Physical applications of solenoids

G. N. Afanas'ev
Joint Institute for Nuclear Research, Dubna

Fiz. Elem. Chastits At. Yadra **24**, 512–593 (March–April 1993)

The wide-ranging physical applications of solenoids are reviewed. The following problems are discussed: static and nonstatic electric and magnetic solenoids, electric vector potentials, electromagnetic-potential waves, the specific realization of static and nonstatic solenoids, the Aharonov–Casher effect for toroidal solenoids, and the experimental verification of the Aharonov–Bohm effect.

1. INTRODUCTION

The toroidal solenoid (TS) is a unique object possessing a number of surprising features. Let us recall only a few of them. Depending on the direction of the current at the solenoid surface, the magnetic field can be completely confined either inside or outside the solenoid.[1–3] This makes the TS useful in setups for studying thermonuclear fusion,[4] for constructing effective electromagnetic-energy storage devices,[5] as an emitter of radio waves,[6] and for testing the foundations of Maxwell electromagnetic theory[7] and quantum mechanics.[8–10] The multipole expansion of the electromagnetic field of a toroidal solenoid contains multipole moments of a new type—toroidal moments.[11,12] Closed chains of arbitrary shape made up of toroidal moments possess a surprising feature: the vector potential is zero outside them, i.e., they are completely self-screened objects.[13] Moreover, the magnetic field of a solenoid at rest or moving uniformly in a vacuum is zero outside the solenoid. In the case of uniform motion in a medium with $\varepsilon\mu \neq 1$ the magnetic field does penetrate the region outside the toroidal solenoid.[14]

In two earlier reviews[15,16] we studied the properties of toroidal solenoids. The purpose of the present review is to discuss the specific physical applications of toroidal solenoids. We shall organize our discussion as follows. In Sec. 2 we give the information about magnetic toroidal solenoids (MTSs) needed for the rest of the discussion. In Sec. 3 we construct a set of MTS vector potentials (VPs) possessing various types of asymptotic behavior.[17] In spite of this, the cross sections for charged-particle scattering on such TSs are the same. This is a reflection of the nonuniqueness of the quantum inverse scattering problem. In Sec. 4 we study the behavior of an MTS in an external magnetic field. For an infinitesimal MTS we obtain a system of equations relating the coordinates of the center of gravity of the TS and its orientation angles. In addition, we explain the physical meaning of the VPs obtained in Sec. 3 with different asymptotic behavior: they correspond to toroidal moments of higher multipole order.[12,18] In Sec. 5 we demonstrate the existence of the Aharonov–Casher effect[19] for a TS and its infinitesimal analogs—the toroidal moments. It turns out that point toroidal solenoids (i.e., moments) must undergo quantum scattering on a Coulomb field. In Sec. 6 we consider self-screened electromagnetic objects.[20] By these we mean configurations of charges and currents for which the magnetic field is equal to zero everywhere, while the electric field is nonzero only in a limited region of space. First a static electric solenoid is constructed from electric dipoles. The electric induction turns out to be nonzero only inside the solenoid. Outside it the electric vector potential is nonzero, and this cannot be eliminated by a gauge transformation. The question arises of the physical interpretation of this potential and the experimental confirmation of its existence. For this we solve some well known electrostatic problems (polarized spheres and an axially symmetric ellipsoid) using both the ordinary scalar potential and the electric vector potential. They lead to the same results. For fixed small semiaxis of the ellipsoid and large semiaxis increasing without bound the electric scalar potential and the electric field E decrease, while the induction D turns out to be concentrated inside the ellipsoid. The electric vector potential of the ellipsoid becomes the electric vector potential of the cylindrical solenoid. Then we consider a nonstatic electric solenoid, which contains both charge and current densities. Outside such a solenoid electromagnetic-potential waves arise and propagate with the speed of light.[21,22] They do not carry energy, since $E=H=0$ in them. The question arises of the physical meaning of such potential waves and their measurability. In Sec. 7 we analyze the concept of quantum impenetrability.[23] A surface is termed impenetrable to incident particles if the normal component of the quantum-mechanical probability current vanishes on it. It turns out that this current can be made to vanish in an infinite number of ways. They correspond to physically distinguishable situations and lead, for example, to different observed cross sections for the scattering of incident particles. In Sec. 8 we consider the possibility of observing the Aharonov–Bohm effect in simply connected spaces.[23] This turns out to be possible, owing to the difference between the mathematical and physical concepts of simple connectedness. In Sec. 9 we study electron scattering on a toroidal solenoid. The well known experiments of Tonomura on the verification of the Aharonov–Bohm effect are analyzed. These fundamental experiments concern the deepest aspects of quantum mechanics.

2. NECESSARY INFORMATION ABOUT TOROIDAL SOLENOIDS

Let us consider a torus. Its surface is defined by the equation

 1063-7796/93/020219-35$10.00

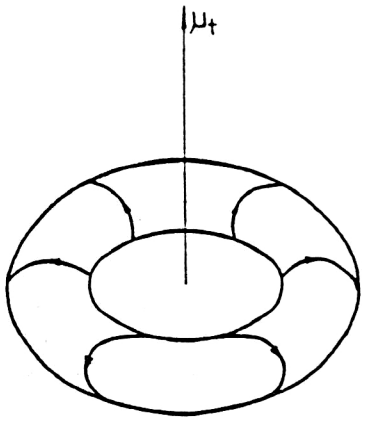

FIG. 1. The poloidal current on the surface of a toroidal solenoid and the associated toroidal moment.

$$(\rho-d)^2+z^2=R^2. \tag{1}$$

Let a constant poloidal current (Fig. 1) flow along the surface of the torus. In order to write down this current explicitly, we introduce the coordinates

$$\rho=d+\tilde{R}\cos\psi, \quad z=\tilde{R}\sin\psi.$$

The value $\tilde{R}=R$ corresponds to the surface of the torus. The infinitesimal volume and surface elements of the torus are

$$\begin{aligned} dV&=\tilde{R}(d+\tilde{R}\cos\psi)d\tilde{R}\,d\psi\,d\varphi,\\ dS&=R(d+R\cos\psi)d\psi\,d\varphi. \end{aligned} \tag{2}$$

The density of the poloidal current in the coordinates $\tilde{R}$ and ψ has the form

$$\mathbf{j}=-\frac{gc}{4\pi}\frac{\delta(\tilde{R}-R)}{d+\tilde{R}\cos\psi}\mathbf{n}_\psi. \tag{3}$$

Here $g=2NI/c$, I is the current in an individual winding, N is the number of windings in the coil of the TS, and $\mathbf{n}_\psi$ is a unit vector defining the direction of the current at the surface of the torus:

$$\mathbf{n}_\psi=\mathbf{n}_z\cos\psi-(\mathbf{n}_x\cos\varphi+\mathbf{n}_y\sin\varphi)\sin\psi. \tag{4}$$

The constant g can also be expressed in terms of the magnetic flux Φ and the geometrical dimensions (Fig. 2) of the torus T: $g=\Phi[2\pi(d-\sqrt{d^2-r^2})]^{-1}$. In the stationary case the magnetic field (MF) H is equal to zero outside the TS. Inside it only the φ component of $\mathbf{H}$ is nonzero: $H_\varphi=g/\rho$. Here ρ is the distance from the symmetry axis of the TS ($\rho=d+\tilde{R}\cos\psi$).

In what follows we shall also need the toroidal coordinates μ, θ, and φ. They are introduced as follows:

$$\begin{aligned} x&=\frac{a\sinh\mu\cos\varphi}{\cosh\mu-\cos\theta}, \quad y=\frac{a\sinh\mu\sin\varphi}{\cosh\mu-\cos\theta},\\ z&=\frac{a\sin\theta}{\cosh\mu-\cos\theta}\\ &(0<\mu<\infty, \quad -\pi<\theta<\pi, \quad 0<\varphi<2\pi). \end{aligned} \tag{5}$$

For a given value of μ the points $P(x,y,z)$ [where x, y, and z are given by (5)] fill the surface of the torus $(\rho-d)^2+z^2=R^2$ with the parameters $d=a\coth\mu$ and $R=a/\sinh\mu$. Let $\mu=\mu_0$ correspond to the surface of the torus T (Fig. 2). Then for $\mu>\mu_0$ the point P lies inside the torus T, and for $\mu<\mu_0$ it lies outside it. The value of the angle θ undergoes a jump from $-\pi$ to π at the intersection of the circle of radius d–R lying in the plane $z=0$. The volume and surface elements (2), the current density (3), and the unit vector (4) in toroidal coordinates become

$$\begin{aligned} dV&=\frac{a^3\sinh\mu\,d\mu\,d\theta\,d\varphi}{(\cosh\mu-\cos\theta)^3}, \quad dS=\frac{a^2\sinh\mu_0\,d\theta\,d\varphi}{(\cosh\mu_0-\cos\theta)^2},\\ \mathbf{j}&=-\frac{gc}{4\pi a^2}\frac{\delta(\mu-\mu_0)}{\sinh\mu_0}(\cosh\mu_0-\cos\theta)^2\mathbf{n}_\theta,\\ \mathbf{n}_\theta&=[(\mathbf{n}_x\cos\varphi+\mathbf{n}_y\sin\varphi)\sinh\mu_0\sin\theta\\ &\quad+\mathbf{n}_z(1-\cosh\mu_0\cos\theta)](\cosh\mu_0-\cos\theta)^{-1}. \end{aligned}$$

The vector potential of the TS was obtained in Ref. 3. The nonzero components of the VP in integral form are

$$\begin{aligned} A_z&=\frac{g\sqrt{R}}{2\pi}\int_0^{2\pi}d\varphi\frac{d-\rho\cos\varphi}{q^{3/2}}Q_{1/2}(\cosh\mu),\\ A_\rho&=\frac{g\sqrt{R}}{2\pi}z\int_0^{2\pi}d\varphi\frac{\cos\varphi}{q^{3/2}}Q_{1/2}(\cosh\mu) \end{aligned} \tag{6}$$

[$\cosh\mu=(r^2+d^2+R^2-2d\rho\cos\varphi)/2Rq$, $q^2=(\rho\cos\varphi-d)^2+z^2$, $r^2=\rho^2+z^2$, and $Q_\nu(x)$ is a Leg-

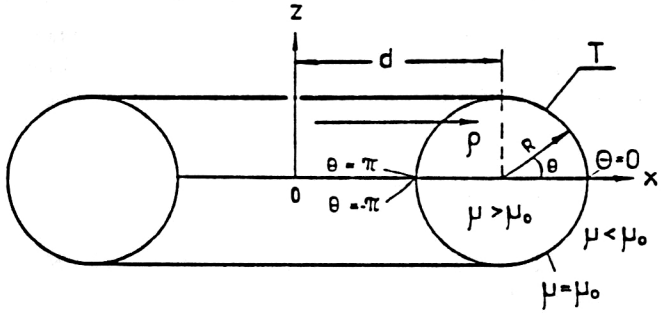

FIG. 2. Geometrical dimensions of the solenoid.

endre function of the second kind]. For a very thin TS ($R \ll d$) these integrals can be evaluated explicitly:

$$A_z=\frac{gR^2}{2(d\rho)^{3/2}}\frac{1}{\sinh\mu_1}\left[\rho Q^1_{1/2}(\cosh\mu_1)\right.$$
$$\left.-dQ^1_{-1/2}(\cosh\mu_1)\right],$$
$$A_\rho=-\frac{gR^2z}{2(d\rho)^{3/2}}\frac{1}{\sinh\mu_1}Q^1_{1/2}(\cosh\mu_1), \quad (7)$$
$$\cosh\mu_1=\frac{r^2+d^2}{2d\rho}.$$

At large distances the VP falls off as r^{-3}:

$$A_z\sim\frac{1}{8}\pi gdR^2\frac{1+3\cos 2\theta_s}{r^3},\quad A_\rho\sim\frac{3}{8}\pi gdR^2\frac{\sin 2\theta_s}{r^3} \quad (8)$$

(r and θ_s are ordinary spherical coordinates).

Instead of the current (3) it is sometimes convenient to introduce the magnetization $\mathbf{j}=c\,\mathrm{curl}\,\mathbf{M}$. It is nonzero everywhere inside the TS and

$$\mathbf{M}=M\mathbf{n}_\varphi,\quad M=\frac{g}{4\pi}\frac{\theta(R-\tilde R)}{d+\tilde R\cos\psi}$$
$$=\frac{g}{4\pi a}\frac{\cosh\mu-\cos\theta}{\sinh\mu}\theta(\mu-\mu_0). \quad (9)$$

Here $\theta(x)$ is the step function [$\theta(x)$ is zero for $x<0$ and unity for $x>0$].

A more general current distribution for which $\mathbf{H}=0$ outside the TS was obtained in Ref. 17. It has the form

$$\mathbf{j}=-\frac{f_1(\tilde R)\theta(R_1-\tilde R)}{d+\tilde R\cos\psi}\mathbf{n}_\psi$$
$$=-\frac{1}{\sinh\mu}f(\mu)\theta(\mu-\mu_1)(\cosh\mu-\cos\theta)^2\mathbf{n}_\theta. \quad (10)$$

The presence of the θ function means that the currents are contained inside a torus of radius $R_1=a/\sinh\mu_1$. The current distribution (3) is obtained for the following special choice of the functions f and f_1:

$$f_1=\frac{gc}{4\pi}\delta(\tilde R-R),\quad f=\frac{gc}{4\pi a^2}\delta(\mu-\mu_0),$$
$$R<R_1,\quad \mu_0>\mu_1.$$

The magnetic field strength, the magnetization, and the flux of the MF corresponding to the current (10) are

$$H_\varphi=\frac{4\pi}{c}\frac{\theta(R-\tilde R)}{d+\tilde R\cos\psi}\int_{\tilde R}^{R}f_1(x)dx$$
$$=\frac{4\pi a}{c}\frac{\cosh\mu-\cos\theta}{\sinh\mu}\int_{\mu_1}^{\mu}f(\mu)d\mu,$$
$$M_\varphi=-\frac{1}{c}\frac{\theta(R-\tilde R)}{d+\tilde R\cos\psi}\int_{\tilde R}^{R}f_1(x)dx$$
$$=-\frac{a}{c}\frac{\cosh\mu-\cos\theta}{\sinh\mu}\int_{\mu_1}^{\mu}f(\mu)d\mu,$$
$$\Phi=\frac{8\pi^2}{c}\int_0^R(d-\sqrt{d^2-x^2})f_1(x)dx$$
$$=\frac{8\pi^2a^3}{c}\int_{\mu_1}^{\infty}(\coth\mu-1)f(\mu)d\mu.$$

The vector potentials corresponding to the current (10) were calculated explicitly in Refs. 16 and 17. In general (i.e., for arbitrary functions f and f_1), at large distances they fall off as r^{-3}:

$$A_\rho\sim\frac{3}{2}\frac{\pi^2a^5}{r^3c}\sin 2\theta_s\alpha(\mu_1),$$
$$A_z\sim\frac{\pi^2a^5}{2r^3c}(1+\cos 2\theta_s)\alpha(\mu_1), \quad (11)$$
$$\alpha(\mu_1)=\int_{\mu_1}^{\infty}d\mu\frac{\cosh\mu}{\sinh^3\mu}f(\mu).$$

These expressions are valid also for a point ($a\to 0$) toroidal solenoid.

3. VECTOR POTENTIALS WITH DIFFERENT ASYMPTOTIC BEHAVIOR

Let us try to arrange the freedom in the choice of the functions f (f_1) so that the asymptote of the VP is changed. For this we need terms of higher order in the asymptotic expansion of the VP. Such an expansion for the current density (3) was obtained in Refs. 16 and 24:

$$A_z=-\frac{1}{2}gR\sum_{l=2}^{\infty}\frac{1}{r^{l+1}}P_l(\cos\theta_s)f^0_l,$$
$$A_\rho=\frac{1}{2}gR\sum_{l=2}^{\infty}\frac{1}{r^{l+1}}\frac{1}{l(l+1)}P^1_l(\cos\theta)f^1_l. \quad (12)$$

Here

$$f^0_l=\int d\psi\cos\psi\rho^lP_l(R\sin\psi/\rho),$$
$$f^1_l=\int d\psi\sin\psi\rho^lP^1_l(R\sin\psi/\rho),$$
$$\rho=(d^2+R^2+2dR\cos\psi)^{1/2}.$$

The summation in (12) runs over even l. The difference between these equations and the analogous ones given in Refs. 16 and 24 is related to the fact that the Legendre polynomials normalized to unity [$Y^m_l=1/\sqrt{2\pi}(-1)^mP^m_l$] were used in Refs. 16 and 24, while the usual normalization

$$\int_{-1}^{1}[P^m_l(x)]^2dx=\frac{2}{2l+1}\frac{(l+m)!}{(l-m)!}$$

is used here. We shall need the first two terms in the expansion (12):

$$A_z \approx \frac{\pi g d R^2}{2r^3}\left[P_2(\cos\theta) - \frac{3}{2}\frac{d^2 - R^2/4}{r^2} P_4(\cos\theta)\right],$$

$$A_\rho \approx \frac{\pi g d R^2}{4r^3}\left[P_2^1(\cos\theta) - \frac{3}{4}\frac{d^2 - R^2/4}{r^2} P_4^1(\cos\theta)\right].$$

Let us consider two concentric solenoids TS_1 and TS_2 (Fig. 3b) with parameters d_1, R_1, Φ_1 and d_2, R_2, Φ_2. The total VP is

$$A_z^{(1,2)} = A_z^{(1)} + A_z^{(2)}, \quad A_\rho^{(1,2)} = A_\rho^{(1)} + A_\rho^{(2)}.$$

We select the solenoid parameters such that the leading terms ($\sim r^{-3}$) in the asymptote of the VP are canceled. This occurs if

$$g_1 d_1 R_1^2 + g_2 d_2 R_2^2 = 0. \tag{13}$$

Substituting into (13) the explicit expressions for g, d, and R for each of the solenoids ($d_i = a\coth\mu_i$, $R_i = a/\sinh\mu_i$, and $g_i = \Phi_i[a(\coth\mu_i - 1)]^{-1}$) and taking $y_i = \coth\mu_i$, we obtain the following relation:

$$\Phi_1 y_1(y_1+1) + \Phi_2 y_2(y_2+1) = 0.$$

This equation can be solved for y_2:

$$y_2 = -\frac{1}{2} + \left[\frac{1}{4} - \frac{\Phi_1}{\Phi_2} y_1(y_1+1)\right]^{1/2}.$$

The total VP now falls off as r^{-5}:

$$A_z^{(1,2)} \sim -\frac{9}{32}\Phi_1 a^2 y_1(y_1+1)(y_1^2 - y_2^2)\frac{1}{r^5} P_4(\cos\theta_s),$$

$$A_\rho^{(1,2)} \sim -\frac{9}{128}\Phi_1 a^2 y_1(y_1+1)(y_1^2 - y_2^2)\frac{1}{r^5} P_4^1(\cos\theta_s). \tag{14}$$

Let us surround TS_1 and TS_2 by an impenetrable (to incident charged particles) torus T. Let the total magnetic flux of TS_1 and TS_2 be Φ (i.e., $\Phi = \Phi_1 + \Phi_2$). The quantum cross section for charged-particle scattering depends only on the geometrical parameters of the impenetrable torus T and the magnetic flux Φ inside the torus (see Sec. 9). This means that the current configurations shown in Fig. 3a (inside T, one TS with magnetic flux Φ) and Fig. 3b (inside T, two TSs with total magnetic flux Φ) are physically indistinguishable despite the different behavior of the VPs ($\sim r^{-3}$ for Fig. 3a and $\sim r^{-5}$ for Fig. 3b). These VPs are not related by a gauge transformation, since they correspond to different distributions of the magnetic field H inside the torus T. This game can be continued. We take (in addition to TS_1 and TS_2) solenoids TS_3 and TS_4 with parameters satisfying the relation $g_3 d_3 R_3^2 + g_4 d_4 R_4^2 = 0$. The total VP of the solenoids TS_3 and TS_4 is

$$A_z^{(3,4)} = -\frac{9}{32}\Phi_3 a^2 y_3(y_3+1)(y_3^2 - y_4^2) r^{-5} P_4(\cos\theta_s),$$

$$A_\rho^{(3,4)} = -\frac{9}{128}\Phi_3 a^2 y_3(y_3+1)(y_3^2 - y_4^2) r^{-5} P_4^1(\cos\theta_s).$$

Here $y_3 = \coth\mu_3$ and $y_4 = \coth\mu_4$. The total VP generated by the solenoids TS_1–TS_4 is

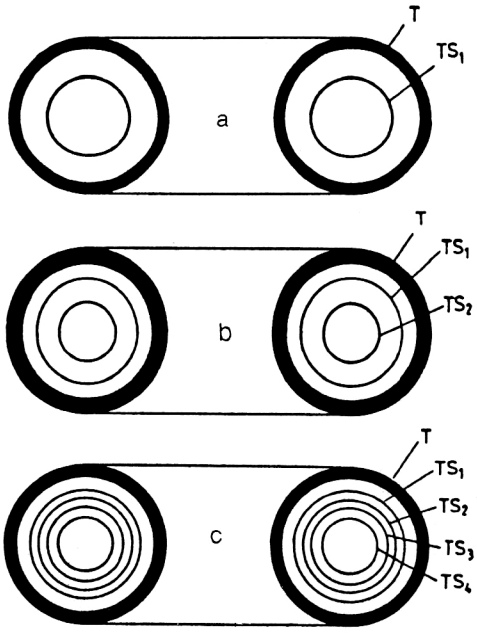

FIG. 3. The current configurations inside an impenetrable torus T. These configurations induce gauge-noninvariant vector potentials giving the same quantum-mechanical charged-particle scattering cross section. The vector potential is concentrated nearer and nearer to the solenoid in going from the figure at the top to the one at the bottom.

$$A_z = A_z^{(1,2)} + A_z^{(3,4)}, \quad A_\rho = A_\rho^{(1,2)} + A_\rho^{(3,4)}.$$

Now we require that the total magnetic flux be Φ ($\Phi_1 + \Phi_2 + \Phi_3 + \Phi_4 = \Phi$) and that the coefficient of r^{-5} vanish. This occurs if

$$\Phi_1 y_1(y_1+1)(y_1^2 - y_2^2) + \Phi_3 y_3(y_3+1)(y_3^2 - y_4^2) = 0.$$

The resulting configuration of four solenoids (Fig. 3c) generates a VP which falls off at large distances as r^{-7}. Now we surround the configuration of four solenoids TS_1–TS_4 by the same impenetrable torus T (Fig. 3c). Then charged particles will undergo the same quantum scattering as in the cases of Figs. 3a and 3b. The fact that the quantum-mechanical cross sections are identical can be interpreted either as nonuniqueness of the quantum inverse scattering problem (the same scattering cross section for different current distributions inside the torus T) or as nonuniqueness of the inverse electromagnetic problem (the same E and H outside the torus T are generated by different current distributions inside the torus T). The magnetic flux is Φ for each of the configurations in Figs. 3a–3c. This implies that $\oint A_l dl$ computed along any closed contour passing through the hole in the torus T is equal to Φ. In particular, this is valid for the integral $\int A_z dz$ computed along the z axis. Since A_z falls off faster in going from the upper part of Fig. 3 to the lower part, the VP is concentrated closer and closer to the torus T. The physical meaning of these VPs will be discussed in Sec. 4.

Realizations of static solenoids (Ref. 13)

Let us consider an arbitrary current configuration **j**. The vector potential is

$$\mathbf{A}=\frac{1}{c}\int G_0(\mathbf{r},\mathbf{r}')\mathbf{j}(\mathbf{r}')dV', \quad G_0=|\mathbf{r}-\mathbf{r}'|^{-1}.$$

Since div $\mathbf{j}=0$, instead of the current j we can introduce the equivalent magnetization M: $\mathbf{j}=c$ curl $\mathbf{M}$. Then

$$\mathbf{A}=\int G_0(\mathbf{r},\mathbf{r}')\text{curl}\,\mathbf{M}(\mathbf{r}')dV'. \tag{15}$$

From this we immediately find that

$$\mathbf{H}=\text{curl}\,\mathbf{A}=\text{grad}\int G_0\,\text{div}\,\mathbf{M}\,dV'+4\pi\mathbf{M}. \tag{16}$$

We see that for div $\mathbf{M}=0$ the strength H is nonzero only inside the solenoid (the magnetization is by definition nonzero only inside the solenoid). Some care should be taken in using the magnetization formalism. In the case just considered of a current j flowing in a vacuum, we introduced a fictitious magnetization using the relation $\mathbf{j}=c$ curl $\mathbf{M}$. In this case $B=H$ everywhere, and H is given by Eq. (16). The situation is changed if we have a real medium with magnetization M. Then (in the absence of currents) we have $\mathbf{B}=\mathbf{H}+4\pi\mathbf{M}$ and div $\mathbf{B}=0$. As before, Eq. (15) holds for the vector potential. In the end we have

$$\mathbf{B}=\text{curl}\,\mathbf{A}=\mathbf{H}+4\pi\mathbf{M}, \tag{17}$$

where

$$\mathbf{H}=\text{grad}\int G_0\,\text{div}\,\mathbf{M}(r')dV'. \tag{18}$$

From this we find that for div $\mathbf{M}=0$ the magnetic field strength H is zero everywhere, and the magnetic induction B is nonzero only inside the solenoid.

It follows from these arguments that solenoids of arbitrary shape can be constructed if the space inside the solenoid is filled with material with solenoidal (div $\mathbf{M}=0$) magnetization. An example is a uniformly magnetized filament of arbitrary shape. Such circular and straight filaments have been used in experiments to test the existence of the Aharonov–Bohm effect.

Let us now represent $\mathbf{M}$ as $\mathbf{M}=$curl $\mathbf{t}$. Then it follows from (15) that

$$\mathbf{A}=\text{grad}\int G_0(\mathbf{r},\mathbf{r}')\text{div}\,\mathbf{t}(\mathbf{r}')dV'+4\pi\mathbf{t}(\mathbf{r}).$$

If div $\mathbf{t}=0$, then $\mathbf{A}=4\pi\mathbf{t}$. Then the vector potential is nonzero only where $\mathbf{t}\neq 0$ (i.e., again inside the solenoid). This means that complete self-screening occurs. In particular, this is valid for the toroidal moments ($\mathbf{j}=c$ curl curl $\mathbf{t}$). Closed chains made of toroidal moments are therefore completely self-screened objects. For an arbitrary deformation of them the vector potential does not penetrate the space outside them.

Solenoids with nontrivial helicity

Let us return to ordinary cylindrical and toroidal solenoids. As is well known, for a cylindrical solenoid with surface current $j\delta(\rho-R)\mathbf{n}_\varphi$ the vector potential A_φ is equal to $\Phi/2\pi\rho$ outside the solenoid ($\rho>R$) and $\Phi\rho/2\pi R^2$ inside it. The magnetic field is nonzero only inside the solenoid: $\mathbf{H}=\mathbf{n}_z\Phi/\pi R^2$. Here Φ is the magnetic flux through the cross section of the solenoid: $\Phi=4\pi^2R^2j/c$. We note that in this case the vector potential is perpendicular to the magnetic field. Therefore, $S=\int\mathbf{A}\cdot\mathbf{H}\,dV=0$. The quantity S is referred to as the helicity.[64–66] Thus, the ordinary cylindrical solenoid has zero helicity. Instead of the current we introduce the equivalent magnetization. For the cylindrical solenoid it is $\mathbf{M}=M_0\mathbf{n}_z$, $M_0=j/c$. The vector potential is related to the magnetization as

$$\mathbf{A}(\mathbf{r})=\int\mathbf{M}(\mathbf{r}')\frac{\mathbf{r}-\mathbf{r}'}{|\mathbf{r}-\mathbf{r}'|^3}dV'.$$

Let us now forget about the current and treat the solenoid as a cylinder filled with magnetic material with magnetization density $\mathbf{M}$. Let the magnetization have a φ component (in addition to the z component already present):

$$\mathbf{M}=M_0(\mathbf{n}_z\cos\alpha+\mathbf{n}_\varphi\sin\alpha)$$

(i.e., the magnetization lines have the shape of spirals uniformly distributed inside the cylinder and having the cylinder axis as their symmetry axis). Let us now give the nonvanishing components of the vector potential and the magnetic field corresponding to this magnetization. Inside the cylinder

$$A_z=4\pi M_0(R-\rho)\sin\alpha, \quad A_\varphi=2\pi\rho M_0\cos\alpha,$$

$$B_z=4\pi M_0\cos\alpha, \quad B_\varphi=4\pi M_0\sin\alpha.$$

Outside the cylinder

$$A_z=0, \quad A_\varphi=2\pi R^2M_0\cos\alpha/\rho, \quad \mathbf{B}=0.$$

Finally, for the helicity of the twisted cylindrical solenoid we find (per unit length of the cylinder)

$$S=\frac{1}{3}16\pi^3M_0^2\sin 2\alpha\cdot R^3.$$

Let us now consider a toroidal solenoid. It can be treated as a torus $(\rho-d)^2+z^2=R^2$ filled with material with magnetization M given by (9). Now let there be a poloidal component (θ) of the magnetization in addition to the already existing toroidal component (φ):

$$\mathbf{M}=M(\mathbf{n}_\varphi\cos\alpha+\mathbf{n}_\theta\sin\alpha) \tag{19}$$

(the magnetization lines have the shape of spirals wound around the axial line $\rho=d$, $z=0$ of the torus). The magnetic field (the induction) is nonzero only inside the torus,

$$B_\varphi=4\pi M\cos\alpha, \quad B_\theta=4\pi M\sin\alpha,$$

and the ρ and z components of the vector potential generated by the toroidal component were given above [see Eqs. (6)–(8), which should be multiplied by $\cos\alpha$]. From them we easily find the required θ component of the vector potential:

$$A_\theta=-[A_\rho\sinh\mu\sin\theta+A_z(1-\cosh\mu\cos\theta)]$$
$$\times(\cosh\mu-\cos\theta)^{-1}.$$

Furthermore, the θ component of $\mathbf{M}$ generates a φ component of $\mathbf{A}$ equal to

$$A_\varphi = -8\pi M_0 \sin\alpha \frac{\cosh\mu - \cos\theta}{\sinh\mu \sin\theta} \times \arctan \frac{\sinh\left(\frac{\mu-\mu_0}{2}\right)\cdot \sin\theta}{\cosh\left(\frac{\mu+\mu_0}{2}\right) - \cosh\left(\frac{\mu-\mu_0}{2}\right)\cdot \cos\theta}$$

inside the torus and zero outside it. From this it follows that the magnetization (19) corresponds to nonzero helicity. We shall write it out explicitly for a very thin torus ($R \ll d$ or $\mu_0 \gg 1$). In this case the required components of the vector potential and the magnetic field inside the torus have the form

$$A_\theta = 4\pi a M_0 [\exp(-\mu) - \mu_0 \cos\theta \exp(-\mu_0)] \cos\alpha,$$

$$A_\varphi = -8\pi a M_0 \exp(-\mu_0) \sin\alpha,$$

$$B_\theta = 4\pi M_0 \sin\alpha, \quad B_\varphi = 4\pi M_0 \cos\alpha.$$

Finally, for the helicity we find

$$S = \int \mathbf{AB}\, dV = \frac{1}{3} 32\pi^4 a^4 M_0^2 \sin 2\alpha \exp(-3\mu_0).$$

The helicity S along with the magnetic flux Φ is one of the topological invariants characterizing the structure of the magnetic field. These invariants remain unchanged for arbitrary but continuous deformations of the solenoid. There are other topological invariants besides Φ and S (Ref. 67). They characterize the more detailed structure of the magnetic field. In Sec. 9 we shall show how the helicity affects the charged-particle scattering cross section.

4. MOTION OF THE TOROIDAL SOLENOID IN AN EXTERNAL MAGNETIC FIELD

The energy of interaction of a TS and an external magnetic field is given by

$$U = -\int \mathbf{H}_{\text{ext}} \mathbf{M} dV. \tag{20}$$

Here $\mathbf{M}$ is the magnetization of the TS (see Sec. 3). Since only the φ component of $\mathbf{M}$ is nonzero, the TS interacts with an external MF if the latter has nonzero projection on the equatorial plane of the TS and nonzero overlap with M_φ. If the source of the MF is sufficiently far from the TS, the MF near the TS can be expanded in a series:

$$\mathbf{H}_{\text{ext}}(\mathbf{r}_s) = \mathbf{H}_{\text{ext}}(\mathbf{r}_0) + (\mathbf{r}\nabla_0)\mathbf{H}_{\text{ext}}(\mathbf{r}_0), \quad \mathbf{r}_s = \mathbf{r}_0 + \mathbf{r}. \tag{21}$$

Here the vector $\mathbf{r}_0$ determines a point near the TS, for example, its center of mass, and $\mathbf{r}$ is a vector going from $\mathbf{r}_0$ to some point lying inside the TS. We substitute this expansion into (20):

$$U = -\mu_d \mathbf{H}_{\text{ext}}(\mathbf{r}_0) - \frac{1}{2}\mu_t \operatorname{curl} \mathbf{H}(\mathbf{r}_0). \tag{22}$$

Here $\mu_t = \int \mathbf{M} dV$ is the dipole magnetic moment, which is zero for the TS. In addition,

$$\mu_t = \int (\mathbf{r}\times\mathbf{M}) dV \tag{23}$$

coincides up to an insignificant constant with the toroidal dipole moment (TDM; Refs. 11, 12, and 18). It points along the symmetry axis of the TS, and its magnitude is

$$\mu_t = \frac{1}{2}\pi g d R^2.$$

For arbitrary orientation θ, φ of the TS symmetry axis

$$\boldsymbol{\mu}_t = (\sin\theta\cos\varphi,\ \sin\theta\sin\varphi,\ \cos\theta)\frac{1}{2}\pi g d R^2.$$

In order to study the motion of the TS in a magnetic field, we use the Lagrangian $L = T - U$. The kinetic energy T is equal to the sum of the energy of the center-of-mass motion $T_{\text{cm}} = \frac{1}{2}M(\dot{x}_0^2 + \dot{y}_0^2 + \dot{z}_0^2)$ and the rotational energy $T_{\text{rot}} = \frac{1}{2}(A\omega_x^2 + B\omega_y^2 + C\omega_z^2)$. Here M is the mass of the TS; x_0, y_0, and z_0 are the coordinates of its center of mass; ω_x, ω_y, and ω_z are the projections of the angular-velocity vector on the axes of inertia attached to the TS:

$$\omega_x = \dot{\theta}\sin\psi - \dot{\varphi}\sin\theta\cos\psi,$$

$$\omega_y = \dot{\theta}\cos\psi + \dot{\varphi}\sin\theta\sin\psi,$$

$$\omega_z = \dot{\varphi}\cos\psi + \dot{\psi},$$

where the angles φ, θ, and ψ determine the orientation of the coordinate system rigidly attached to the TS relative to the lab frame; A, B, and C are the moments of inertia of the TS [$A = \int (y^2+z^2)\rho dV / \int \rho dV$, and so on]:

$$A = B = \frac{1}{2} d^2 M (1 + 5R^2/4d^2),$$

$$C = d^2 M (1 + 3R^2/4d^2).$$

Using the Maxwell equation $\operatorname{curl}\mathbf{H} = (1/c)\dot{\mathbf{E}}_{\text{ext}} + (4\pi/c)\mathbf{j}_{\text{ext}}$ and the fact that the expansion (21) is valid at large distances from the source of the MF (where $j_{\text{ext}} = 0$), we obtain

$$U = -\frac{1}{2c}\dot{\mathbf{E}}_{\text{ext}}\boldsymbol{\mu}_t, \quad \dot{\mathbf{E}} = \frac{\partial \mathbf{E}}{\partial t}. \tag{24}$$

This expression simplifies if the field E_{ext} points along the z axis: $U = -(1/2c)\dot{\mathbf{E}}_z(\mathbf{r}_0)\mu_t \cos\theta$, where θ is the angle $\boldsymbol{\mu}_t$ makes with the z axis. From this it follows that the potential energy of the TDM depends both on the center-of-mass coordinates of the TDM and on the TDM orientation. The Lagrange equation $[(d/dt)(\partial L/\partial \dot{q}_1) - (\partial L/\partial q_i) = 0, q_i = x_0, y_0, z_0, \varphi, \theta, \psi]$ leads to a coupled system of equations which completely determine the TDM motion. The classical equations of motion are easily quantized. As a result, we arrive at the following Schrödinger equation:

$$i\hbar\frac{\partial \psi}{\partial t} = H\Psi, \quad H = T + V,$$

$$T = -\frac{\hbar^2}{2M}\nabla_0^2 + \frac{\hbar^2}{2MA^2}\mathbf{L}^2 + \frac{\hbar^2}{2M}\left(\frac{1}{C^2} - \frac{1}{A^2}\right)L_z^2,$$

$$V=-\frac{1}{2c}\dot{\mathbf{E}}_z(\mathbf{r}_0)\mu_t\mathbf{n}_t.$$

Here L_i are the Cartesian components of the ordinary angular momentum, $\mathbf{L}^2=\Sigma L_i^2$. The classical and quantum equations for the magnetic dipole moment have recently been obtained in Ref. 68. The TDM is an important characteristic of the TS, but is not the only one. To verify this we return to the current configuration shown in Fig. 3. The corresponding magnetization and TDM have the form

$$M_{12}=\frac{1}{4\pi a}\frac{\cosh\mu-\cos\theta}{\sinh\mu}\left[g_1\theta(\mu-\mu_1)+g_2(\mu-\mu_2)\right], \tag{25}$$

$$\mu_t^{(1,2)}=\frac{1}{2}\pi(g_1d_1R_1^2+d_2d_2R_2^2).$$

In view of (13) the TDM vanishes for this configuration. This means that the next term in the expansion of H_{ext} must be included. It is $\frac{1}{2}(\mathbf{r}\nabla_0)^2H_{\text{ext}}$. Substituting it into (20), we find

$$U=-\frac{1}{3}\frac{\partial}{\partial x_{0i}}(\text{curl}\,H_{\text{ext}})_j\int x_i(\mathbf{r}\times\mathbf{M}_{12})_j dV.$$

It is easily verified that the integrals on the right-hand side vanish for the magnetization (25). Substituting the next term $\frac{1}{6}(\mathbf{r}\nabla_0)^3H_{\text{ext}}$ into the expansion of H_{ext} in (20), we find

$$U=-\frac{1}{8}\frac{\partial^2}{\partial x_{0i}\partial x_{0j}}(\text{curl}\,H_{\text{ext}})_k\int x_ix_j(\mathbf{r}\times\mathbf{M}_{12})_k dV. \tag{26}$$

The nonvanishing integrals on the right-hand side are

$$\int x^2(\mathbf{r}\times\mathbf{M}_{12})_z dV=\int y^2(\mathbf{r}\times\mathbf{M}_{12})_z dV$$

$$=\frac{7}{32}\Phi_1a^4y_1(y_1+1)(y_1^2-y_2^2),$$

$$\int z^2(\mathbf{r}\times\mathbf{M}_{12})_z dV=\frac{1}{16}\Phi_1a^4y_1(y_1+1)(y_1^2-y_2^2),$$

$$\int xz(\mathbf{r}\times\mathbf{M}_{12})_x dV=\int yz(\mathbf{r}\times\mathbf{M}_{12})_y dV$$

$$=-\frac{1}{32}\Phi_1a^4y_1(y_1+1)(y_1^2-y_2^2),$$

$$y_i=\coth\mu_i. \tag{27}$$

Therefore, for the current configuration of Fig. 3b the interaction energy is given by (26). The integrals on the right-hand side of (26) are usually defined as the higher-order (or multipole-order) toroidal moments.[12,18] Let us now turn to the configuration of Fig. 3c. Instead of (26) we find

$$U=-\frac{1}{8}\frac{\partial^2[\text{curl}\,\mathbf{H}_{\text{ext}}(\mathbf{r}_0)]_k}{\partial x_{0i}\partial x_{0j}}$$

$$\times\int\int x_ix_j[\mathbf{r}\times(M_{12}+M_{34})]_k dV. \tag{28}$$

Here M_{34} is given by an expression analogous to (25). It follows directly from (28) that this expression vanishes for the current configuration in Fig. 3c. The interaction arises when the higher-order terms in the expansion of $\mathbf{H}_{\text{ext}}$ are included. In the end we obtain a physical interpretation of the current configurations shown in Fig. 3: they generate the toroidal moments of various multipole orders.

5. THE AHARONOV–CASHER EFFECT FOR TOROIDAL SOLENOIDS

First let us give the well known arguments illustrating the existence of the Aharonov–Casher effect[19] for a cylindrical solenoid. We consider a particle of charge e in the field of a cylindrical solenoid at rest. The following term in the Lagrangian describes their interaction:[19]

$$\frac{e}{c}\mathbf{v}_e\mathbf{A}(\mathbf{r}_e-\mathbf{r}_s). \tag{29}$$

Here $\mathbf{r}_e$ and $\mathbf{r}_s$ are the radius vectors of the charged particle and the cylindrical solenoid, $\mathbf{v}_e$ is the velocity of the charged particle, and $\mathbf{A}(\mathbf{r}_e-\mathbf{r}_s)$ is the vector potential generated by the solenoid at the location of the charged particle. Considerations of Galilean invariance allow us to write down the interaction in the case where both the charge and the cylindrical solenoid are moving:

$$\frac{e}{c}(\mathbf{v}_e-\mathbf{v}_s)\mathbf{A}(\mathbf{r}_e-\mathbf{r}_s). \tag{30}$$

Here $\mathbf{v}_s$ is the velocity of the cylindrical solenoid. Aharonov and Casher[19] showed that the additional term

$$-\frac{e}{c}\mathbf{v}_s\mathbf{A}(\mathbf{r}_e-\mathbf{r}_s) \tag{31}$$

describes the quantum scattering of neutral particles possessing a magnetic dipole moment on an infinitesimally thin charged filament (the Aharonov–Casher effect). Experiments in which neutrons were scattered on such a filament were carried out in 1989 (Ref. 25). They confirmed the existence of the Aharonov–Casher effect.

Let us now return to the toroidal solenoid. The interaction of a charged particle with a TS at rest is again described by (29), but $\mathbf{A}$ is now the vector potential of the TS. Experiments in which electrons were scattered by the magnetic field of an impenetrable TS [the Aharonov–Bohm (AB) effect] have been carried out by Tonomura.[8] They confirmed the existence of the AB effect. The theoretical description of these experiments is given in Refs. 9 and 10.

When both the charge and the toroidal solenoid are moving, the requirement of Galilean invariance leads to Eq. (30). Our immediate goal is to obtain and interpret the additional term (31) for the toroidal solenoid. Let a TS with poloidal current $\mathbf{j}$ (which generates a vector potential $\mathbf{A}$ with magnetic field $\mathbf{H}$ equal to zero outside the TS) move with velocity $\mathbf{v}_s$ in an external electric field with strength E and scalar potential φ ($\mathbf{E}=-\text{grad}\,\varphi$). According to the special theory of relativity, the motion of the current $\mathbf{j}$ induces a charge density $\rho=\gamma(\mathbf{v}_s\cdot\mathbf{j})/c^2$. The factor $\gamma=(1-\beta_s^2)^{-1/2}$ can be dropped if we remain within the

Galilean-invariant theory. The interaction of the moving TS with an external electrostatic field is given by

$$U=\int \varphi(\mathbf{r}_s-\mathbf{r}_e)\rho(\mathbf{r}_s)dV_s=\frac{1}{c^2}\int \varphi(\mathbf{v}_s\mathbf{j})dV_s. \quad (32)$$

We replace the current by the equivalent magnetization ($\mathbf{j}=c$ curl $\mathbf{M}$) and integrate by parts:

$$U=\frac{1}{c}\mathbf{v}_s\int [\mathbf{E}(\mathbf{r}_s-\mathbf{r}_e)\times\mathbf{M}]dV_s \quad (33)$$

(the integration is carried out inside the TS, where $M\neq 0$). At large distances from the source of the electrostatic field (or for small size of the TS) the electric field $\mathbf{E}$ near the TS can be expanded in a series:

$$\mathbf{E}(\mathbf{r}_s-\mathbf{r}_e)=\mathbf{E}(\mathbf{r}_0-\mathbf{r}_e)+(\mathbf{r}\nabla_0)\mathbf{E}(\mathbf{r}_0-\mathbf{r}_e), \quad \mathbf{r}_s=\mathbf{r}_0+\mathbf{r}. \quad (34)$$

Here $\mathbf{r}_0$ refers to some point near the TS. For definiteness we take this point to be the center of mass of the TS. In addition, $\mathbf{r}$ is the distance from the center of mass to a flowing point inside the TS. We substitute this expansion into (33). Then

$$U=\frac{1}{c}\mathbf{v}_s(\mathbf{E}\times\boldsymbol{\mu}_d)-\frac{1}{2c}(\mathbf{v}_s\nabla_0)(\mathbf{E}\boldsymbol{\mu}_t). \quad (35)$$

Here $\boldsymbol{\mu}_d=\int \mathbf{M}dV$ is the magnetic dipole moment, and $\boldsymbol{\mu}_t=\int(\mathbf{r}\times\mathbf{M})dV$ is the toroidal moment of the TS. It turns out that for the TS $\boldsymbol{\mu}_d=0$. The toroidal moment $\boldsymbol{\mu}_t$ points along the symmetry axis of the TS (see Fig. 1). Its absolute value is $\mu_t=\frac{1}{2}\pi g d R^2$. Here $g=\Phi[2\pi(d-\sqrt{d^2-R^2})]^{-1}$, Φ is the magnetic flux inside the TS, and d and R are the geometrical dimensions of the TS $(\rho-d)^2+z^2=R^2$. In obtaining (35) we dropped the term containing div $\mathbf{E}$, since the expansion (34) is valid outside the electric-field source. Therefore,

$$U=-\frac{1}{2c}(\mathbf{v}_s\nabla_0)(\mathbf{E}\boldsymbol{\mu}_t). \quad (36)$$

We ask ourselves: what electric field $\mathbf{E}$ substituted into (36) can reproduce the term (31)? We equate these expressions:

$$e\mathbf{v}_s\mathbf{A}(\mathbf{r}_0-\mathbf{r}_e)=-\frac{1}{2}(\mathbf{v}_s\nabla_0)[\mathbf{E}(\mathbf{r}_0-\mathbf{r}_e)\boldsymbol{\mu}_t]. \quad (37)$$

The minus sign in (37) arose because the potential energy in the Lagrangian has negative sign. In addition, we have used the fact that the vector potential of the TS is an even function of the coordinates[3] (in contrast to the vector potential of a cylindrical solenoid). Equating the coefficients of $\mathbf{v}_s$ in (37), we find

$$e\mathbf{A}(\mathbf{r})=-\frac{1}{2}\nabla[\boldsymbol{\mu}_t\mathbf{E}(r)], \quad \mathbf{r}=\mathbf{r}_0-\mathbf{r}_e. \quad (38)$$

Without loss of generality we can assume that the symmetry axes of the TS on both sides of (38) are parallel to the z axis. Since it was obtained using the expansion (34), which is valid for large separations between the TS and the source, for the vector potential on the left-hand side of (38) we must use the asymptotic expression (8):

$$A_x\sim\frac{3}{4}\pi g d R^2\frac{xz}{r^5}, \quad A_y\sim\frac{3}{4}\pi g d R^2\frac{yz}{r^5},$$

$$A_z\sim\frac{\pi g d R^2}{4}\frac{3z^2-r^2}{r^5}.$$

Then from (38) we obtain the following equations:

$$3e\frac{xz}{r^5}=-\frac{\partial E_z}{\partial x}, \quad 3e\frac{yz}{r^5}=-\frac{\partial E_z}{\partial y}, \quad e\frac{3z^2-r^2}{r^5}=-\frac{\partial E_z}{\partial z}.$$

It is easily checked that these equations are satisfied for $E_z=ez/r^3$, which is the z component of $\mathbf{E}=e\mathbf{r}/r^3$. This means that the term (31) restoring the Galilean symmetry of the Lagrangian describes the motion of the TS in a Coulomb field at large distances. If the current distribution (or the magnetization) in the TS is such that the TDM vanishes, we must keep higher-order terms in the expansion of $\mathbf{E}$. In this case, instead of (36) we obtain

$$U=-\frac{1}{8c}(\mathbf{v}_s\nabla_0)\frac{\partial^2 E_i}{\partial x_{0j}\partial x_{0k}}\int x_j x_k(\mathbf{r}\times\mathbf{M})_i dV$$

(with a summation over repeated indices). Replacing $\mathbf{M}$ by the magnetization M_{12} given by (25) and using Eq. (27) obtained earlier, we find

$$\frac{\partial^2 E_i}{\partial x_{0j}\partial x_{0k}}\int x_j x_k(\mathbf{r}\times\mathbf{M}_{12})_i dV$$

$$=\alpha\left[\frac{7}{32}\left(\frac{\partial^2 E_z}{\partial x_0^2}+\frac{\partial^2 E_z}{\partial y_0^2}\right)+\frac{1}{16}\frac{\partial^2 E_z}{\partial z_0^2}\right.$$

$$\left.-\frac{1}{16}\left(\frac{\partial^2 E_z}{\partial x_0\partial z_0}+\frac{\partial^2 E_z}{\partial y_0\partial z_0}\right)\right],$$

$$\alpha=\Phi_1 a^4 y_1(y_1+1)(y_1^2-y_2^2).$$

Using the fact that outside the source div $\mathbf{E}=0$, we transform this expression to the form

$$-\frac{3}{32}\alpha\frac{\partial^2 E_z}{\partial z_0^2}.$$

As a result, we obtain

$$U=\frac{3}{256}\frac{\alpha}{c}(\mathbf{v}_s\nabla_0)\frac{\partial^2 E_z}{\partial z_0^2}. \quad (39)$$

Equating this to (31), we find

$$e\mathbf{A}=\frac{3}{256}\alpha\nabla_0\frac{\partial^2 E_z}{\partial z^2}. \quad (40)$$

Using the fact that the asymptotic behavior of $\mathbf{A}$ for the configuration of Fig. 3b under consideration is given by (14), we verify the fact that (40) is satisfied for $E_z=ez/r^3$. The difference between Eqs. (36) and (39) means only that the toroidal moments of higher multipole order interact with the same external electric field in a more complicated way than do the toroidal dipole moments. To find the

electric field E at finite distances, we return to (32), in which we have not yet expanded in the external field. Equating (31) and (32), we obtain

$$\frac{e}{c}(\mathbf{v}_s A)=\frac{1}{c^2}\int \varphi(\mathbf{v}_s\mathbf{j})dV'.$$

Or, equating the coefficients of $\mathbf{v}_s$,

$$e\mathbf{A}(\mathbf{r})=\frac{1}{c}\int \varphi(\mathbf{r}-\mathbf{r}')\mathbf{j}(\mathbf{r}')dV'. \tag{41}$$

We use the fact that the vector potential $\mathbf{A}$ satisfies the equation $\Delta\mathbf{A}=-(4\pi/c)\mathbf{j}$. Its solution has the form

$$\mathbf{A}=\frac{1}{c}\int \frac{1}{|\mathbf{r}-\mathbf{r}'|}\mathbf{j}(\mathbf{r}')dV'. \tag{42}$$

Comparing (41) and (42), we find that $\varphi=e|\mathbf{r}-\mathbf{r}'|^{-1}$, which corresponds to the electric potential of a point charge. Therefore, the additional term (31) describes the motion of the TS in a Coulomb field. From the Lagrangian

$$L=\frac{1}{2}m_e v_e^2+\frac{1}{2}m_s v_s^2+\frac{e}{c}(\mathbf{v}_e-\mathbf{v}_s)\mathbf{A}(\mathbf{r}_e-\mathbf{r}_s) \tag{43}$$

we find $\dot{\mathbf{v}}_e=0$ and $\dot{\mathbf{v}}_s=0$, which implies the absence of classical scattering. After fixing the location of the Coulomb center ($\mathbf{v}_e=\mathbf{r}_e=0$, $\mathbf{v}_s\equiv\mathbf{v}$, $\mathbf{r}_s\equiv\mathbf{r}$), we arrive at the Lagrangian $L=\frac{1}{2}mv^2-(e/c)\mathbf{v}\mathbf{A}$ describing the scattering of a TS by a Coulomb center. For an infinitesimally small TS this Lagrangian can be written as $L=\frac{1}{2}mv^2+(1/2c)(\mathbf{v}\nabla)(\mathbf{E}\mu_t)$, which corresponds to the scattering of a dipole toroidal moment by a Coulomb field. Classical scattering is again absent ($\dot{\mathbf{v}}=0$). The corresponding Schrödinger equations have the form

$$\begin{aligned}&-\frac{\hbar^2}{2m}\left(\nabla+\frac{ie}{\hbar c}\mathbf{A}\right)^2\Psi=\mathscr{E}\Psi,\\&-\frac{\hbar^2}{2m}\left(\nabla-\frac{i}{2\hbar c}\nabla(\mathbf{E}\mu_t)\right)^2\Psi=\mathscr{E}\Psi,\quad \mathbf{E}=er/r^3.\end{aligned} \tag{44}$$

They describe the quantum scattering of the TS and the toroidal dipole moment by a Coulomb field (Fig. 4). The question arises of how to verify the existence of the Aharonov–Casher effect for this case. We must find neutral particles with nonvanishing toroidal moment (and zero dipole moment). According to Ref. 26, Majorana neutrinos are just such particles. The second way is to study the scattering of ferromagnetic microparticles (which, according to Ref. 27, possess a toroidal dipole moment) by a Coulomb field. We note that the region containing the sources of the Coulomb field need not be multiply connected. This effect has been pointed out earlier in Ref. 28 for the case of the scattering of ordinary magnetic dipoles.

6. ELECTRIC VECTOR SOLENOIDS

The physical meaning of the magnetization

First let us explain the physical meaning of the magnetization (9). We write down the expression for the magnetization again:

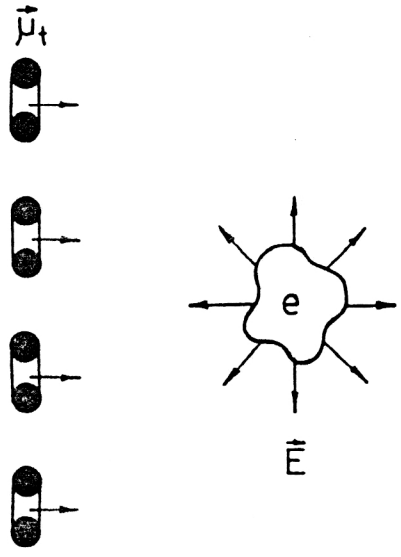

FIG. 4. Theory predicts that toroidal moments must undergo scattering by a Coulomb field.

$$\mathbf{M}=M\mathbf{n}_\varphi,\quad M=\frac{1}{4\pi}g\frac{\theta(R-\tilde{R})}{d+\tilde{R}\cos\psi}$$

$$=\frac{g}{4\pi}\theta(R-\sqrt{(\rho-d)^2+z^2})/\rho. \tag{45}$$

For an infinitesimally thin TS ($R\ll d$) and fixed magnetic flux Φ we have

$$M=\frac{1}{4\pi}\Phi\delta(\rho-d)\delta(z). \tag{46}$$

The vector potential satisfying the equation $\Delta\mathbf{A}=-4\pi\,\mathrm{curl}\,\mathbf{M}$ is expressed in terms of the magnetization as[29,30]

$$\mathbf{A}=\int\left(\mathbf{M}(\mathbf{r}')\times\frac{\mathbf{r}-\mathbf{r}'}{|\mathbf{r}-\mathbf{r}'|^3}\right)dV'. \tag{47}$$

Equations (46) and (47) imply that an infinitesimally thin TS can be realized as a chain of magnetic dipoles (Fig. 5).

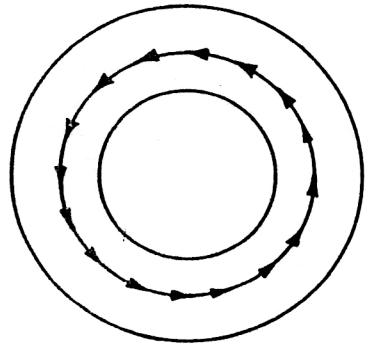

FIG. 5. Explicit realization of a magnetic (electric) toroidal solenoid by means of a circular chain of magnetic (electric) dipoles.

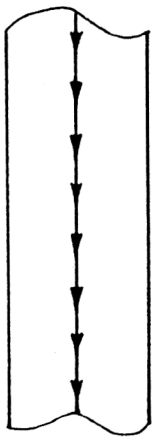

FIG. 6. Explicit realization of a magnetic (electric) cylindrical solenoid by means of a linear chain of magnetic (electric) dipoles.

In fact, the VP at the point r generated by a magnetic dipole located at $\mathbf{r}_0$ is (see, for example, Ref. 29)

$$\mathbf{A}=m\left(\mathbf{n}\times\frac{\mathbf{r}-\mathbf{r}_0}{|\mathbf{r}-\mathbf{r}_0|^3}\right). \tag{48}$$

Here $\mathbf{n}$ and m are the direction and strength of the magnetic dipole. Let us integrate this expression over a circle of radius d lying in the plane $z=0$. Then $\mathbf{n}=\mathbf{n}_\varphi$ is a unit vector tangent to this circle ($\mathbf{n}_\varphi=\mathbf{n}_y\cos\varphi-\mathbf{n}_x\sin\varphi$), $\mathbf{r}_0$ is its radius vector ($\mathbf{r}_0=d\mathbf{n}_\rho$, $\mathbf{n}_\rho=\mathbf{n}_x\cos\varphi+\mathbf{n}_y\sin\varphi$). Finally, we arrive at the vector potential of an infinitesimally thin TS found in Sec. 2 [see (7)]. Here $g=4m/R^2$ or $\Phi=4\pi m/d$. In addition, Eqs. (45) and (47) imply that a TS of finite thickness can be realized as a closed spin tube of radius R. In fact, let us integrate (48) over the volume of the torus. Here m represents the spin density inside the torus, which coincides with the magnetization M. In the end we arrive at the vector potential of a TS of finite thickness (6). A spin tube of this type (a ferromagnetic ring with magnetization independent of the external fields) was used in the experiments of Ref. 8 to verify the existence of the AB effect (see Sec. 9).

The cylindrical solenoid presents a simpler case. It can be realized in the form of a linear spin chain (Fig. 6). In fact, integrating (48) along the z axis, we obtain the VP of a cylindrical solenoid: $\mathbf{A}=\mathbf{n}_\varphi\Phi/2\pi\rho$, $\Phi=4\pi m$. A spin chain (magnetized filament) of this type was used in the early experiments to verify the AB effect (see, for example, the review of Ref. 31).

So far we have discussed only the magnetization and the vector potential. The question arises of what are the magnetic induction B and the field strength H. The general relation is $\mathbf{B}=\mathbf{H}+4\pi\mathbf{M}$. Since div $\mathbf{M}=0$ for the magnetizations (45) and (46), according to (16) and (17) $H=0$ everywhere and $\mathbf{B}=4\pi\mathbf{M}$, i.e., the magnetic induction B is nonzero only inside the solenoid.

Electric toroidal solenoids (ETSs)

Let us now replace the magnetic dipoles by electric ones. Then the electric polarization is $\mathbf{P}=\mathbf{n}_\varphi\Phi\delta(\rho-d)\delta(z)/4\pi$ for a chain of electric dipoles and $\mathbf{P}=g\theta(R-\sqrt{(\rho-d)^2+z^2})/4\pi\rho$ for a finite tube of dipoles. In the absence of free charges the Maxwell equations take the form

$$\text{div}\,\mathbf{D}=0, \tag{49}$$

$$\text{curl}\,\mathbf{E}=0, \tag{50}$$

$$\mathbf{D}=\mathbf{E}+4\pi\mathbf{P}. \tag{51}$$

Eliminating $\mathbf{E}$ from them, we find the equations for $\mathbf{D}$:

$$\text{div}\,\mathbf{D}=0, \tag{52}$$

$$\text{curl}\,\mathbf{D}=4\pi\,\text{curl}\,\mathbf{P}. \tag{53}$$

Equation (52) is satisfied automatically if we introduce the electric vector potential $\mathbf{A}_e$:

$$\mathbf{D}=\text{curl}\,\mathbf{A}_e,\quad \text{div}\,\mathbf{A}_e=0. \tag{54}$$

Substituting these expressions into (53), we obtain the equation for $\mathbf{A}_e$:

$$\Delta\mathbf{A}_e=-4\pi\,\text{curl}\,\mathbf{P}.$$

From this

$$\mathbf{A}_e=\int\frac{1}{|\mathbf{r}-\mathbf{r}'|}\,\text{curl}\,\mathbf{P}\,dV'=\int\left(\mathbf{P}\times\frac{\mathbf{r}-\mathbf{r}'}{|\mathbf{r}-\mathbf{r}'|^3}\right)dV', \tag{55}$$

which coincides with (47). Applying the curl operation to (55), we obtain $\mathbf{D}=\text{curl}\,\mathbf{A}_e=4\pi\mathbf{P}$. Then from (51) it follows that $\mathbf{E}=0$.

The ETS problem is obviously a purely electrostatic one. Such a problem is usually fully determined by the charge density $\rho(r)$. From it, it is easy to find the electric potential Φ, the field strength E, the induction D, and the polarization P. In this case the induction and polarization are constructed from the elementary electric dipole moments. The question arises of how to construct the multipole expansion for the electric VP and the induction. For a magnetic spin tube the problem is simplified by introducing a real surface current equivalent to the magnetization, and making a multipole expansion for the VP generated by this current. For an electric spin tube we can formally[32] introduce an equivalent current of magnetic momopoles $\mathbf{j}=c\,\text{curl}\,\mathbf{P}$ and make a multipole expansion for the corresponding VP. In the end the following alternatives arise:

1) A description of the electric field of the ETS in terms of the charge density is possible (although at this stage it is not known how). This would seem strange, because the magnetization $\mathbf{M}$, which has the same functional form as the polarization $\mathbf{P}$, is constructed from completely different building blocks—the elementary currents.

2) The description of the electric field of the ETS in terms of the charge density is incomplete.

Finally, we note that for the ETS the toroidal moments constructed using the polarization $\mathbf{P}$ are of independent interest. In fact, for the MTS there is the standard[33,34] expansion of the vector potentials in the complete set of electric, magnetic, and longitudinal multipoles. As shown in Ref. 24, the toroidal form factors and moments reduce

to the standard electric ones, so they specify a different representation of the MTS electromagnetic field. There is no such standard expansion for the ETS (owing to the impossibility of setting up a monopole current in the solenoid windings). On the other hand, the electric toroidal moments can be constructed just like the magnetic ones (see Sec. 3). By combining electric dipole tubes with different polarizations, we easily reproduce the entire set of electric toroidal moments of higher multipole order (Fig. 3). They interact differently with an external electric field.

The electric vector potential

In order to explain the physical meaning of the electric vector potential [see (54) and (55)], let us consider a case well known in physics: a polarized sphere of radius a. Let the polarization $\mathbf{P}$ be constant inside the sphere and directed along the z axis:

$$\mathbf{P}=P_0\mathbf{n}_z\theta(a-r). \tag{56}$$

In the absence of free charges the Maxwell equations become

$$\operatorname{div}\mathbf{D}=0, \tag{57}$$

$$\operatorname{curl}\mathbf{E}=0. \tag{58}$$

They are related as

$$\mathbf{D}=\mathbf{E}+4\pi\mathbf{P}. \tag{59}$$

We shall solve this system of equations in two ways. In the first case[35] we use (59) to eliminate $\mathbf{D}$ from (57) and obtain the following system of equations for $\mathbf{E}$:

$$\operatorname{div}\mathbf{E}=-4\pi\operatorname{div}\mathbf{P}, \tag{60}$$

$$\operatorname{curl}\mathbf{E}=0. \tag{61}$$

The second of these equations is automatically satisfied if we set

$$\mathbf{E}=-\operatorname{grad}\Phi. \tag{62}$$

Then from (60) we obtain the equations for

$$\Delta\Phi=4\pi\operatorname{div}\mathbf{P}, \quad \operatorname{div}\mathbf{P}=-P_0\cos\theta\cdot\delta(r-a).$$

From this

$$\Phi=-\int\frac{\operatorname{div}\mathbf{P}(\mathbf{r}')}{|\mathbf{r}-\mathbf{r}'|}dV'.$$

Or, explicitly,

$$\Phi=\frac{1}{3}4\pi P_0\frac{a^3}{r^2}\cos\theta \quad \text{for } r>a,$$

$$\Phi=\frac{4}{3}\pi P_0 r\cos\theta \quad \text{for } r<a. \tag{63}$$

From this we easily find

$$E_r=\frac{8}{3}\pi P_0\frac{a^3}{r^3}\cos\theta, \quad E_\theta=\frac{4}{3}\pi P_0\frac{a^3}{r^3}\sin\theta,$$

$\mathbf{D}=\mathbf{E}$ outside the sphere $(r>a)$,

$$E_r=-\frac{4}{3}\pi P_0\cos\theta, \quad E_\theta=\frac{4}{3}\pi P_0\sin\theta,$$

$$D_r=\frac{8}{3}\pi P_0\cos\theta, \quad D_\theta=-\frac{8}{3}\pi P_0\sin\theta \tag{64}$$

inside the sphere.

The second way of solving the system (57)–(59) is to eliminate $\mathbf{E}$ and write out the equation for $\mathbf{D}$. Applying the curl operation to (59), we rewrite it as

$$\operatorname{curl}\mathbf{D}=4\pi\operatorname{curl}\mathbf{P}. \tag{65}$$

For (57) to be satisfied automatically we take

$$\mathbf{D}=\operatorname{curl}\mathbf{A}_e, \quad \operatorname{div}\mathbf{A}_e=0. \tag{66}$$

Substituting this expression into (65), we obtain the following equation for the electric vector potential:

$$\Delta\mathbf{A}_e=-4\pi\operatorname{curl}\mathbf{P}, \quad \operatorname{curl}\mathbf{P}=P_0\sin\theta\cdot\delta(r-a)\mathbf{n}_\varphi.$$

From this

$$\mathbf{A}_e=\int\frac{1}{|\mathbf{r}-\mathbf{r}'|}\operatorname{curl}\mathbf{P}(\mathbf{r}')dV',$$

or, explicitly,

$$\mathbf{A}_e=\frac{4\pi}{3}P_0\frac{a^3}{r^2}\sin\theta\cdot\mathbf{n}_\varphi \quad \text{for } r>a \text{ and}$$

$$\mathbf{A}_e=\frac{4\pi}{3}P_0 r\sin\theta\cdot\mathbf{n}_\varphi \quad \text{for } r<a. \tag{67}$$

Substituting $\mathbf{A}_e$ into (66) and (59), we find the expressions (64) obtained earlier for $\mathbf{D}$ and $\mathbf{E}$. This means that for a sphere with constant polarization the fields $\mathbf{E}$ and $\mathbf{D}$ can be found in two different ways. They are, respectively, expressed in terms of the scalar and vector electric potentials. Since the space outside the sphere is simply connected, these potentials are uniquely given in terms of $\mathbf{E}$ and $\mathbf{D}$, so that in this case they have only an auxiliary nature.

As a second example, let us consider a prolate ellipsoid

$$\frac{x^2+y^2}{b^2}+\frac{z^2}{c^2}=1, \quad c>b, \tag{68}$$

with constant polarization directed along the z axis. We introduce spheroidal coordinates:

$$x=a\sinh\mu\sin\theta\cos\varphi, \quad y=a\sinh\mu\sin\theta\sin\varphi,$$

$$z=a\cosh\mu\cos\theta.$$

Let the value $\mu=\mu_0$ correspond to the ellipsoid (68). Then the polarization is

$$\mathbf{P}=P_0\mathbf{n}_z\theta(\mu_0-\mu). \tag{69}$$

The usual method[35] of solving the Maxwell equations (57)–(59) with the polarization (69) is to eliminate $\mathbf{D}$ and introduce the electric scalar potential Φ: $\mathbf{E}=-\operatorname{grad}\Phi$. As a result, for the scalar electric potential Φ, the field strength $\mathbf{E}$, and the induction $\mathbf{D}$ we find

$$\Phi=4\pi P_0 a\sinh^2\mu_0\cos\theta\cdot f_{10}(\mu,\mu_0),$$

$$E_\mu = -4\pi P_0 \sinh^2 \mu_0 \frac{\cos\theta}{(\cosh\mu - \cos\theta)^{1/2}} \frac{df_{10}(\mu,\mu_0)}{d\mu},$$

$$E_\theta = -4\pi P_0 \sinh^2 \mu_0 \frac{\sin\theta}{(\cosh\mu - \cos\theta)^{1/2}} f_{10}(\mu,\mu_0),$$

$$\mathbf{D} = \mathbf{E} + 4\pi\mathbf{P}. \tag{70}$$

Here

$$f_{lm}(\mu,\mu_0) = \begin{cases} Q_l^m(\cosh\mu) P_l^m(\cosh\mu_0), & \mu > \mu_0, \\ P_l^m(\cosh\mu) Q_l^m(\cosh\mu_0), & \mu < \mu_0, \end{cases}$$

where P_l^m and Q_l^m are the Legendre functions. The values $\mu < \mu_0$ and $\mu > \mu_0$ correspond to points, respectively, lying inside and outside the ellipsoid.

An alternative method of solving Eqs. (57)–(59) is to eliminate $\mathbf{E}$ and introduce the electric vector potential: $\mathbf{D} = \text{curl}\, \mathbf{A}_e$. For $\mathbf{A}_e$ we find

$$\mathbf{A}_e = A\mathbf{n}_\varphi, \quad A = -2\pi P_0 a \cosh\mu_0 \sinh\mu_0 \sin\theta \cdot f_{11}. \tag{71}$$

Using the expressions $\mathbf{D} = \text{curl}\, \mathbf{A}_e$ and $\mathbf{E} = \mathbf{D} - 4\pi\mathbf{P}$, we arrive at Eq. (70). Therefore, these electrostatic problems can be solved equally successfully by using either the electric scalar or the vector potential.

Now we let the large semiaxis c of the ellipsoid (68) increase to infinity, while the small semiaxis b remains unchanged. For this we must set $a = b/\sinh\mu_0$ and $\mu_0 \to 0$ in Eqs. (70) and (71). Then in this limit $\Phi \to 0$ and $\mathbf{E} \to 0$ both outside and inside the ellipsoid: $\mathbf{A}_e \to 2\pi P_0 b^2 \mathbf{n}_\varphi/\rho$, $\mathbf{D} \to 0$ outside the ellipsoid and $\mathbf{A}_e \to 2\pi P_0 \rho \mathbf{n}_\varphi$, $\mathbf{D} \to 4\pi\mathbf{P}$ inside it. In the end we obtain the electromagnetic field of an electric cylindrical solenoid of radius b. This situation (vanishing of the electric scalar potential Φ and of the field strength $\mathbf{E}$, and survival of the electric vector potential $\mathbf{A}_e$ and of the induction $\mathbf{D}$) is also valid for the electric toroidal solenoid.

The possibility of introducing electric vector potentials was suggested in Ref. 36. Some applications of these potentials are given in Ref. 37.

How can we tell if an electric field exists inside an electric solenoid?

In the same way as for a magnetic solenoid. Let us briefly list the ways.

1) The electromagnetic field penetrates the space outside a TS uniformly moving in a medium with $\varepsilon\mu \neq 1$ (Refs. 14 and 16).

2) The electromagnetic field penetrates the space outside an accelerated TS.[24]

3) The interaction of an external electric field with the electric dipoles forming an electric solenoid is given by

$$U = -\int \mathbf{E}_{\text{ext}} \mathbf{P} dV.$$

At large distances from the sources of an external electric field (or for small dimensions of the electric TS) this expression takes the form

$$U = -\frac{1}{2}\varepsilon_t \,\text{curl}\, \mathbf{E}_{\text{ext}} = \frac{1}{2c}\frac{\partial H_{\text{ext}}(\mathbf{r})}{\partial t}\varepsilon_t, \tag{72}$$

Here $\varepsilon_t = \int (\mathbf{r}\times\mathbf{P}) dV$ is the electric toroidal dipole moment.[32] For the electric polarization $\mathbf{P}$ defined above, it is directed along the symmetry axis of the ETS and is $\varepsilon_t = \frac{1}{2}\pi g d R^2$. Equation (72) means that at large distances the ETS interacts with a time-varying magnetic field.[32] This expression was used in Ref. 38 to explain the experimentally observed[39] rotation of nonmagnetic molecules in a uniform magnetic field slowly varying in time. This situation becomes much simpler for an electric cylindrical solenoid, which consists of a linear chain of electric dipoles (Fig. 6). Such a solenoid tries to orient itself along the external electric field. The question arises of the practical realization of an ETS. Materials called electrets exist in nature.[35] They are electrically neutral (i.e., uncharged), but possess a constant electric dipole moment. Of the various types of electrets, the ferroelectrics (the electric analogs of ferromagnets) are most suitable for our purposes. Such materials can be used in the construction of an uncharged toroidal ring carrying an electric toroidal dipole moment (just as a ferromagnet was used to construct a ring for experiments to verify the AB effect[8]).

By distributing electric and magnetic dipoles inside a torus, we arrive at a static electromagnetic TS for which the electric and magnetic inductions $\mathbf{D}$ and $\mathbf{B}$ are nonzero only inside the TS. There are nonzero electric and magnetic vector potentials outside the solenoid.

The physical meaning of the electric vector potential

In the examples considered above we either forced the electromagnetic field to penetrate the region outside the ETS by putting the ETS in motion or we allowed an external electric field to penetrate inside the ETS and interact with the electric dipoles forming it. Now we shall fix the position of the ETS. Outside it is a nonvanishing electric VP. As in the case of the magnetic solenoid, this VP cannot be eliminated by a gauge transformation, since $\oint A_e dl = \Phi$ for any closed contour passing through the hole in the solenoid. Is it possible to determine whether or not an electric VP is present outside an ETS without penetrating it? We do not know any obvious answer. In fact, the analog of the AB effect for this case would be the scattering of free magnetic charges on an electric VP outside the ETS. However, so far monopoles have not been discovered in nature. We conclude by rephrasing the question posed by Aharonov and Bohm in 1959: does the electric vector potential of an electric toroidal solenoid have any physical meaning?

Nonstatic electric solenoids (Ref. 20)

In Ref. 1 a pointlike electric solenoid was constructed by using the following (nonstatic) point charge and current densities:

$$\rho = D\exp(-i\omega t)\Delta\delta^3(\mathbf{r}), \quad \mathbf{j} = i\omega D \exp(-i\omega t)\nabla\delta^3(\mathbf{r}) \tag{73}$$

(D is a constant). The following electromagnetic potentials are the sources of (73):

$$\Phi=-\exp(-i\omega t)\,D\left[4\pi\delta^3(\mathbf{r})+k^2\frac{\exp(ikr)}{r}\right],$$
$$\mathbf{A}=ikD\exp(-i\omega t)\nabla\frac{\exp(ikr)}{r}. \tag{74}$$

Only the electric field is nonzero:

$$\mathbf{E}=-\nabla\Phi-\frac{1}{c}\frac{\partial\mathbf{A}}{\partial t}=4\pi D\exp(-i\omega t)\nabla\delta^3(\mathbf{r}). \tag{75}$$

These relations are easily generalized to the case of charge and current distributions of finite size. We choose ρ and $\mathbf{j}$ in the form

$$\rho=\exp(-i\omega t)\Delta f,\quad \mathbf{j}=i\omega\nabla f\exp(-i\omega t). \tag{76}$$

The following potentials and field strength correspond to these sources:

$$\Phi=-\exp(-i\omega t)\left[4\pi f+k^2\int G(\mathbf{r},\mathbf{r}')f\,dV'\right],$$
$$G=\frac{\exp(ik|\mathbf{r}-\mathbf{r}'|)}{|\mathbf{r}-\mathbf{r}'|},$$
$$\mathbf{A}=ik\exp(-i\omega t)\nabla\int G f\,dV', \tag{77}$$
$$\mathbf{E}=4\pi\exp(-i\omega t)\nabla f,\quad \mathbf{H}=0$$

[the factor $\exp(-i\omega t)$ will be omitted below when it is obvious].

Equations (73)–(75) are obviously obtained for $f=D\delta^3(\mathbf{r})$. It follows from (77) that if the function f is nonzero inside some region of space, E and H are nonzero in this region. On the other hand, the electromagnetic potentials Φ and $\mathbf{A}$ are nonzero also outside this region. Therefore, Eqs. (76) and (77) for this chcice of f realize a nonstatic electric solenoid. In particular, f can be chosen to be nonzero inside the torus $(\rho-d)^2+z^2=R^2$. One way of obtaining this is to take $f=D\theta(R-\sqrt{(\rho-d)^2+z^2})$, where D is a constant.

In Ref. 21 a nonstatic solenoid was realized in the form of a cylindrical capacitor. It was studied experimentally in the interesting work of Ref. 40. Instead of this we consider a spherical capacitor obtained by a special choice of the function f. We have

$$\rho=\frac{e}{4\pi r^2}[\delta(r-r_1)-\delta(r-r_2)],$$
$$\mathbf{j}=\frac{i\omega e}{4\pi r^3}\mathbf{r}\theta(r-r_1)\theta(r_2-r),\quad r_1<r_2. \tag{78}$$

This spherical capacitor consists of two oppositely charged spheres and a radial current flowing between them. Using the general expressions

$$\Phi=\int G\rho(\mathbf{r}')dV',\quad \mathbf{A}=\frac{1}{c}\int G\mathbf{j}(\mathbf{r}')dV',$$

we easily find the scalar and vector potentials (only the radial component of the vector potential is nonzero):

$$\Phi=ikeh_0^{(1)}(kr)[j_0(1)-j_0(2)],$$
$$A_r=-keh_1^{(1)}(kr)[j_0(1)-j_0(2)]\quad \text{for } r>r_2,$$
$$\Phi=ikej_0(kr)[h_0^{(1)}(1)-h_0^{(1)}(2)],$$
$$A_r=-kej_1(kr)[h_0^{(1)}(1)-h_0^{(1)}(2)]\quad \text{for } r<r_1, \tag{79}$$
$$\Phi=ike[h_0^{(1)}(kr)j_0(1)-j_0(kr)h_0^{(1)}(2)],$$
$$A_r=ek[j_1(kr)h_0^{(1)}(2)-h_1^{(1)}(kr)j_0(1)]$$
$$-\frac{ie}{kr^2}\quad \text{for } r_1<r<r_2,$$
$$j_l(x)=\sqrt{\frac{\pi}{2x}}J_{l+1/2}(x),\quad h_l^{(1)}(x)=\sqrt{\frac{\pi}{2x}}H_{l+1/2}^{(1)}(x),$$
$$j_l(1)\equiv j_l(kr_1),\ \text{and so on.}$$

The electromagnetic field is zero outside the spherical capacitor, i.e., for $r>r_2$ and $r<r_1$. Inside it only the radial component of $\mathbf{E}$ is nonzero:

$$E_r=e/r^2,\quad \mathbf{H}=0.$$

From Eqs. (74), (77), and (79) we find that electromagnetic-potential waves appear outside a nonstatic electric solenoid. This was noted earlier in Refs. 21 and 22. The question arises of the physical meaning of such waves and the possibility of detecting them experimentally. Let the region S in which E and H are nonzero be inaccessible to observation. Can an observer located outside S verify the existence of electromagnetic potential-waves? Since $E=H=0$ in such waves, they do not carry energy. Therefore, they can be detected only at the quantum level. This is the case because the Schrödinger equation

$$i\hbar\frac{\partial\Psi}{\partial t}=H\Psi,\quad H=-\frac{\hbar^2}{2m}\left(\nabla-\frac{ie}{\hbar c}\mathbf{A}\right)^2+e\Phi$$

involves the potentials Φ and $\mathbf{A}$ rather than the fields $\mathbf{E}$ and $\mathbf{H}$.

The transformation

$$\Psi\to\Psi'=\Psi\exp\left(-\frac{ie\chi}{\hbar c}\right),\quad \chi=ik\exp(-i\omega t)\int G f\,dV' \tag{80}$$

eliminates the electromagnetic potentials outside S. If χ is a single-valued function outside S, Eq. (80) is a unitary transformation between single-valued wave functions in the presence and absence of electromagnetic potentials outside S. In this case the presence of electromagnetic-potential waves outside S does not lead to observable consequences. On the other hand, if χ is discontinuous outside S (which, in turn, is determined by the choice of the source function f), the possibility in principle arises of observing electromagnetic-potential waves, for example, by observing a phase difference acquired by the wave function of a charged particle as the particle travels around a closed

contour. A necessary condition is that the region of space accessible to charged test particles be multiply connected. This is the case because multivalued wave functions are allowed only in non-simply connected spaces.

Let us consider a general nonstatic solenoid.[13] For this we write the expansion of the scalar and vector potentials in scalar and vector harmonics.[33,34] Outside the region S ($\rho,\mathbf{j}\neq 0$ only in S) we have

$$\Phi=4\pi ik\sum h_l Y_l^m q_l^m,\quad \mathbf{A}=\frac{4\pi ik}{c}\sum \mathbf{A}_l^m(\tau)a_l^m(\tau). \tag{81}$$

Here $\mathbf{A}_l^m(\tau)$ are elementary vector potentials, the vector solutions of the Helmholtz equation. In what follows τ will denote the electric (E), magnetic (M), and longitudinal (L) multipoles. The vector functions $\mathbf{A}$ are[1)]

$$\mathbf{A}_l^m(L)=\frac{1}{k}\nabla h_l Y_l^m,$$

$$\mathbf{A}_l^m(M)=h_l\mathbf{L}Y_l^m,\quad \mathbf{L}=-i(\mathbf{r}\times\nabla),$$

$$\mathbf{A}_l^m(E)=-\frac{1}{k}\frac{1}{\sqrt{l(l+1)}}\operatorname{curl}(\mathbf{r}\times\nabla)h_l Y_l^m. \tag{82}$$

The $\mathbf{A}_l^m(\tau)$ are eigenfunctions of the total angular momentum and its third projection, and are orthogonal on a sphere of arbitrary radius:

$$\int d\Omega\mathbf{A}_l^m(\tau)\mathbf{A}_{l'm'}^{m'*}(\tau')=\text{const}\cdot\delta_{ll'}\delta_{mm'}\delta_{\tau\tau'}.$$

The functions q_l^m and $a_l^m(\tau)$ depend on the charge and current distributions:

$$q_l^m=\int j_l Y_l^{m*}\rho dV,\quad a_l^m(\tau)=\int \mathbf{B}_l^{m*}(\tau)\mathbf{j}dV,$$

$$\rho=\frac{1}{i\omega}\operatorname{div}\mathbf{j},\quad q_l^m=\frac{i}{c}a_l^m(L).$$

The vector functions $\mathbf{B}_l^m(\tau)$ are obtained from the $\mathbf{A}_l^m(\tau)$ by replacing the spherical Hankel functions h_l by the Bessel functions j_l. It follows from (82) that

$$\operatorname{curl}\mathbf{A}_l^m(L)=0,\quad \operatorname{curl}\mathbf{A}_l^m(M)=ik\mathbf{A}_l^m(E),$$

$$\operatorname{curl}\mathbf{A}_l^m(E)=-ik\mathbf{A}_l^m(M).$$

Acting on $\mathbf{A}$ by the curl operator, we obtain

$$\mathbf{H}=\frac{1}{c}4\pi k^2\sum[\mathbf{A}_l^m(M)a_l^m(E)-\mathbf{A}_l^m(E)a_l^m(M)].$$

Since $\mathbf{A}_l^m(E)$ and $\mathbf{A}_l^m(M)$ are linearly independent and orthogonal, the condition $H=0$ reduces to the following:

$$a_l^m(E)=a_l^m(M)=0. \tag{83}$$

To understand the physical meaning of these conditions, we parametrize the current density in several different ways. The simplest parametrization is the following:[36]

$$\mathbf{j}=\operatorname{grad}\Psi+\operatorname{curl}\mathbf{M},\quad \operatorname{div}\mathbf{M}=0.$$

Substitution of this expression into (83) leads to the conditions

$$\int j_l(kr)Y_l^{m*}(\theta,\varphi)(\mathbf{rM})dV=\int j_l(kr)\mathbf{Y}_l^{m*}(\theta,\varphi)\times(\mathbf{r}\operatorname{curl}\mathbf{M})dV=0.$$

For the Helmholtz parametrization

$$\mathbf{j}=\operatorname{grad}f_1+\operatorname{curl}(\mathbf{r}f_2)+\operatorname{curl}\operatorname{curl}(\mathbf{r}f_3)$$

the analogous conditions become

$$\int j_l(kr)Y_l^{m*}(\theta,\varphi)\left[2r\frac{df_2}{dr}+6f_2+k^2r^2f_2+r\frac{\partial}{\partial r}\operatorname{div}(\mathbf{r}f_2)\right]dV=0,$$

$$\int j_l(kr)Y_l^{m*}(\theta,\varphi)\left[2\operatorname{div}(\mathbf{r}f_3)+k^2r^2f_3+r\frac{\partial}{\partial r}\operatorname{div}(\mathbf{r}f_3)\right]dV=0.$$

Finally, we consider the parametrization

$$\mathbf{j}=[\mathbf{r}f_{lm}^{(1)}+f_{lm}^{(2)}\nabla+f_{lm}^{(3)}(\mathbf{r}\times\nabla)]Y_l^m$$

(an arbitrary vector function can be represented in this form; see, for example, Ref. 41). The functions $f_{lm}^{(i)}$ depend only on the radial coordinate r. Substituting this expression into (83), we find the following conditions satisfied by the functions $f^{(1)}$ and $f^{(3)}$:

$$\int j_l(kr)f_{lm}^{(1)}(r)r^2dr=\int j_l(kr)f_{lm}^{(3)}(r)r^2dr.$$

Since the Bessel functions $j_l(kr)$ form a complete set, it would seem at first glance that these integrals vanish only when $f_{lm}^{(1)}=f_{lm}^{(3)}=0$. This would be valid if we required that the integrals vanish for all values of k. However, for fixed k (as in the case under consideration), it is always possible to find nontrivial (i.e., nonzero) functions $f_{lm}^{(i)}$ which make the integrals vanish.

Using the conditions (83), we rewrite the electromagnetic potentials as

$$\mathbf{A}=\frac{4\pi i}{ck}\nabla\sum h_l Y_l^m\int\nabla(j_l Y_l^{m*})\mathbf{j}dV,$$

$$\Phi=4\pi ik\sum h_l Y_l^m\int j_l Y_l^{m*}\rho dV,$$

$$\operatorname{div}\mathbf{A}+\frac{1}{c}\dot{\Phi}=0$$

(the dot stands for differentiation with respect to time).

It is easily verified that these potentials correspond to zero magnetic ($\mathbf{H}=\operatorname{curl}\mathbf{A}$) and electric ($\mathbf{E}=-\nabla\Phi-(1/c)\dot{A}$) fields. The electromagnetic potentials can be written as

$$\mathbf{A}=\operatorname{grad}\chi,\quad \Phi=-\frac{1}{c}\dot{\chi},$$

where

$$\chi=\frac{1}{c}4\pi i\exp(-i\omega t)\sum h_l Y_l^m a_l^m(L),$$

$$a_l^m(L)=\frac{1}{k}\int\nabla(j_l Y_l^{m*})\mathbf{j}dV=-icq_l^m.$$

The electromagnetic potentials are eliminated from the Schrödinger equation by a unitary transformation:

$$\Psi\to\Psi'=\Psi\exp(ie\chi/\hbar c).$$

Since the function χ is everywhere single-valued and continuous, at first glance it would appear that the electromagnetic potentials are eliminated by means of a single-valued, continuous transformation and therefore are unobservable in the region where $E=H=0$. In fact, this is not so. The point is that in obtaining the electromagnetic potentials it was implicitly assumed that the current and charge densities are concentrated in a simply connected region of space S including the origin, while the electromagnetic potentials were calculated outside S. In this case the electromagnetic potentials are really unobservable. The situation is changed if the region is multiply connected. As an illustration let us consider the case where charge and current densities are enclosed inside the torus T: $(\rho-d)^2+z^2=R^2$. Then the expressions given above are valid outside the sphere of radius $d+R$. Inside the sphere of radius $d-r$ we have

$$\mathbf{A}=\text{grad}\,\chi_{\text{in}},\quad\Phi=-\frac{1}{c}\dot{\chi}_{\text{in}},$$

$$\chi_{\text{in}}=\frac{1}{c}4\pi i\exp(-i\omega t)\sum j_l(kr)Y_l^m(\theta,\varphi)b_l^m(L),$$

$$b_l^m(L)=\frac{1}{k}\int\nabla(h_l Y_l^{m*})\mathbf{j}dV=-icq_l^m,$$

$$q_l^m=\int h_l Y_l^{m*}\rho dV.$$

Although both for $r>d+R$ and for $r<d-R$ the electromagnetic potentials can be represented as derivatives of χ, the functions χ themselves are, in general, different in these regions. This still does not mean that the electromagnetic potentials are observable outside the torus for any ρ and $\mathbf{j}$ inside the torus. They are observable for any ρ and $\mathbf{j}$ for which the complete function χ composed of χ_{in} and χ_{out}, respectively defined in the regions $r<d-R$ and $r>d+R$, actually are discontinuous. In this case the initial wave function Ψ satisfying the Schrödinger equation with nonzero potential is not equivalent to the transformed wave function $\Psi'=\Psi\exp(ie\chi/\hbar c)$ satisfying the Schrödinger equation without electromagnetic potentials. Discontinuity of the function χ leads to discontinuity of the wave function Ψ' (the initial function is assumed to be continuous). As an illustration, let us consider a static toroidal solenoid with poloidal current (3). In this case an explicit expression is known for the function χ in toroidal coordinates.[3,15] It changes discontinuously by the value of the magnetic flux at the intersection of the circle of radius $d-R$ lying in the equatorial plane $(z=0)$ of the solenoid. On the other hand, this function can also be expressed in spherical coordinates (see the Appendix). For an infinitesimally thin solenoid $(R\ll d)$ we have

$$\chi_{\text{out}}=-\frac{1}{4}\pi gR^2\sum(-1)^n\frac{(2n+1)!!}{2^n(n+1)!}\frac{d^{2n+1}}{r^{2n+2}}P_{2n+1}(\cos\theta)$$

for $r>d$ and

$$\chi_{\text{in}}=-\frac{1}{2}\pi gR^2\sum(-1)^n\frac{(2n-1)!!}{2^n n!}\frac{r^{2n+1}}{d^{2n+2}}P_{2n+1}(\cos\theta)$$

for $r<d$. We see that for a static toroidal solenoid with poloidal current (3) the functions χ_{in} and χ_{out}, although they are single-valued in the regions where they are defined, do not coincide on their boundary (i.e., at $r=d$).

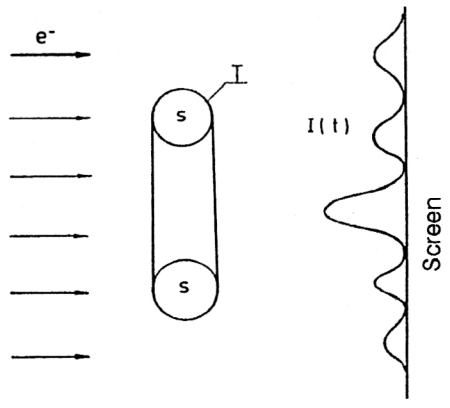

FIG. 7. Basic setup for detecting and recording electromagnetic-potential waves. The phase of a charged-particle beam is modulated by time-varying electromagnetic potentials, which at the screen leads to an interference pattern which also varies in time.

If we were able to find nonstatic distributions of ρ and $\mathbf{j}$ inside the torus for which $H=E=0$ outside the torus, this would provide a means of transferring information without loss of energy. A possible scheme for an experiment is shown in Fig. 7. Charged particles (for example, electrons) fall on a toroidal solenoid inside which the charge and current densities vary with time in some definite way. The electromagnetic field strengths are zero outside the solenoid, but the potentials are nonzero. This causes the phase of the electron wave function to also vary with time, this variation being different for electrons passing through the hole in the solenoid and outside it. A screen is placed sufficiently far from the solenoid, and the time-varying interference pattern is observed on it. This pattern can in principle be recorded. Energy is not stored inside the solenoid. It "flows into (out of)" the solenoid from its windings as the current in them is increased (decreased). The fundamental problem is the practical realization of ρ and $\mathbf{j}$ which generate zero field strengths outside the torus. The following configuration of periodic currents and charges would seem to satisfy these requirements:

$$\rho=ik(\text{div}\,\mathbf{N}+\Delta\Psi),\quad\mathbf{j}=c(\text{curl curl}\,\mathbf{N}-k^2\mathbf{N})-ck^2\nabla\Psi$$

[the factor $\exp(-i\omega t)$ has again been dropped]. Here Ψ and $\mathbf{N}$ are arbitrary scalar and vector functions specifying

the current and charge distributions and are nonzero only inside the torus. The electromagnetic potentials and field strengths are

$$\Phi=ik\chi-4\pi ik\Psi, \quad \mathbf{A}=\nabla\chi+4\pi\mathbf{N},$$

$$\mathbf{H}=4\pi \operatorname{curl}\mathbf{N}, \quad \mathbf{E}=4\pi ik(\mathbf{N}+\nabla\Psi),$$

$$\chi=\int G_k(\operatorname{div}\mathbf{N}-k^2\Psi)dV',$$

$$G_k=\exp(ik|\mathbf{r}-\mathbf{r}'|)/|\mathbf{r}-\mathbf{r}'|.$$

From this it follows that the fields are nonzero only inside the torus, while the potentials are nonzero both inside and outside it. Let Φ be the magnetic flux through the transverse cross section of the solenoid. Then $\Phi=\int \mathbf{H}d\mathbf{S}=\oint_C A_l dl$. Here C is a closed contour not intersecting the torus, but passing through the hole in it. Since by definition $\mathbf{N}=0$ outside the torus, χ is a multivalued (more precisely, discontinuous) function outside the torus. Furthermore, the vector function $\mathbf{N}$ must be singular inside the torus. This follows directly from the Stokes theorem, according to which

$$\int \mathbf{H}d\mathbf{S}=\Phi=4\pi \oint_C N_l dl.$$

From this it would follow that $\mathbf{N}\neq 0$ outside the torus, which contradicts the initial assumption about the vanishing of $\mathbf{N}$ outside the torus. However, the Stokes theorem is applicable only to vector functions which are not too singular. Therefore, $\mathbf{N}$ and, consequently, ρ and $\mathbf{j}$ are singular inside the torus. Applying the Stokes theorem to both sides of the Maxwell equation $\operatorname{curl}\mathbf{E}=-(1/c)\dot{\mathbf{H}}$, we obtain $\oint_C E_l dl=ik\Phi$. From this one might incorrectly conclude that $E\neq 0$ outside the torus. The singularity of $\mathbf{E}$ again makes it incorrect to use the Stokes theorem. In addition, it is not clear how to solve the Helmholtz equation with such singular sources. These complications show that this realization of the charge and current densities is not very successful, and the question of the possibility of generating and detecting electromagnetic-potential waves remains unanswered. Currents and charges satisfying the conditions (83) do not radiate, so $\mathbf{E}=\mathbf{H}=0$ outside the torus. On the other hand, it turns out to be possible to construct nonradiating currents and charges with $E, H\neq 0$ outside them.

This will occur if the radial component of the Poynting vector falls off faster than r^{-2} for $r\to\infty$. Let us consider the explicit expressions for the electromagnetic potentials:

$$\Phi=\int G_k(\mathbf{r},\mathbf{r}')\rho(\mathbf{r}')dV',$$

$$\mathbf{A}=\frac{1}{c}\int G_k(\mathbf{r},\mathbf{r}')\mathbf{j}(\mathbf{r}')dV'.$$

At large distances

$$\Phi_0=\frac{1}{r}\exp(ikr)\int \exp(-ik\mathbf{n}_r\mathbf{r}')\rho(\mathbf{r}')dV', \quad \mathbf{n}_r=\mathbf{r}/|\mathbf{r}|,$$

$$\mathbf{A}_0=\frac{1}{cr}\exp(ikr)\int \exp(-ik\mathbf{n}_r\mathbf{r}')\mathbf{j}(r')dV',$$

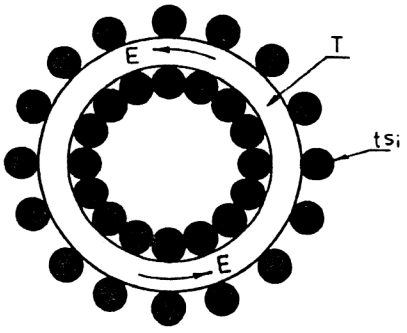

FIG. 8. Torus T on which toroidal solenoids ts_i with variable currents in their windings are wound. When the solenoids ts_i are infinitesimally thin and densely cover the torus, the electromagnetic field does not extend beyond T.

$$\mathbf{E}=-ik\mathbf{n}_r\Phi_0+ik\mathbf{A}_0, \quad \mathbf{H}=ik(\mathbf{n}_r\times\mathbf{A}_0).$$

Terms of order r^{-2} and higher order have been dropped, since they do not contribute to the energy flux. The radial component of the Poynting vector has the form

$$\begin{aligned}S_r&=\frac{1}{4\pi c}(\mathbf{n}_r(\mathbf{E}\times\mathbf{H}))\\&=\frac{k^2}{4\pi c}\mathbf{n}_r(\mathbf{A}_0\times(\mathbf{A}_0\times\mathbf{n}_r))\\&=\frac{k^2}{4\pi c}(|\mathbf{A}_0|^2-|\mathbf{n}_r\mathbf{A}_0|^2)\\&=\frac{k^2}{4\pi c}(|\mathbf{A}_0|^2-|\mathbf{A}_{0r}|^2)\\&=\frac{k^2}{4\pi c}(|A_{0\theta}|^2+|A_{0\varphi}|^2).\end{aligned}$$

From this we immediately obtain the well known condition that the energy flux in the surrounding space vanishes if $A_{0\theta}=A_{0\varphi}=0$.

The nonstatic electric solenoids just considered contained a current density and a charge density which were both nonzero. The author of Ref. 42 proposed a current configuration (with no charge density) which realizes a nonstatic toroidal solenoid. Toroidal solenoids ts_i are wound on the torus T (Fig. 8) with parameters d and R. In the limit where the solenoids ts_i are infinitesimally thin they completely cover the surface of the torus T. In Ref. 42 it was maintained that when there is a variable current in the windings of ts_i the electromagnetic field is concentrated inside the torus. We shall now show by direct calculation that this does not occur, at least for an infinitesimally thin torus ($R\ll d$). In this case the toroidal solenoids ts_i become infinitesimally small and reduce to toroidal moments:[12,18]

$$\mathbf{t}=\exp(-i\omega t)t\mathbf{n}_\varphi\delta(\rho-d)\delta(z).$$

This toroidal moment corresponds to the current

$$\mathbf{j}=c\operatorname{curl}\operatorname{curl}\mathbf{t}.$$

The solenoid configuration under consideration reduces to a chain of toroidal moments (see Fig. 5, where the arrows should now be understood as toroidal moments). It corresponds to the vector potential

$$\mathbf{A}=\frac{1}{c}\exp(-i\omega t)\int G\mathbf{j}dV'$$

$$=\exp(-i\omega t)\int G\,\mathrm{curl}\,\mathrm{curl}\,\mathbf{t}dV'.$$

Obviously, here the integration runs along the toroidal chain. Transferring the curl curl operation to the Green function, we obtain

$$\mathbf{A}=\exp(-i\omega t)(\mathrm{grad}\,\mathrm{div}-\Delta)\mathbf{I}$$

$$=\exp(-i\omega t)(\mathrm{grad}\,\mathrm{div}+k^2)\mathbf{I}+4\pi\exp(-i\omega t)\mathbf{t}(\mathbf{r}).$$

Here

$$\mathbf{I}=G\mathbf{t}(\mathbf{r}')dV'.$$

Substituting in the explicit expression for $\mathbf{t}$, we can write this integral as

$$\mathbf{I}=n_\varphi I,\quad I=\int\frac{\exp(ikZ)}{Z}\cos\varphi\,d\varphi,$$

$$Z=(r^2+d^2-2d\rho\cos\varphi)^{1/2},\quad r^2=\rho^2+z^2.$$

Since I is independent of φ, $\mathrm{div}\,\mathbf{I}=0$. Therefore,

$$A=\exp(-i\omega t)(4\pi\mathbf{t}+k^2\mathbf{n}_\varphi I).$$

Now let us calculate I:

$$I=\frac{i\pi^2}{(\tilde{r}\tilde{d})^{1/2}}\sum_{n=0}^{\infty}\left(2n+\frac{3}{2}\right)J_{2n+3/2}(k\tilde{d})$$

$$\times H^{(1)}_{2n+3/2}(k\tilde{r})\frac{1}{2^{4n}}\frac{2n+1}{n+1}\binom{2n}{2}^2.$$

Here

$$\tilde{r}=\frac{1}{2}(r_1+r_2),\quad \tilde{d}=\frac{1}{2}(d_1-d_2),$$

$$r_1=[(\rho+d)^2+z^2]^{1/2},\quad r_2=[(\rho-d)^2+z^2]^{1/2}.$$

Finally, outside the chain of toroidal moments we have

$$A_\varphi=\exp(-i\omega t)k^2I,\quad E_\varphi=k^3\exp(-i\omega t)I,$$

$$H_r=\frac{1}{r\sin\theta}\frac{\partial}{\partial\theta}(\sin\theta A_\varphi),\quad H_\theta=-\frac{1}{r}\frac{\partial}{\partial r}(rA_\varphi).$$

Since $I\neq 0$, the fields E and H are nonzero outside the toroidal chain. This means that the configuration shown in Fig. 8 is not a solenoid. However, we must be careful. We have proved that E and H are nonzero outside an infinitesimally thin torus. But the measurements described in Ref. 42 were carried out for a torus of finite thickness. It is known that for a periodic current flowing in the windings of a cylindrical solenoid, the vector potential $\mathbf{A}$ (and, consequently, the magnetic field H) vanishes outside the solenoid for certain values of kR ($k=\omega/c$ and R is the radius of the solenoid). We assume that the current configuration shown in Fig. 8 has the same property. Then the vanishing of the electromagnetic field outside the torus discovered in Ref. 42 can be attributed to the radius of the torus used in Ref. 42 being close to the critical value discussed above.

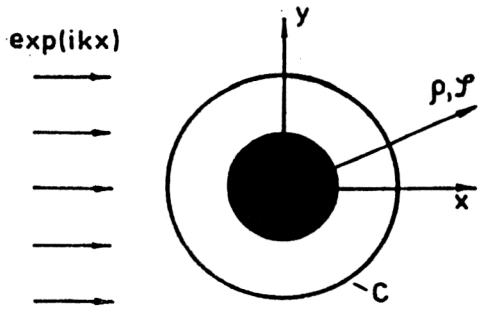

FIG. 9. An infinite cylindrical solenoid (shaded) surrounded by an impenetrable cylinder C of radius R. The arrows indicate the wave vector of the incident particles.

7. QUANTUM IMPENETRABILITY

The Aharonov–Bohm effect is often explained as the quantum consequence of the presence of fields inaccessible to particles. Inaccessibility of the fields is ensured by surrounding the region containing nonzero electromagnetic fields by an impenetrable screen S of suitable geometrical shape. We shall assume that the screen S is impenetrable to incident particles if the component of the quantum-mechanical probability current normal to S is zero.

Scattering on an impenetrable cylinder

As our first example let us consider the scattering of spinless charged particles on an impenetrable cylinder C of radius $\mathbf{R}$ (Fig. 9) containing a cylindrical solenoid. In the nonrelativistic case the probability current is

$$\mathbf{j}=\frac{\hbar}{2i\mu}(\bar{\Psi}\nabla\Psi-\Psi\nabla\bar{\Psi})-\frac{e}{\mu c}\mathbf{A}|\Psi|^2. \tag{84}$$

In this case the only nonzero component of the vector potential is $A_\varphi=\Psi/2\pi\rho$ (Φ is the magnetic flux inside the solenoid). Therefore, the condition that the cylinder C be impenetrable reduces to

$$\bar{\Psi}\frac{\partial\Psi}{\partial\rho}-\Psi\frac{\partial\bar{\Psi}}{\partial\rho}=0,\quad \rho=R. \tag{85}$$

This condition is usually satisfied by assuming that

$$\Psi=0\ \text{for}\ \rho=R. \tag{86}$$

The condition (85) can be satisfied in many ways. Two of the simplest, different from (86), are

$$\frac{\partial\Psi}{\partial\rho}=0\ \text{for}\ \rho=R, \tag{87}$$

$$\frac{\partial\Psi}{\partial\rho}=\alpha\Psi\ \text{for}\ \rho=R \tag{88}$$

(α is an arbitrary real constant). In any of these cases the wave function (WF) can be written as

$$\Psi=\Psi_{AB}+\Psi_s. \tag{89}$$

Here Ψ_{AB} is the wave function corresponding to scattering on an infinitesimally thin solenoid:

$$\Psi_{AB}=\sum \exp[i\pi(|m|-|m-\gamma|)+im\varphi]J_{|m-\gamma|}(k\rho) \tag{90}$$

($k^2=2\mu E/\hbar^2$ and $\gamma=e\Phi/hc$). Here and below, when there is no index, there is understood to be a summation from $-\infty$ to $+\infty$. An asymptotic expression for Ψ_{AB} valid for all scattering angles was first obtained in Ref. 43:

$$\Psi_{AB}\sim\exp[ikx+i\gamma(\varphi-\pi)]+i\sin\pi\gamma\exp(i\varphi/2)\frac{\exp(ik\rho)}{(1-2\pi ik\rho\sin^2\varphi/2)^{1/2}}.$$

For scattering angles φ which are not too small [$k\rho\sin^2(\varphi/2)\gg 1$] we arrive at the expression obtained in Ref. 44:

$$\Psi_{AB}\sim\exp[ikx+i\gamma(\varphi-\pi)]+\frac{1}{\sqrt{\rho}}\exp(ik\rho)\cdot f_{AB}(\varphi),$$

$$f_{AB}=-\frac{1}{\sqrt{2\pi ik}}\frac{\exp(i\varphi/2)}{\sin\varphi/2}\sin\pi\gamma, \tag{91}$$

$$\sigma_{AB}=\frac{1}{2\pi k}\frac{\sin^2\pi\gamma}{\sin^2\varphi/2}.$$

(For definiteness and without loss of generality we assume that $0\leqslant\gamma\leqslant\frac{1}{2}$.) The second term in (89) takes into account the finiteness of the solenoid dimensions and its screening:

$$\Psi_s=\sum \exp[i\pi(|m|-\tfrac{1}{2}|m-\gamma|)+im\varphi]H^{(1)}_{|m-\gamma|}\times(k\rho)C_m.$$

The coefficients C_m are determined by the boundary condition at $\rho=R$:

$$C_m=-\frac{J_{|m-\gamma|}}{H^{(1)}_{|m-\gamma|}} \text{ with the condition (86),}$$

$$C_m=-\frac{\dot{J}_{|m-\gamma|}}{\dot{H}^{(1)}_{|m-\gamma|}} \text{ with the condition (87),}$$

$$C_m=-\frac{k\dot{J}_{|m-\gamma|}-\alpha J_{|m-\gamma|}}{k\dot{H}^{(1)}_{|m-\gamma|}-\alpha H^{(1)}_{|m-\gamma|}} \text{ with the condition (88).}$$

Here and below, we shall omit the argument of the Bessel and Hankel functions if it is kR. The dot denotes differentiation of these functions with respect to their argument. For $\rho\to\infty$ we obtain

$$\Psi_s\sim\frac{1}{\sqrt{\rho}}\exp(ik\rho)\cdot f_s(\varphi),$$

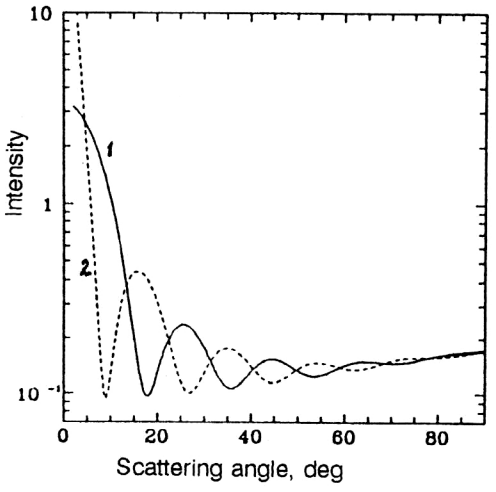

FIG. 10. Nonrelativistic intensity of scattering on a cylinder in the case where the boundary condition (86) is imposed. The intensity is defined as the ratio of the scattering cross section (93) and the geometrical cross section ($=2R$). The intensity thus defined is dimensionless. Curves *1* and *2* correspond to the absence of magnetic flux inside the solenoid and the value $\gamma=1/2$, respectively. The parameter is $kR=10$.

$$f_s(\varphi)=\left(\frac{2}{\pi ik}\right)^{1/2}\sum C_m\cdot\exp[i\pi(|m|-|m-\gamma|)+im\varphi]. \tag{92}$$

The total amplitude and cross section have the form

$$f=f_{AB}+f_s,\quad \sigma=|f|^2. \tag{93}$$

Let us find the dependence of the scattering cross section on the specific realization of the impenetrability condition (85). Typical cross sections are shown in Figs. 10–12. There is a strong dependence on the choice of impenetrability conditions.

The conditions (86)–(88), which are trivial from the mathematical point of view (they correspond to Dirichlet–Neumann boundary-value problems and the mixed boundary-value problem), correspond to different types of

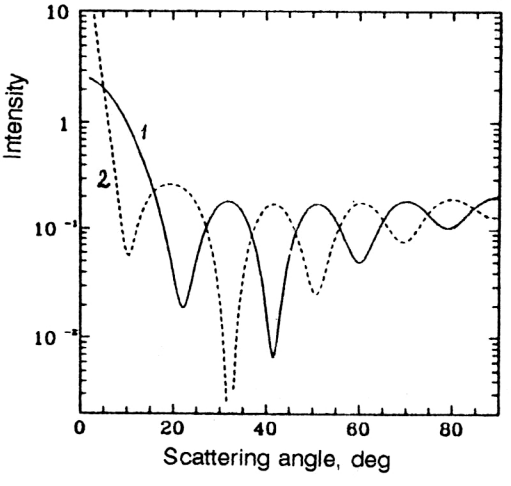

FIG. 11. The same as in Fig. 10 for the boundary condition (87).

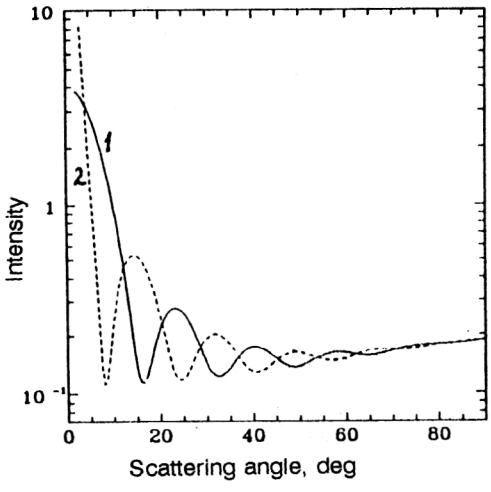

FIG. 12. The same as in Fig. 10 for the boundary condition (88).

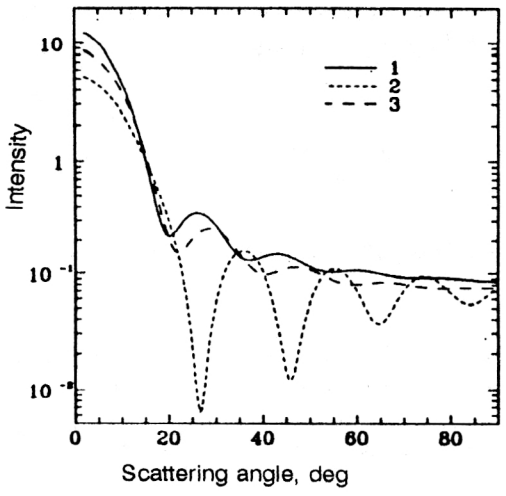

FIG. 13. Nonrelativistic cross sections for scattering on an impenetrable sphere S of radius R. The intensity is defined as the ratio of the scattering cross section (98) to the geometrical cross section ($=\pi R^2$). Curves *1*, *2*, and *3* refer to the impenetrability conditions (95), (96), and (97) (for $\alpha=1$), respectively. The parameter is $kR=10$.

physical impenetrability. It is important to find out what type of physical impenetrability is realized in experiments to verify the existence of the AB effect. At this stage we are not interested in the behavior of the WF inside the cylinder C. For example, in order to make the WF inside C vanish with the boundary condition (86), we need to generate infinite three-dimensional repulsion inside the cylinder C and a δ-function repulsive potential on the surface of the cylinder C. The latter is necessary to obtain the correct value of the jump of the normal derivative of Ψ in crossing the boundary of C [in fact, $\partial\Psi/\partial\rho$ is zero inside the cylinder and nonzero on the outside of the cylinder for the boundary condition (86)]. Finally, we make note of Refs. 45 and 46, where the effect of changing the boundary conditions on the scattering process was studied (without reference to the AB effect).

Scattering on an impenetrable sphere

Let us now consider an impenetrable sphere S of radius R. In the absence of a magnetic field the condition that the normal component of the probability current vanish on the surface of S becomes

$$\bar{\Psi}_0\frac{\partial\Psi_0}{\partial r}-\Psi_0\frac{\partial\bar{\Psi}_0}{\partial r}=0 \text{ for } r=R. \tag{94}$$

The simplest realizations of (94) are the following:

$$\Psi_0=0 \text{ for } r=R, \tag{95}$$

$$\frac{\partial\Psi_0}{\partial r}=0 \text{ for } r=R, \tag{96}$$

$$\frac{\partial\Psi_0}{\partial r}=\alpha\Psi \text{ for } r=R \tag{97}$$

(α is an arbitrary real constant). In any of these cases the wave function, amplitude, and scattering cross section have the form

$$\Psi_0=\exp(ikz)+\sqrt{\frac{\pi}{2kr}}\sum i^l(2l+1)C_l$$

$$\times H^{(1)}_{l+1/2}(kr)P_l(\cos\theta),$$

$$f(\theta)=\frac{1}{ik}\sum(2l+1)C_lP_l(\cos\theta), \quad \sigma=|f(\theta)|^2. \tag{98}$$

The coefficients C_l are

$$C_l=-J_{l+1/2}/H^{(1)}_{l+1/2} \text{ with the condition (95)},$$

$$C_l=-\frac{(l+1)J_{l+1/2}-kRJ_{l-1/2}}{(l+1)H^{(1)}_{l+1/2}-kRH^{(1)}_{l-1/2}} \text{ with the condition (96)},$$

$$C_l=-\frac{(l+1+\alpha R)J_{l+1/2}-kRJ_{l-1/2}}{(l+1+\alpha R)H^{(1)}_{l+1/2}-kRH^{(1)}_{l-1/2}}$$

with the condition (97).

Typical cross sections $\sigma=|f|^2$ are shown in Fig. 13. As in the case of the impenetrable cylinder, we find that the cross sections depend strongly on the specific realization of the impenetrability conditions.

Relativistic impenetrability conditions

A relativistic impenetrable cylinder

Let us consider the relativistic AB effect. There are several studies of it. In the first[47] it was proved that for an infinitesimally thin cylindrical solenoid the relativistic AB cross section differs from the nonrelativistic one by the factor $(1-\beta^2)^{1/2}$, $\beta=v/c$. The authors of Ref. 48, in which scattering on an impenetrable cylindrical solenoid of finite radius R was studied, state that it is impossible to make all the components of the Dirac WF vanish on the solenoid boundary. The relativistic scattering of charged particles on a cylindrical potential barrier of finite height (with a solenoid inside) was studied in Ref. 49. There it was shown that it is impossible to make all the components of the Dirac wave function and their derivatives match at the

barrier boundary. In view of the fact that in typical experiments to verify the existence of the AB effect[8] the electron energy is of order 100 keV, which corresponds to $\beta \approx 0.6$, it becomes necessary to study this question in more detail.

Outside the cylinder C the WF satisfies the Dirac equation

$$H\Psi = \mathscr{E}\Psi, \quad H = -i\hbar c\alpha\left(\nabla - \frac{ie}{\hbar c}\mathbf{A}\right) + \mu c^2\beta,$$

$$\alpha = \begin{pmatrix} 0 & \sigma \\ \sigma & 0 \end{pmatrix}, \quad \beta = \begin{pmatrix} 1 & 0 \\ 0 & -1 \end{pmatrix}.$$

We expand Ψ in states with definite angular-momentum projection:

$$J_3 = \frac{\hbar}{i}\frac{\partial}{\partial\varphi} + \frac{1}{2}\hbar\Sigma_3, \quad \Sigma = \begin{pmatrix} \sigma & 0 \\ 0 & \sigma \end{pmatrix},$$

$$\Psi = \sum \Psi_m, \quad J_3\Psi_m = \hbar\left(m + \frac{1}{2}\right)\Psi_m, \quad \Psi_m = \begin{bmatrix} \Psi_{1m} \\ \Psi_{2m} \\ \Psi_{3m} \\ \Psi_{4m} \end{bmatrix},$$

$$\Psi_{1m} = u_{1m}\exp(im\varphi), \quad \Psi_{2m} = u_{2m}\exp[i(m+1)\varphi],$$

$$\Psi_{3m} = u_{3m}\exp(im\varphi), \quad \Psi_{4m} = u_{4m}\exp[i(m+1)\varphi]. \tag{99}$$

The functions u_{1m} and u_{2m} are linear combinations of Bessel functions:

$$u_{1m} = A_m[J_{m-\gamma}(k\rho) + B_m H^{(1)}_{m-\gamma}(k\rho)],$$

$$u_{2m} = C_m[J_{m+1-\gamma}(k\rho) + D_m H^{(1)}_{m+1-\gamma}(k\rho)],$$

$$k^2 = (\mathscr{E}^2 - \mu^2c^4)^{1/2}/\hbar c.$$

The small components of the Dirac WF are expressed in terms of u_{1m} and u_{2m} as follows:

$$u_{3m} = -\frac{i\eta}{k}\left(\frac{d}{d\rho} + \frac{m+1-\gamma}{\rho}\right)u_{2m}$$

$$= -i\eta C_m[J_{m-\gamma}(k\rho) + D_m H^{(1)}_{m-\gamma}(k\rho)],$$

$$u_{4m} = -\frac{i\eta}{k}\left(\frac{d}{d\rho} - \frac{m-\gamma}{\rho}\right)u_{1m}$$

$$= -i\eta A_m[J_{m+1-\gamma}(k\rho) + B_m H^{(1)}_{m+1-\gamma}(k\rho)],$$

$$\eta = \left(\frac{\mathscr{E} - \mu c^2}{\mathscr{E} + \mu c^2}\right)^{1/2}. \tag{100}$$

The coefficients A_m and C_m are fixed by the condition that the correct expression be obtained for the incident wave, which we choose to be propagating in the $+x$ direction with positive helicity and energy:

$$\sum\left(\mathbf{p} - \frac{e}{c}\mathbf{A}\right)\Psi_{\text{inc}} = p\Psi_{\text{inc}}, \quad p = \hbar k,$$

$$\Psi_{\text{inc}} = \exp[ikx + i\gamma(\varphi - \pi)]u_\eta, \quad u_\eta = \begin{bmatrix} 1 \\ 1 \\ \eta \\ \eta \end{bmatrix}.$$

Finally, we obtain

$$A_m = \exp\left(i\pi\frac{m+\gamma}{2}\right), \quad B_m = \exp\left(i\pi\frac{m+1+\gamma}{2}\right).$$

Substituting these coefficients into (99), we bring Ψ to the form

$$\Psi = (\Psi_{\text{AB}} + \Psi_s^0)u_\eta + \Psi_s. \tag{101}$$

Here Ψ_{AB} is defined by (90):

$$\Psi_s^0 = i\sin\pi\gamma\sum_{m=0}^{-\infty}\exp\left(i\pi\frac{\gamma-m}{2}\right)$$

$$\times H^{(1)}_{\gamma-m}(k\rho)\exp(im\varphi),$$

$$\Psi_s = \begin{bmatrix} \Psi_1^{(s)} \\ \Psi_2^{(s)} \\ \Psi_3^{(s)} \\ \Psi_4^{(s)} \end{bmatrix},$$

$$\Psi_1^{(s)} = \sum\exp\left(i\pi\frac{m+\gamma}{2}\right)B_m H^{(1)}_{m-\gamma}(k\rho)\exp(im\varphi),$$

$$\Psi_2^{(s)} = \sum\exp\left(i\pi\frac{m+\gamma}{2}\right)D_{m-1}H^{(1)}_{m-\gamma}(k\rho)\exp(im\varphi),$$

$$\Psi_3^{(s)} = \eta\sum\exp\left(i\pi\frac{m+\gamma}{2}\right)D_m H^{(1)}_{m-\gamma}(k\rho)\exp(im\varphi),$$

$$\Psi_4^{(s)} = \eta\sum\exp\left(i\pi\frac{m+\gamma}{2}\right)B_{m-1}H^{(1)}_{m-\gamma}(k\rho)\exp(im\varphi).$$

Here and below, when the limits of summation are not indicated, there is understood to be a summation over all m from $-\infty$ to $+\infty$. For $\rho \to \infty$ we have the following asymptotic behavior of Ψ:

$$\Psi \sim \exp[ikx + i\gamma(\varphi - \pi)]u_\eta + \frac{\exp(ik\rho)}{\sqrt{\rho}}f(\varphi), \tag{102}$$

where $f(\varphi)$ is the spinor scattering amplitude, given by

$$f = \begin{bmatrix} f_1 \\ f_2 \\ \eta f_2\exp(-i\varphi) \\ \eta f_1\exp(i\varphi) \end{bmatrix},$$

$$f_1 = \sqrt{\frac{2}{\pi ik}}\exp(i\pi\gamma)\sum B_m\exp(im\varphi),$$

$$f_2 = \sqrt{\frac{2}{\pi ik}}\exp(i\pi\gamma)\sum D_{m-1}\exp(im\varphi). \tag{103}$$

Finally, the scattering cross section is

$$\sigma = \frac{1}{2}(|f_1|^2 + |f_2|^2). \tag{104}$$

The coefficients B_m and D_m are determined by the boundary condition at $\rho=R$. For example, we require that at $\rho=R$ the large components u_{1m} and u_{2m} of the Dirac WF vanish. This gives

$$D_{m-1}=B_m=-J_{m-\gamma}/H^{(1)}_{m-\gamma}. \tag{105}$$

Substituting these values into (100), for $\rho=R$ we obtain

$$|u_{3m}|^2=\frac{4\eta^2}{\pi^2k^2R^2}\,(J^2_{m-\gamma}+Y^2_{m-\gamma})^{-1},$$

$$|u_{4m}|^2=\frac{4\eta^2}{\pi^2k^2R^2}\,(J^2_{m+1-\gamma}+Y^2_{m+1-\gamma})^{-1}.$$

In typical experiments on the AB effect[8] $kR\sim10^6$. We replace the Bessel and Neumann functions by their asymptotic expressions. Then

$$|u_{3m}|^2\approx|u_{4m}|^2\approx\frac{2\eta^2}{\pi kR}\ll1.$$

Therefore, although the small components of the WF actually are nonzero for $\rho=R$ (Ref. 48), in real experiments they can be neglected. Substituting (105) into (103) and (104), we have

$$f_1=f_2=f,\quad \sigma=|f|^2,$$

$$f=-\sqrt{\frac{2}{\pi ik}}\exp(i\pi\gamma)\sum\frac{J_{m-\gamma}}{H^{(1)}_{m-\gamma}}\exp(im\varphi). \tag{106}$$

This sum contains Bessel functions with both positive and negative index. We get rid of the latter by using (for $m-\gamma<0$) the identities

$$J_{-\nu}(x)=i\sin\pi\nu H^{(1)}_\nu(x)+J_\nu\exp(-i\pi\nu),$$

$$H^{(1,2)}_{-\nu}=\exp(i\pi\nu)H^{(1,2)}_\nu.$$

Then

$$f=-\sqrt{\frac{2}{\pi ik}}\left\{\frac{1}{2}\sin\pi\gamma\frac{\exp(i\varphi/2)}{\sin\varphi/2}+\sum\exp[i\pi(|m|-|m-\gamma|)+im\varphi]J_{|m-\gamma|}/H^{(1)}_{|m-\gamma|}\right\}, \tag{107}$$

which has the same form as the nonrelativistic scattering amplitude (93) corresponding to the boundary condition (86). More precisely, the nonrelativistic cross section (93) becomes the relativistic one (86) when the nonrelativistic momentum $k_{\text{nonrel}}=\sqrt{2\mu E}/\hbar$ is replaced by the relativistic momentum $k_{\text{rel}}=k_{\text{nonrel}}(1-\beta^2)^{-1/2}$. A typical cross section is shown in Fig. 14. For an infinitesimally thin solenoid ($kR\ll1$) the sum in (107) can be neglected. Then

$$\int^{\text{rel}}_{\text{AB}}=-\frac{1}{\sqrt{2\pi ik}}\sin\pi\gamma\frac{\exp(i\varphi/2)}{\sin\varphi/2}.$$

This expression differs from the nonrelativtic one (91) by the symbol k. Therefore, for the infinitesimally thin solenoid $\sigma^{\text{rel}}_{\text{AB}}=\sigma^{\text{nonrel}}_{\text{AB}}\sqrt{1-\beta^2}$, which is confirmed by the results of Ref. 47. The fact that the nonrelativistic expressions transform into the relativistic ones is verified *a posteriori* by

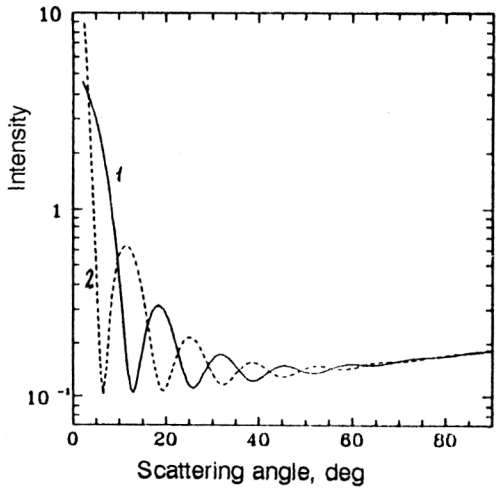

FIG. 14. Relativistic cross section for electron scattering on an impenetrable cylinder C of radius R for $\gamma=0$ (curve *1*) and $\gamma=1/2$ (curve *2*). The impenetrability condition corresponds to the vanishing of the large components of the Dirac wave function. The electron kinetic energy is 150 keV. The parameter is $kR=10$.

the fact that the individual components of the Dirac WF satisfy a second-order equation of the same form as the Schrödinger equation, differing only in that it involves the relativistic instead of the nonrelativistic momentum. The fact that the small components of the Dirac WF do not vanish for $\rho=R$ (although it is of an academic nature, owing to the numerical smallness of u_{3m} and u_{4m} for $\rho=R$) is related to the nonrelatistic nature of the boundary condition. The impenetrability condition can be satisfied exactly by imposing a relativistic boundary condition, namely, by requiring the vanishing (as in the theory of quark bags; see, for example, Ref. 50) of the component of the probability current normal to the surface of the impenetrable cylinder C: $\mathbf{j}\cdot\mathbf{n}=0$. Here n is the normal to the surface of C, and $\mathbf{j}$ is the Dirac probability current: $\mathbf{j}=ec\Psi^+\boldsymbol{\alpha}\Psi$. As a result, we obtain

$$\Psi^+\boldsymbol{\alpha}\mathbf{n}\Psi=0\ \text{ for }\ \rho=R. \tag{108}$$

This expression is inconvenient for practical use. The following relativistic condition, which is linear in the components of the Dirac WF, is also widely used in bag theory:[50]

$$i\boldsymbol{\alpha}\mathbf{n}\Psi=\beta\Psi\ \text{ for }\ \rho=R. \tag{109}$$

The proof that (108) follows from (109) takes only two lines. We take the Hermitian conjugate of (109):

$$i\Psi^+\boldsymbol{\alpha}\mathbf{n}=-\Psi^+\beta. \tag{110}$$

Multiplying (109) on the left by Ψ^+ and (110) on the right by Ψ, we obtain

$$i\Psi^+\boldsymbol{\alpha}\mathbf{n}\Psi=\Psi^+\beta\Psi=-\Psi^+\beta\Psi=0.$$

Therefore, $\Psi^+\boldsymbol{\alpha}\cdot\mathbf{n}\Psi=0$ if the condition (109) is satisfied. The converse does not, in general, hold, i.e., Eq. (108) is more general than (109). Henceforth we shall restrict ourselves to (109). We apply it to the Dirac WF (99). This gives

$$u_{4m}=-iu_{1m},\quad u_{3m}=-iu_{2m}\ \text{for}\ \rho=R. \tag{111}$$

From this we find the coefficients B_m and D_m:

$$B_m=-\frac{J_{m-\gamma}+\eta J_{m+1-\gamma}}{H^{(1)}_{m-\gamma}+\eta H^{(1)}_{m+1-\gamma}},$$

$$D_m=-\frac{J_{m+1-\gamma}-\eta J_{m-\gamma}}{H^{(1)}_{m+1-\gamma}-\eta H^{(1)}_{m-\gamma}}.$$

We substitute these expressions into (103):

$$f_1=-\sqrt{\frac{2}{\pi ik}}\left\{\frac{1}{2}\sin\pi\gamma\frac{\exp(i\varphi/2)}{\sin\varphi/2}\right.$$
$$+\exp(i\pi\gamma)\sum_{m=1}^{\infty}\frac{J_{m-\gamma}+\eta J_{m+1-\gamma}}{H^{(1)}_{m-\gamma}+\eta H^{(1)}_{m+1-\gamma}}\exp(im\varphi)$$
$$\left.+\exp(-i\pi\gamma)\sum_{m=0}^{-\infty}\frac{J_{\gamma-m}-\eta J_{\gamma-m-1}}{H^{(1)}_{\gamma-m}-\eta H^{(1)}_{\gamma-m-1}}\exp(im\varphi)\right\},$$

$$f_2=-\sqrt{\frac{2}{\pi ik}}\left\{\frac{1}{2}\sin\pi\gamma\frac{\exp(i\varphi/2)}{\sin\varphi/2}+\exp(i\pi\gamma)\right.$$
$$\times\sum_{m=0}^{\infty}\frac{J_{m+1-\gamma}-\eta J_{m-\gamma}}{H^{(1)}_{m+1-\gamma}-\eta H^{(1)}_{m-\gamma}}\exp[i(m+1)\varphi]$$
$$+\exp(-i\pi\gamma)\sum_{m=-1}^{-\infty}\frac{J_{\gamma-m-1}+\eta J_{\gamma-m}}{H^{(1)}_{\gamma-m-1}+\eta H^{(1)}_{\gamma-m}}$$
$$\left.\times\exp[i(m+1)\varphi]\right\}. \tag{112}$$

Let us consider limiting cases of these expressions.

a) The magnetic flux inside the solenoid is equal to zero ($\gamma=0$):

$$f_1=-\sqrt{\frac{2}{\pi ik}}\sum\frac{J_m+\eta J_{m+1}}{H^{(1)}_m+\eta H^{(1)}_{m+1}}\exp(im\varphi),$$

$$f_2=-\sqrt{\frac{2}{\pi ik}}\sum\frac{J_{m+1}-\eta J_m}{H^{(1)}_{m+1}-\eta H^{(1)}_m}\exp[i(m+1)\varphi)]. \tag{113}$$

b) The screening cylinder is infinitesimally thin ($kR\ll 1$). For $0<\gamma<1/2$:

$$f_1=-\frac{1}{\sqrt{2\pi ik}}\sin\pi\gamma\frac{\exp(-i\varphi/2)}{\sin\varphi/2},$$

$$f_2=-\frac{1}{\sqrt{2\pi ik}}\sin\pi\gamma\frac{\exp(i\varphi/2)}{\sin\varphi/2}.$$

For $\frac{1}{2}<\gamma<1$:

$$f_1=-\frac{\sin\pi\gamma}{\sqrt{2\pi ik}}\frac{\exp(i\varphi/2)}{\sin\varphi/2},$$

$$f_2=-\frac{\sin\pi\gamma}{\sqrt{2\pi ik}}\frac{\exp(3i\varphi/2)}{\sin\varphi/2}. \tag{114}$$

In this case the scattering cross section is

$$\sigma^{\text{rel}}_{AB}=\frac{1}{2\pi k}\frac{\sin^2\pi\gamma}{\sin^2\varphi/2}. \tag{115}$$

This has the same form as the nonrelativistic expression (91), differing from it only in that (115) involves the relativistic momentum. Therefore, as above,

$$\sigma^{\text{rel}}_{AB}=\sigma^{\text{nonrel}}_{AB}\sqrt{1-\beta^2}.$$

It is surprising that the initial expressions (112) for f_1 and f_2 are continuous functions of γ, while the amplitudes f_1 and f_2 in (114) are discontinuous for $\gamma=1/2$. The reason for this apparent contradiction becomes clear if we consider the limit of (112) for $kR\to 0$ for arbitrary γ. Keeping only the nonvanishing terms in (112), we obtain

$$f_1(kR\to 0,\gamma)=-\sqrt{\frac{2}{\pi ik}}\sin\pi\gamma\left(\frac{1}{2}\frac{\exp(i\varphi/2)}{\sin\varphi/2}\right.$$
$$\left.-i\eta\frac{1}{\frac{J_{-\gamma}}{J_{\gamma-1}}\exp(i\pi\gamma)+\eta}\right),$$

$$f_2(kR\to 0,\gamma)=-\sqrt{\frac{2}{\pi ik}}\sin\pi\gamma\left(\frac{1}{2}\frac{\exp(i\varphi/2)}{\sin\varphi/2}\right.$$
$$\left.+i\eta\frac{\exp(i\varphi)}{\frac{J_{\gamma-1}}{J_{-\gamma}}\exp(-i\pi\gamma)+\eta}\right).$$

Now we take into account the fact that for $kR\to 0$

$$\frac{J_{-\gamma}(kR)}{J_{\gamma-1}(kR)}\sim\left(\frac{kR}{2}\right)^{1-2\gamma}\frac{\Gamma(\gamma)}{\Gamma(1-\gamma)}.$$

We write the first factor in this expression as

$$\left(\frac{kR}{2}\right)^{1-2\gamma}=\exp\left((1-2\gamma)\ln\frac{kR}{2}\right).$$

If kR is so small that $|(1-2\gamma)\ln(kR/2)|\gg 1$, then

$$\left(\frac{kR}{2}\right)^{1-2\gamma}=\begin{cases}0\ \text{for}\ 0<\gamma<\frac{1}{2}\\ \infty\ \text{for}\ \frac{1}{2}<\gamma<1,\end{cases}$$

and we arrive at (114). On the other hand, if γ is close enough to 1/2 that $|(1-2\gamma)\ln(kR/2)|\ll 1$, then

$$\left(\frac{kR}{2}\right)^{1-2\gamma}\approx 1+(1-2\gamma)\ln\frac{kR}{2}.$$

Substituting this expression into f_1 and f_2, we obtain

$$f_1\left(\gamma=\frac{1}{2},\ kR\to 0\right)\sim-\sqrt{\frac{2}{\pi ik}}\left(\frac{1}{2}\frac{\exp(i\varphi/2)}{\sin\varphi/2}-\frac{\eta}{1-i\eta}\right),$$

$$f_2\left(\gamma=\frac{1}{2},\ kR\to 0\right)\sim\sqrt{\frac{2}{\pi ik}}\left(\frac{1}{2}\frac{\exp(i\varphi/2)}{\sin\varphi/2}\right.$$

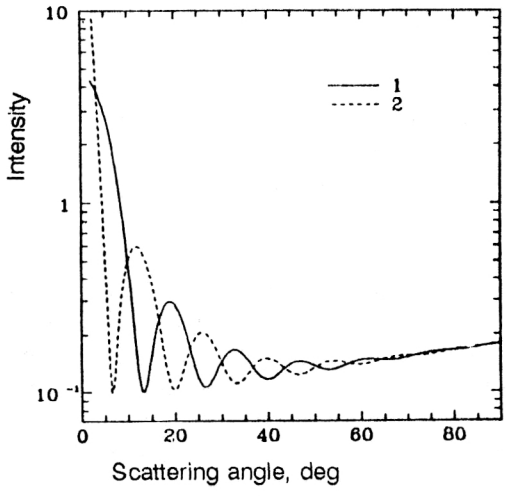

FIG. 15. The same as in Fig. 14 for the impenetrability condition (109).

$$-\frac{\eta}{1+i\eta}\exp(i\varphi)\Big). \tag{116}$$

Equations (114) and (116) correspond to different physical situations. The fact that different orders of taking the limit can lead to different physics is not new. In particular, this is related to the recent discussion[51] about the validity of the first Born approximation for describing the AB effect. In Fig. 15 we give the relativistic scattering cross sections corresponding to the exact relativistic boundary condition (109). Comparing these with the approximate relativistic cross sections corresponding to the vanishing of the large components of the Dirac wave function at $\rho=R$, we see that they are in excellent agreement despite the great difference between the scattering amplitudes (103) and (112).

Scattering on a relativistically impenetrable sphere

Let us now consider relativistic scattering on an impenetrable sphere of radius R. Let the incident wave propagate in the $+z$ direction with positive energy $\mathscr{E}$ and helicity. Then

$$\Psi_{\text{inc}}=\exp(ikz)\begin{bmatrix}1\\0\\\eta\\0\end{bmatrix},\quad \eta=\left(\frac{\mathscr{E}-\mu c^2}{\mathscr{E}+\mu c^2}\right)^{1/2},$$

$$k=\frac{1}{\hbar c}(\mathscr{E}^2-\mu^2c^4)^{1/2}.$$

The total wave function is

$$\Psi=\Psi_{\text{inc}}+\Psi_s.$$

For $r\to\infty$

$$\Psi_s=\frac{\exp(ikr)}{r}f(\varphi),\quad f(\varphi)=\begin{bmatrix}f_1\\f_2\\f_3\\f_4\end{bmatrix}.$$

The components f_i of the spinor scattering amplitude depend on the choice of impenetrability condition. For example, we can require that the large components of the Dirac WF vanish at $r=R$. Then

$$f_1=\frac{i}{k}\sum(2l+1)\frac{J_{l+1/2}}{H^{(1)}_{l+1/2}}P_l(\cos\theta),\quad f_2=0,$$

$$f_3=\frac{i\eta}{k}\sum\left[l\frac{J_{l-1/2}}{H^{(1)}_{l-1/2}}+(l+1)\frac{J_{l+3/2}}{H^{(1)}_{l+3/2}}\right]P_l(\cos\theta), \tag{117}$$

$$f_4=\frac{i\eta}{k}\exp(i\varphi)\sum\left(\frac{J_{l-1/2}}{H^{(1)}_{l-1/2}}-\frac{J_{l+3/2}}{H^{(1)}_{l+3/2}}\right)P^1_l(\cos\theta).$$

It turns out that for $r=R$ the small component is $\Psi_3=0$, and Ψ_4 is of order $(kR)^{-2}$.

Now let us require that the Dirac probability current vanish exactly at $r=R$. This is equivalent to the condition

$$i\alpha\mathbf{n}\Psi=\beta\Psi \text{ for } r=R,\qquad \mathbf{n}=(\sin\theta\cos\varphi,\ \sin\theta\sin\varphi,\ \cos\theta,\ 0). \tag{118}$$

This impenetrability condition corresponds to the following components of the relativistic spinor amplitude:

$$f_1=\frac{i}{k}\sum[(l+1)g_{l+1}+lf_l]P_l(\cos\theta),$$

$$f_2=-\frac{i}{k}\exp(i\varphi)\sum(g_{l+1}-f_l)P^1_l(\cos\theta),$$

$$f_3=\frac{i\eta}{k}\sum[(lg_l+(l+1)f_{l+1}]P_l(\cos\theta), \tag{119}$$

$$f_4=\frac{i\eta}{k}\sum(g_l-f_{l+1})P^1_l(\cos\theta),$$

$$g_l=\frac{J_{l-1/2}+\eta J_{l+1/2}}{H^{(1)}_{l-1/2}+\eta H^{(1)}_{l+1/2}},\quad f_l=\frac{J_{l+1/2}-\eta J_{l-1/2}}{H^{(1)}_{l+1/2}-\eta H^{(1)}_{l-1/2}}.$$

For each of these impenetrability conditions we have the scattering cross section

$$\sigma=\frac{1}{1+\eta^2}(|f_1|^2+|f_2|^2+|f_3|^2+|f_4|^2).$$

Typical dependences are shown in Fig. 16. As for scattering on a cylinder, we find excellent agreement between the cross sections corresponding to different relativistic impenetrability conditions. Here the scattering amplitudes (117) and (119) have quite different functional forms.

8. THE AHARONOV-BOHM EFFECT IN SIMPLY CONNECTED REGIONS OF SPACE

A typical discussion about the absence of the AB effect in simply connected regions of space goes as follows. Let the fields E and H be nonzero in a bounded simply connected region of space S. Outside S the scalar and vector potentials Φ and A are nonzero. Let us consider an arbitrary contour C lying entirely outside S. It is easy to see that $\oint A_l dl$ calculated for this contour is always zero. In

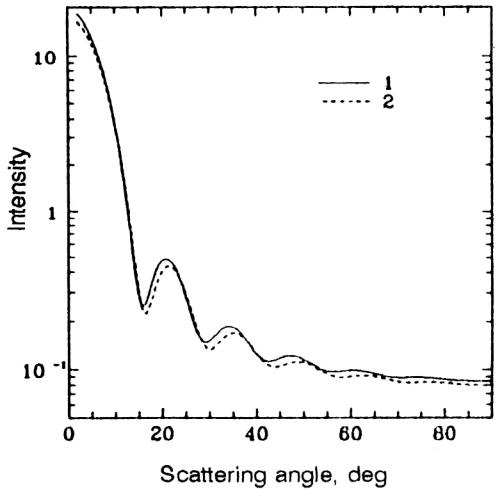

FIG. 16. Relativistic intensity of electron scattering on an impenetrable sphere S of radius R. Curves *1* and *2* correspond to vanishing of the large components of the Dirac wave function on the surface of S and the impenetrability condition (118), respectively.

fact, the contour C can always be spanned by a surface lying entirely outside S. According to the Stokes theorem,

$$\oint A_l dl = \int \mathbf{H} d\mathbf{S}.$$

Since $E=H=0$ outside S, $\oint A_l dl=0$, which proves our assertion. Since the presence of nontrivial paths along which $A_l dl \neq 0$ is a necessary condition for the existence of the AB effect,[52] we conclude that this effect is absent in this case.

A counterexample given in Ref. 53 casts doubt on this argument and leads us to reconsider the possibility that the AB effect exists in simply connected spaces.

The authors of Ref. 53 consider a toroidal cavity T (Fig. 17) given by $a_1<\rho<a_2$, $|z|<b_1$, inside which the magnetic field H is nonzero:

$$H_\rho=H_z=0, \quad H_\varphi=\Phi[2b_1(a_2-a_1)]^{-1} \tag{120}$$

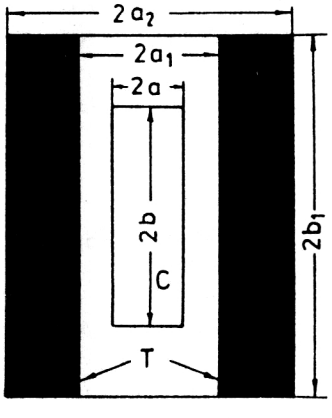

FIG. 17. A toroidal cavity T inside which the magnetic field H is nonzero. In the cylindrical cavity C, where $H=0$, two different vector potentials related by a gauge transformation lead to different eigenvalues (according to Ref. 53).

(Φ is the magnetic flux).

Outside T the magnetic field is zero. Furthermore, the authors of Ref. 53 give two vector potentials producing the same magnetic field H. They are zero for $|z|>b_1$. For $|z|<b_1$ they are given by the expressions

$$A_z^{(1)}=\begin{cases} \dfrac{\Phi}{2b_1} & \text{for } \rho<a_1 \\ \Phi\dfrac{1}{2b_1}\dfrac{a_2-\rho}{a_2-a_1} & \text{for } a_1<\rho<a_2 \\ 0 & \text{for } \rho>a_2, \end{cases} \tag{121}$$

$$A_z^{(2)}=\begin{cases} 0 & \text{for } \rho<a_1 \\ -\dfrac{\Phi}{2b_1}\dfrac{\rho-a_1}{a_2-a_1} & \text{for } a_1<\rho<a_2 \\ -\dfrac{\Phi}{2b_1} & \text{for } \rho>a_2. \end{cases} \tag{122}$$

Now let a charged particle be present in the cylindrical cavity C: $|z|<b$ ($b<b_1$), $\rho<a$ ($a<a_1$). On the WF Ψ we impose the Dirichlet condition in the radial variable ($\Psi=0$ for $\rho=a$) and the periodicity condition in the variable z:

$$\Psi(z=b)=\Psi(z=-b). \tag{123}$$

The solutions of the Schrödinger equation

$$-\frac{\hbar^2}{2\mu}\left[\frac{\partial^2\Psi}{\partial\rho^2}+\frac{1}{\rho}\frac{\partial\Psi}{\partial\rho}+\frac{1}{\rho^2}\frac{\partial^2\Psi}{\partial\varphi^2}+\left(\frac{\partial}{\partial z}-\frac{ie}{\hbar c}A_z^{(1,2)}\right)^2\Psi\right] =E\Psi \tag{124}$$

inside C with the selected boundary conditions are the following WFs:

$$\Psi_{nsm}^{(1,2)}\sim\exp\left(\frac{in\pi z}{b}\right)\exp(im\varphi)J_m(\lambda_{ms}\rho/R). \tag{125}$$

Here λ_{ms} is the sth nonzero root of the Bessel function $J_m(x)$. These WFs correspond to the eigenvalues

$$E_{nms}^{(1)}=\frac{\hbar^2}{2\mu}\left[\frac{\lambda_{ms}^2}{R^2}+\left(\frac{n\pi}{b}-\frac{e\Phi}{\hbar c}\frac{1}{2b_1}\right)^2\right],$$
$$E_{nms}^{(2)}=\frac{\hbar^2}{2\mu}\left[\frac{\lambda_{ms}^2}{R^2}+\left(\frac{n\pi}{b}\right)^2\right]. \tag{126}$$

Obviously, $E_{nms}^{(1)}\neq E_{nms}^{(2)}$, i.e., the eigenvalues in the simply connected region (where $H=0$) depend on the particular choice of WF. This seems very strange, since the vector potentials $A_z^{(1)}$ and $A_z^{(2)}$ are related by a gauge transformation:

$$A_z^{(1)}=A_z^{(2)}+\text{grad}\,\chi. \tag{127}$$

The function χ is equal to $\Phi z/2b_1$ for $|z|<b_1$, $\Phi/2$ for $z>b_1$, and $-\Phi/2$ for $z<-b_1$. We note that the eigenvalues $E^{(1,2)}$ correspond to wave functions $\Psi^{(1,2)}$ satisfying the same boundary condition (123) for $z=\pm b$. Meanwhile, a gauge transformation of the VP (127) corresponds to the following transformation of the WF:

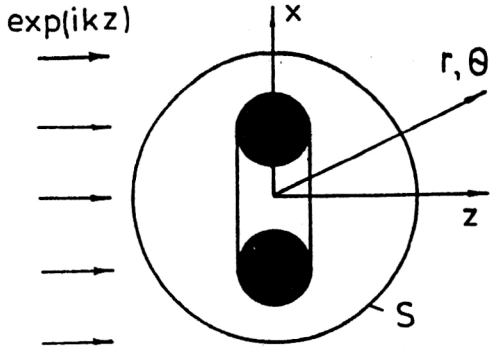

FIG. 18. A toroidal solenoid (shaded) inside a sphere S. For the same boundary condition on the surface the charged-particle scattering cross section depends on the value of the magnetic current inside the solenoid.

$$\Psi_1=\tilde{\Psi}_2\exp\left(\frac{ie\chi}{\hbar c}\right). \tag{128}$$

From this it follows that if Ψ_1 satisfies the boundary condition (123), the transformed WF $\tilde{\Psi}_2$ does not, in general, satisfy this condition:

$$\tilde{\Psi}_2(z=-b)=\tilde{\Psi}_2(z=b)\exp\left(\frac{ie\Phi}{\hbar c}\right)\neq\tilde{\Psi}_2(z=b). \tag{129}$$

Therefore, the difference between the eigenvalues E_1 and E_2 arises from the fact that the corresponding Ψ_1 and Ψ_2 are not related by a gauge transformation. The boundary conditions which the WFs satisfy must also change under a gauge transformation.

Let us now consider the scattering of charged spinless particles on a sphere S inside which a TS is located (Fig. 18). Let the following boundary condition be satisfied at the surface of the sphere:

$$\Psi(z=R)=f_0(\theta,\varphi). \tag{130}$$

The scattering problem is completely defined. The space outside the sphere is simply connected. Will the scattering cross section depend on the value of the magnetic field inside the sphere S [for the same boundary condition (130)]? The answer is surprising. In fact, let the boundary condition (130) be specified in the absence of a magnetic field. For this condition we can find the wave function Ψ_0, the amplitude, and the scattering cross section.[2)] Now we switch on the magnetic field inside the TS. Using the gauge transformation

$$\Psi=\Psi'\exp\left(\frac{ie}{\hbar c}\frac{\partial\alpha}{\partial z}\right) \tag{131}$$

we eliminate the VP outside the sphere S. The function α was obtained in Refs. 3 and 15. The wave function Ψ' satisfies the free Schrödinger equation with boundary condition

$$\Psi'(r=R)=f_0\exp\left(-\frac{ie}{\hbar c}\frac{\partial\alpha}{\partial z}\right)\Big|_{r=R}.$$

Since the transformation (131) is unitary, all the observables for Ψ and Ψ' are the same. Since Ψ_0 and Ψ' satisfy the free Schrödinger equation with different boundary conditions, they describe different physical situations. In view of the unitary equivalence of Ψ and Ψ', this implies that for the same boundary condition at $r=R$ the situations in the presence and absence of a magnetic field inside the sphere turn out to be physically different. These situations are equivalent in the following two cases. First, when a boundary condition explicitly depending on the magnetic field inside the TS is imposed on the surface S,

$$\Psi=f_0\exp\left(\frac{ie}{\hbar c}\frac{\partial\alpha}{\partial z}\right)\Big|_{r=R}.$$

In fact, after the unitary transformation (131) we arrive at a WF Ψ' satisfying the boundary condition (130). In the second case a gauge-invariant boundary condition is imposed on the surface of the sphere. Since the probability current is a gauge-invariant quantity, the vanishing of its normal component on the surface of the sphere is a gauge-invariant condition. We thus have on the surface of the sphere

$$\bar{\Psi}\frac{\partial\Psi}{\partial z}-\Psi\frac{\partial\bar{\Psi}}{\partial z}-\frac{2ie}{\hbar c}A_z|\Psi|^2=0 \text{ for } r=R.$$

After the gauge transformation (131) we arrive at the WF Ψ' satisfying the boundary condition

$$\bar{\Psi}'\frac{\partial\Psi'}{\partial z}-\Psi'\frac{\partial\bar{\Psi}'}{\partial z}=0 \text{ for } r=R.$$

We choose one of the particular realizations of this boundary condition:

$$\frac{\partial\Psi'}{\partial z}\Big|_{r=R}=0. \tag{132}$$

The explicit solution for this realization was obtained in Sec. 7. Then, using the same transformation (131), we return to the initial WF Ψ. The explicit form of the boundary condition for Ψ is obtained by substituting $\Psi'=\Psi\exp[(-ie/\hbar c)\,(\partial\alpha/\partial z)]$ into (132). Then

$$\frac{\partial\Psi}{\partial z}-\frac{ic}{\hbar c}A_z\Psi=0. \tag{133}$$

Therefore, if in the absence of a magnetic field inside the sphere a boundary condition is specified on its surface in the form

$$\frac{\partial\Psi_0}{\partial z}=0,$$

to obtain the same physical situation in the presence of a magnetic field it is necessary to impose the boundary condition (133). A natural nonrelativistic boundary condition preserving its functional form for all values of the magnetic flux inside the sphere is the condition $\Psi=0$ on the spherical boundary.

We conclude that we must be careful when dealing with the AB effect in a simply connected space; in particular, we must define what we mean by a given impenetrability condition. We have unwittingly become like the character described by Montaigne: "I know one such man:

when I ask him about something, even though it is well known to him, he immediately seeks a book to consult for the needed answer; and he never decides to say that he has mange on his backside until he has looked up in his dictionary exactly what mange and backside mean" (Montaigne, Essays).

9. EXPERIMENTAL CONFIRMATION OF THE AHARONOV–BOHM EFFECT

The discussions of recent years about the existence of the Aharonov–Bohm effect are concerned with the fact that multivalued WFs are allowed in multiply connected regions of space.[15,54] It turns out that the naive use of multivalued WFs (i.e., the solution of the Schrödinger equations using multivalued WFs) causes the AB effect to disappear,[54,55] as it only occurs when single-valued WFs are used. The well known proof by Pauli[56] of the single-valuedness of the WF is valid only in simply connected regions of space. Therefore, this theoretical uncertainty can be resolved only by experiment. The first experiments (see, for example, the review of Ref. 31), in which electrons were scattered on cylindrical solenoids, are now viewed as insufficient. The main reasons are the poor asymptotic form of the WF (owing to slow falloff of the VP) and the presence of a return magnetic flux and leakage of the magnetic field due to the finite length of a real cylindrical solenoid. This makes it possible to relate the experimentally observed shift of the diffraction pattern to electron scattering on the magnetic-field leakage.[57] These defects are absent for the toroidal solenoid. The rapid falloff of the VP ($\sim r^{-3}$; see Sec. 2) leads to the normal asymptotic form of the WF. Electron scattering on toroidal solenoids was studied in the excellent experiments carried out by Japanese physicists (see their description in Ref. 8). We shall refer to these experiments as the Tonomura experiments. Let us briefly discuss the existing theoretical approaches. Frauenhofer diffraction of electrons on a TS was studied in the important work of Ref. 9. Unfortunately, this approximation is inapplicable under the conditions of the Tonomura experiment. A suitable approach was found in Ref. 10. Our immediate goal is to use the results of these studies to describe these experiments.

The following WF (Ref. 10) describes the scattering of an electron plane wave on an impenetrable TS:

$$\Psi=\exp(ikz)+\Psi_s,$$

$$\Psi_s=i\frac{1+\cos\theta}{2}\exp(ikr)\exp\left(ik\frac{d^2+R^2}{2r}\right). \qquad (134)$$

$$[\exp(i\omega)W_1-\exp(2i\pi\gamma-i\omega)\cdot W_2].$$

Here d and R are the parameters of the impenetrable torus $(\rho-d)^2+z^2=R^2$ with magnetic flux Φ inside it (Fig. 19); $\gamma=e\Phi/hc$; θ and r are the scattering angle and the distance from the TS to the observation point P; k is the wave number; $\omega=kdR/r$; W_1 and W_2 are linear combinations of Lommel functions of two variables:

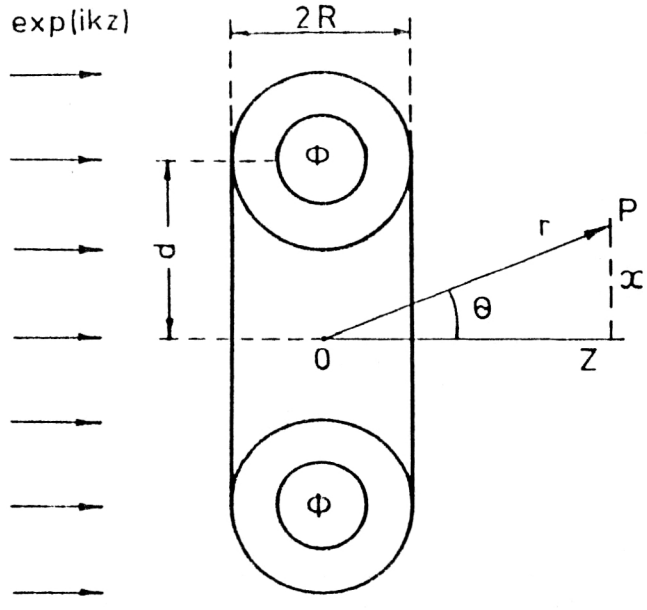

FIG. 19. Schematic depiction of charged-particle scattering on an impenetrable toroidal solenoid with magnetic flux Φ. Here d and R are the parameters of the toroidal solenoid, and z and x are the location of the observation plane and the distance of the observation point from the symmetry axis of the solenoid.

$$W_{1,2}=U_1\left[\frac{k(d\pm R)^2}{r},\ k(d\pm R)\sin\theta\right]$$

$$-iU_2\left[\frac{k(d\pm R)^2}{r},\ k(d\pm R)\sin\theta\right].$$

The scattering intensity is determined by the squared absolute value of Ψ: $I=|\Psi|^2$. Let us now discuss the conditions under which Eq. (134) is valid. It was obtained by Fresnel–Kirchhoff diffraction theory.[58] In it, it is assumed that the WF vanishes at the surface of the torus, while outside the torus, in the $z=0$ plane, the WF coincides with a plane wave $\exp(ikz)$. Furthermore, at an arbitrary point P the WF is determined by the diffraction integral. It reduces to Eq. (134) if the following conditions are satisfied:

$$k(d-R)\gg 1, \qquad (135)$$

$$\delta\sin^2\theta\ll\pi \quad (\delta=kd^2/2r). \qquad (136)$$

In the experiments under discussion[8] $d\approx 2\times10^{-4}$ cm, $R\approx 1\times10^{-4}$ cm, and $k\approx 2\times10^{10}$ cm^{-1} (this corresponds to electron energy $E\approx 150$ keV). We shall calculate the electron intensities in the planes $z=10$ cm and $z=100$ cm. They correspond to the values $\delta=4$ and 0.4, respectively. Then Eq. (136) leads to the following constraint on $\sin\theta$: $\sin^2\theta\ll\frac{1}{4}\pi$ for $z=10$ cm and $\sin^2\theta\ll 2\pi$ for $z=100$ cm. In the Tonomura experiments the measurements were made at x lying inside the hole of the torus ($x\leqslant d-R$) and close to the TS. We assume (to be on the safe side) that $x_{\max}=2(d+R)\approx 6\times10^{-4}$ cm. Then $\sin\theta_{\max}=x_{\max}/z\approx 6\times10^{-5}$ (for $z=10$ cm) and 6×10^{-6} (for $z=100$ cm). Thus, the condition (136) is certainly satisfied. In addition, in this case $k(d-R)\approx 2\times10^6$. In view of this, the

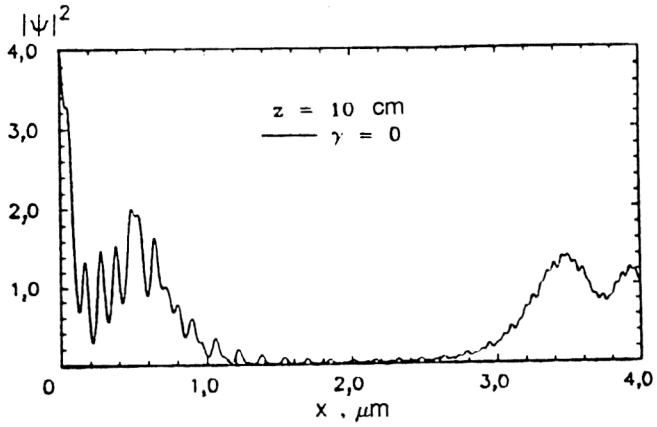

FIG. 20. Electron scattering intensity in the plane $z=10$ cm in the absence of magnetic flux inside the solenoid ($\gamma=e\Phi/hc=0$). The ranges $0<x<1$ and $1<x<3$ correspond to the hole in the solenoid and the shadow region.

condition (135) is also satisfied. Physically, this implies that sufficiently many wavelengths fit into the hole of the torus. Since the incident wave near the torus differs from a plane wave at distances of the order of several wavelengths and since the WF vanishes at the torus surface because of the impenetrability of the torus, the conditions for the applicability of Fresnel–Kirchhoff diffraction theory are satisfied. Special measures were taken in the Tonomura experiments to ensure impenetrability of the torus. According to Ref. 8, only 10^{-6} of the incident particles reach the region inside the torus where $H\neq 0$. The condition (135) does not at all imply the transition to geometrical optics and the absence of diffraction. The condition (136) directly determines the angular range in which the Fresnel theory of diffraction is valid. According to Ref. 59, it is important that the transverse dimensions of the beam significantly exceed the detector dimensions. In that study excellent, clear diffraction patterns are shown for which the ratio of the scatterer size and the electron wavelength is of order 10^4.

Numerical analysis of electron diffraction by a toroidal solenoid

In Figs. 20–23 we show the typical electron intensities in the plane $z=$const. The parameters R, d, and k are the same as in the Tonomura experiments: $R\approx 10^{-4}$ cm, $d=2\times 10^{-4}$ cm, and $k=2\times 10^{10}$ cm^{-1}. The calculations were carried out for $\gamma=0$ and $\gamma=\frac{1}{2}$. This does not imply loss of generality, since the theory is invariant under the replacement $\gamma\to\gamma+n$ (where n is an integer). It is for such values of γ (integer and half-integer) that the Tonomura experiments were carried out. Let us first consider the case where the distance z from the plane $z=0$ to the observation plane is 10 cm (Figs. 20 and 21). The low intensity in the shadow region ($1<x<3$) should be noted. At large distances from the z axis the electron intensity is the same for $\gamma=0$ and $\gamma=1/2$. It oscillates about the value $|\Psi|^2=1$, with the amplitude of the oscillations decreasing with increasing x. For x lying inside the hole in the torus ($x<1$) the intensities for $\gamma=0$ and $\gamma=1/2$ differ significantly (Fig. 22). Most of the oscillations in this angular range are out of phase. In Fig. 23 we show the scattering intensities in the plane $z=100$ cm. We see that only one oscillation is observed inside the hole in the torus. The shadow region, as expected, is not as clearly expressed as in the preceding case. In Fig. 24 we show the intensities along the z axis. In this case Ψ simplifies considerably and we obtain

$$|\Psi|^2=1-8\sin\left[\frac{k(d-R)^2}{4z}\right]\times\sin\left(\frac{kdR}{z}-\pi\gamma\right)\cos\left[\frac{k(d+R)^2}{4z}-\pi\gamma\right].$$

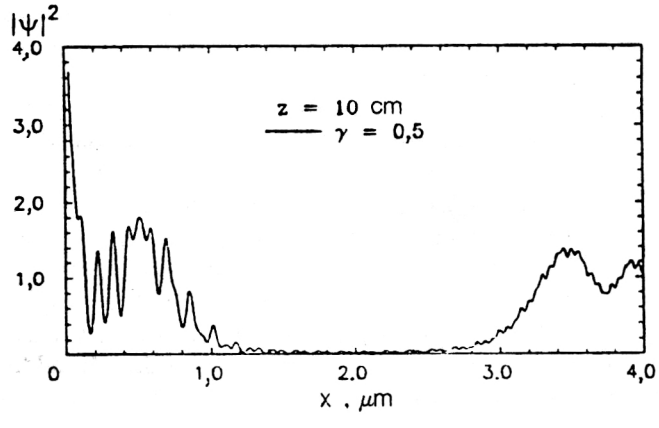

FIG. 21. The same as in Fig. 20 for $\gamma=1/2$.

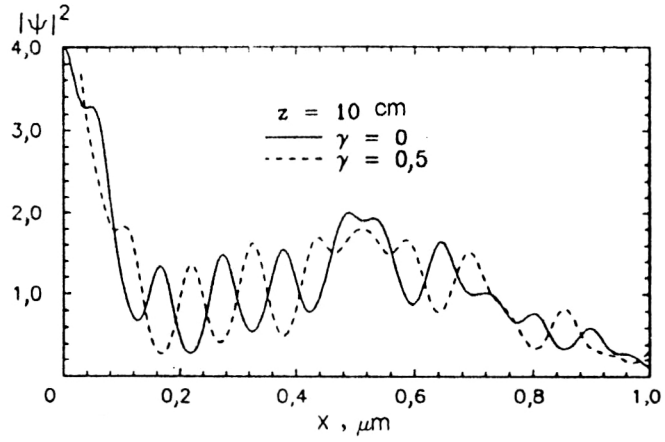

FIG. 22. The same as in Figs. 20 and 21 inside the hole in the solenoid.

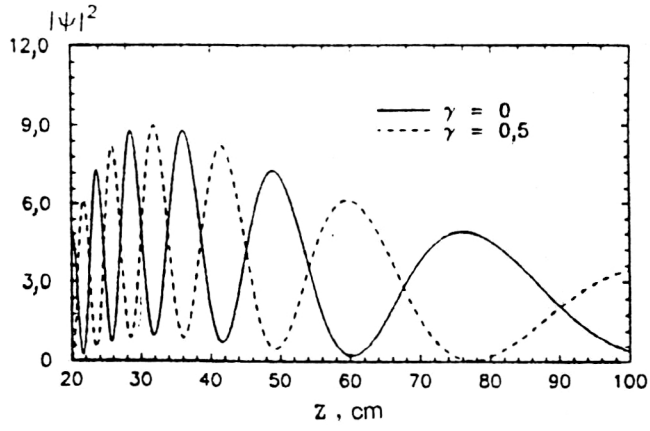

FIG. 24. Scattering intensity along the z axis.

We see that the maxima of $|\Psi|^2$ on the symmetry axis are macroscopically separated for $\gamma=0$ and $\gamma=1/2$. However, it is not clear how this measurement could be carried out in practice. Actually, the smallness of the hole in the torus (2 μm in diameter) and the finiteness of the dimensions of a real detector necessarily lead to averaging of the intensity. Owing to particle flux conservation, these averaged intensities will be practically identical for $\gamma=0$ and $\gamma=1/2$, and can hardly be distinguished experimentally.

The Tonomura experiments

In the preceding subsection we considered the diffraction of an electron plane wave on an impenetrable TS. However, the Tonomura experiments were carried out in a slightly different way (Fig. 25). The incident electron beam was split into two parts. The first, as before, was incident on the TS. The second part of the beam (which will be referred to as the reference wave Ψ_{ref}) was directed toward the first by means of an electron optical system, and the two beams met behind the TS. As a result, an interference pattern arises in this region. These experiments show that in region II (where Ψ_{ref} interferes with the part of the beam Ψ_{out} which did not pass through the hole in the solenoid) the interference pattern remains the same for any value of the magnetic flux Φ inside the TS. In region I (where Ψ_{ref} interferes with the part of the beam Ψ_{in} which passed through the hole in the TS) the interference pattern shifts as Φ varies.

The qualitative treatment

The standard explanation of the observed shift of the diffraction pattern is the following. We assume that in the absence of a magnetic field the WFs Ψ_{in} and Ψ_{out} can be approximated by plane waves: $\Psi_{in}=\Psi_{out}=\exp(ikz)$. Furthermore, let the wave vector of the reference wave have components $k_x=k\sin\alpha$ and $k_z=k\cos\alpha$. Then $\Psi_{ref}=\exp[ik(x\sin\alpha+z\cos\alpha)]$. In the absence of a magnetic field we have, in regions I and II,

$$\Psi_0=\exp(ikz)+\Psi_{ref} \text{ and } |\Psi_0|^2$$
$$=2\{1+\cos[kx\sin\alpha-kz(1-\cos\alpha)]\}.$$

In the plane $z=$const (where the measurements were made) the maxima of $|\Psi_0|^2$ are located at

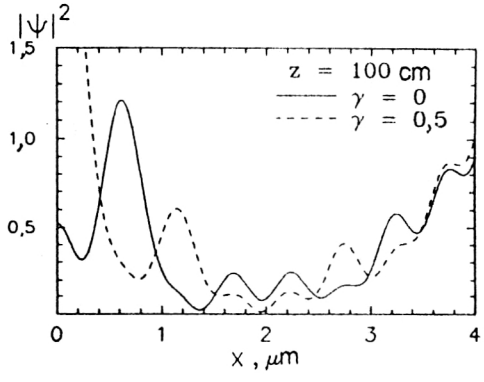

FIG. 23. Electron scattering intensity in the plane $z=100$ cm.

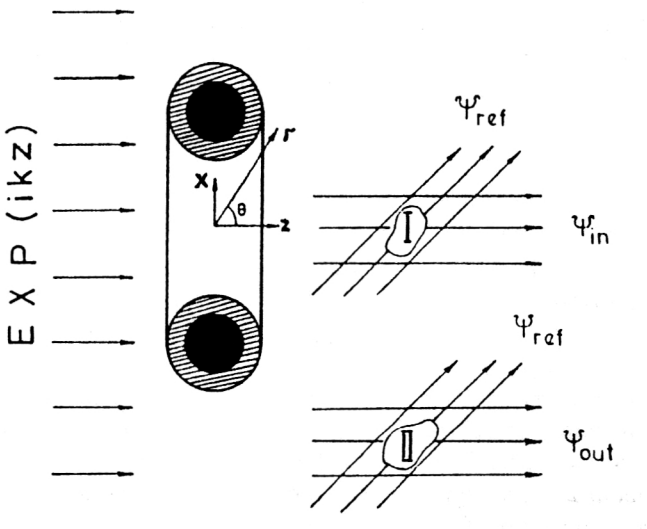

FIG. 25. Schematic depiction of the Tonomura experiments.

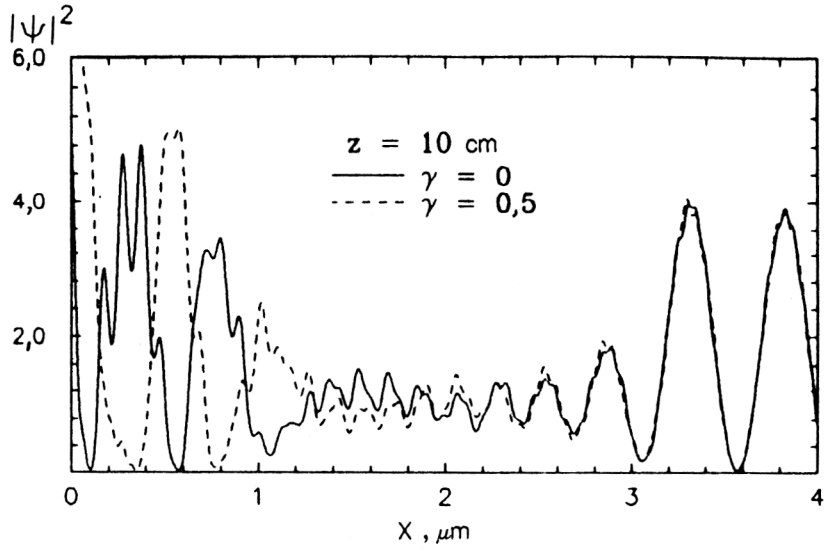

FIG. 26. Scattering intensity corresponding to interference of the scattered wave and the reference wave in the plane $z=10$ cm. The angle of incidence of the reference wave is $\alpha=2\pi\times10^{-6}$ rad.

$x_n^0=[2\pi n+kz(1-\cos\alpha)]/k\sin\alpha$. The distance between them is $\Delta x_n^0=2\pi/k\sin\alpha$. The presence of the magnetic field can be taken into account by the Dirac phase factor (see, for example, Ref. 60):

$$\Psi_{\text{in}}^{\Phi}=\Psi_{\text{out}}^{\Phi}=\exp(ikz)\exp\left(\frac{ie}{\hbar c}\int_{-\infty}^{z}A_z(x,z)dz\right).$$

Here A_z is the vector potential of the TS. In spite of the fact that these functions have the same form, they actually differ, owing to the different values of x in them. Due to the short-range nature of A_z ($\sim r^{-3}$ at large distances), the upper limit of the z integration can be replaced by $+\infty$ already at distances of the order of a fraction of a centimeter. Since $\int_{-\infty}^{\infty}A_z(x,z)$ is equal to Φ if the integration axis passes inside the hole of the solenoid and zero otherwise, $\Psi_{\text{out}}=\exp(ikz)$ and $\Psi_{\text{in}}=\exp(ikz)\exp(2i\pi\gamma)$. This implies that in region II the interference picture remains the same as in the absence of a magnetic field, while in region I

$$|\Psi_I^{\Phi}|^2=2\{1+\cos[kx\sin\alpha-kz(1-\cos\alpha)-2\pi\gamma]\}.$$

The maxima of $|\Psi_I^{\Phi}|^2$ are located at $x_n^{\Phi}=x_n^0+2\pi\gamma/k\sin\alpha$. This means that when the magnetic field is switched on they are shifted by $\Delta=2\pi\gamma/k\sin\alpha$. Because of the periodicity of $|\Psi_I^{\Phi}|^2$ in γ it is sufficient to consider the interval $0<\gamma<1$. The largest shift of the interference patterns occurs for $\gamma=1/2$. It is $\Delta=\pi/k\sin\alpha$.

The quantitative treatment

To obtain quantitative results we form the superposition of the WF (134) and Ψ_{ref}. The results of the calculations are shown in Figs. 26 and 27. The angle of incidence α was taken to be $2\pi\times10^{-6}$ rad. We see that the maxima of the intensity $|\Psi+\Psi_{\text{ref}}|^2$ are sufficiently separated inside the hole of the torus. The intensity oscillates about 1 in the shadow region (since there Ψ is small and $|\Psi_{\text{ref}}|=1$) and about 2 in the region outside the torus ($x>3$) (since there Ψ_{ref} and Ψ are of order 1, but have different phases). In one of the Tonomura papers[61] the angle of incidence was estimated to be 10^{-3} rad. The calculated interference pattern is shown in Fig. 28 for this α and $z=100$ cm. We note the scale on the horizontal axis: the entire interference pattern is developed in a range of 10^{-2} μm. From this figure we can estimate the distance between adjacent maxima to be $\approx3.2\times10^{-3}$ μm, and the shift of the interference pattern when the magnetic field is switched on (for $\gamma=1/2$) is estimated to be half this value. This is consistent with the qualitative estimates made above ($\Delta x_n^0\sim3.14\times10^{-3}$ μm and $\Delta\sim1.58\times10^{-3}$ μm). This interference picture is written on film. Then the holographic method is used to reconstruct the original diffraction pattern (i.e., in the absence of the reference wave). From the figures given in Refs. 8 and 61 we can estimate the distance between adjacent maxima to be 0.5 μm, while the shift of an individual maximum when the magnetic field is switched on (for $\gamma=1/2$) is about 0.25 μm. To compare this with the theory it is necessary to specify the distance z between the TS and the observation plane. In all the Tonomura studies known to us there is no information about this distance. From Figs. 20–23 we can estimate the shift of the diffraction pattern to

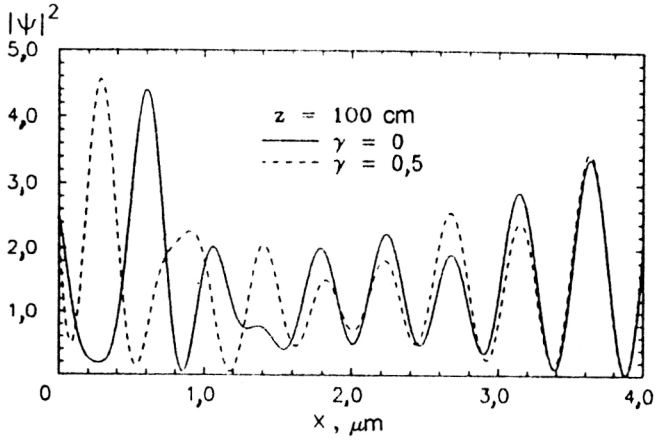

FIG. 27. The same as in Fig. 25 in the plane $z=100$ cm.

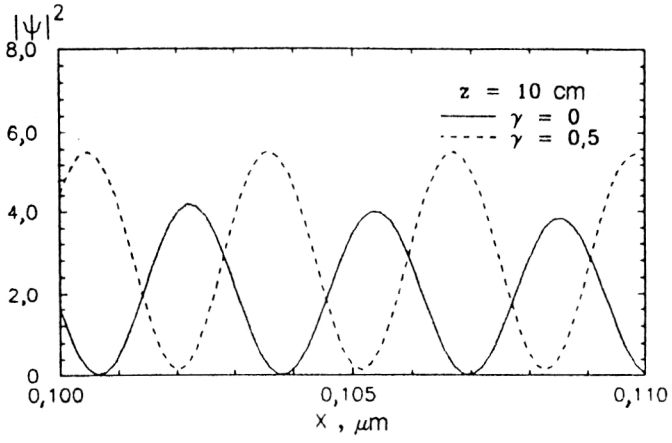

FIG. 28. The same as in Fig. 25 for angle of incidence equal to 10^{-3} rad. Only part of the interference pattern is shown ($0.1\ \mu m \leqslant x \leqslant 0.11\ \mu m$).

be $\Delta \approx 0.06\ \mu m$ for $z=10$ cm and $\Delta \approx 0.4\ \mu m$ for $z=100$ cm. Therefore, the observation plane in the Tonomura experiments must lie between these values of z. We note that even though the qualitative treatment gives practically the same shift of the interference pattern as the quantitative treatment, there is a fundamental difference between them. In fact, after reconstructing the original (i.e., in the absence of the reference wave) interference pattern in the first case we obtain $|\Psi|^2=1$ both for $\rho<d-R$ and for $\rho=d+R$. On the other hand, the quantitative treatment using the wave function (134) leads to the interference patterns shown in Figs. 20–24. We conclude that it is the minimal difference between the qualitative and quantitative interference patterns (before the holographic reconstruction) which leads to the correct description of these experiments.

Let us make several concluding remarks. First, the diffraction pattern observed in the Tonomura experiments is produced by the superposition of individual electron events. By these we mean the scattering of an individual electron on the TS and its subsequent collapse onto the detection screen. The incident electron intensity was so low[8,61] that only one electron was located inside the experimental setup at a given instant of time. Second, the applicability of the Fresnel–Kirchhoff diffraction theory for describing electron scattering is confirmed by careful analysis of the theoretical and experimental diffraction patterns.[62] Third, we should note the recent study[63] on the use of coherent point sources of low-energy ($\sim$20–50 keV) electrons to study crystal lattice structure. According to the authors of that study, a 150 000-fold magnification of the diffraction pattern (compared with that for a plane wave) can be obtained for small distances between the electron emitter and the object studied. This reveals new possibilities for studying the quantum effects of inaccessible fields.

In Sec. 3 we noted that the magnetic field distribution inside a magnetized torus is characterized by the helicity S (in addition to the magnetic flux Φ). The magnetization vector $\mathbf{M}$ has the following dependence on the angle α determining the amount of twisting of the magnetic field lines inside T:

$$\mathbf{M}=M(\cos\alpha\cdot\mathbf{n}_\varphi+\sin\alpha\cdot\mathbf{n}_\theta).$$

Is it possible to detect a nontrivial helicity inside a torus by performing experiments outside the torus (can the torus be surrounded by an impenetrable screen)? At the beginning of this section we explained that the cross section for charged-particle scattering on an impenetrable magnetic torus depends on the geometrical dimensions of the torus and on the part of the magnetic flux which "sees" the charged particle in a circuit around a closed path passing through the hole in the solenoid. This part of the flux is equal to $\Phi\cos\alpha$. Since the scattering cross section is a periodic function of the magnetic flux [see, for example, Eq. (134)], the cross section will vary periodically as the twist angle α changes. This will occur in the range $0\leqslant\alpha\leqslant\alpha_0$. Here $\alpha_0=\arccos(2\gamma)^{-1}$ and $\gamma=e\Phi/hc$. As α is increased further (i.e., for $\alpha_0\leqslant\alpha\leqslant\pi/2$) the cross section approaches the cross section for scattering on an impenetrable torus in the absence of a magnetic field.

CONCLUSION

Let us briefly recall the subjects touched upon here.

1. We considered a family of toroidal solenoids with constant current, the vector potentials of which fall off at large distances as r^{-2n-1}. The charged-particle scattering cross section is the same for a given total magnetic flux and the same impenetrable torus surrounding the toroidal solenoids. In spite of this, the vector potentials of different families are not related by a gauge transformation. Toroidal solenoids with different asymptotic behavior realize toroidal moments of different multipole orders.

2. We have given a practical recipe for constructing solenoids of arbitrary geometrical shape. For this it is sufficient to fill an arbitrary region of space with matter with solenoidal magnetization.

3. We have given a specific realization of toroidal solenoids with nontrivial helicity, which (along with the magnetic flux) is one of the invariants characterizing the topological structure of the magnetic field.

4. We have found the classical and quantum equations of motion of the toroidal moments in an external electromagnetic field.

5. We have found the three-dimensional analog of the Aharonov–Casher effect. It turns out that toroidal solenoids of different multipole orders must undergo quantum scattering on a Coulomb center. Here there is no classical scattering.

6. We have demonstrated the possibility that nontrivial electric vector potentials exist. We have given a specific realization of systems possessing such potentials. The simplest ones are toroidal and cylindrical electric solenoids.

7. We have studied nonstatic configurations of currents and charges outside which the fields $\mathbf{E}$ and $\mathbf{H}$ are zero, but the electromagnetic potentials $\mathbf{A}$ and Φ are nonzero. We have formulated the conditions under which these potentials have physical meaning and can be observed. This re-

veals the possibility in principle of information transfer without loss of energy (by phase modulation of the wave function of the scattered particles).

8. We have studied different versions of quantum impenetrability, which is defined as the condition that the normal component of the quantum-mechanical probability current vanish (at the boundary of the impenetrable region). It turns out that different versions of impenetrability lead to different physical consequences, which must be taken into account in designing experiments.

9. We have considered recent experiments to verify the existence of the Aharonov-Bohm effect. In particular, we have given a quantitative description of the well known Tonomura experiments in which electrons are scattered on impenetrable toroidal magnetic solenoids.

APPENDIX. VECTOR SOLUTIONS OF THE LAPLACE EQUATION

Instead of the elementary vector potentials $\mathbf{A}_l^m(\tau)$ and $\mathbf{B}_l^m(\tau)$, we introduce the vector spherical harmonics (VSHs):

$$\begin{aligned}
&\mathbf{A}_l^m(M)=-h_l\mathbf{Y}_{ll}^m,\\
&\mathbf{A}_l^m(E)=(\sqrt{l+1}h_{l-1}\mathbf{Y}_{l,l-1}^m-\sqrt{l}h_{l+1}\mathbf{Y}_{l,l+1}^m)/\sqrt{2l+1},\\
&\mathbf{A}_l^m(L)=(\sqrt{l+1}h_{l+1}\mathbf{Y}_{l,l+1}^m+\sqrt{l}h_{l-1}\mathbf{Y}_{l,l-1}^m)/\sqrt{2l+1}\\
&\mathbf{B}_l^m(M)=-j_l\mathbf{Y}_{ll}^m,\\
&\mathbf{B}_l^m(E)=(\sqrt{l+1}j_{l-1}\mathbf{Y}_{l,l-1}^m-\sqrt{l}j_{l+1}\mathbf{Y}_{l,l+1}^m)/\sqrt{2l+1},\\
&\mathbf{B}_l^m(L)=(\sqrt{l+1}j_{l+1}\mathbf{Y}_{l,l+1}^m+\sqrt{l}j_{l-1}\mathbf{Y}_{l,l-1}^m)/\sqrt{2l+1}.
\end{aligned}\tag{A1, A2}$$

They are vectorially coupled objects constructed from the ordinary scalar spherical harmonics and spherical unit vectors $[\mathbf{n}_0=\mathbf{n}_z,\ \mathbf{n}_{\pm1}=\mp1/\sqrt{2}(n_x\pm in_y)]$:

$$\mathbf{Y}_{jl}^m=\sum_\mu C(1,-\mu,l,m+\mu;jm)\,Y_l^{m+\mu}\mathbf{n}_{-\mu}.$$

The VSHs are orthogonal on a sphere of arbitrary radius:

$$\int \mathbf{Y}_{jl}^m\cdot\mathbf{Y}_{jl'}^{m'}d\Omega=\delta_{jj'}\delta_{mm'}\delta_{\tau\tau'}.$$

Then the vector potential can be written as

$$\begin{aligned}
&\mathbf{A}=\frac{1}{c}4\pi ik\sum h_l(kr)\mathbf{Y}_{jl}^m\cdot J_{jl}^m,\\
&J_{jl}^m=\int j_l(kr)\mathbf{Y}_{jl}^{m*}\cdot\mathbf{j}dV.
\end{aligned}\tag{A3}$$

In the static limit this expression becomes

$$\begin{aligned}
&\mathbf{A}=\frac{1}{c}4\pi\sum\frac{1}{2l+1}\frac{1}{r^{l+1}}\mathbf{Y}_{jl}^m\cdot J_{jl}^m,\\
&J_{jl}^m=\int r^l\mathbf{Y}_{jl}^{m*}\cdot\mathbf{j}dV.
\end{aligned}\tag{A4}$$

Here $r^l\mathbf{Y}_{jl}^m$ and $r^{-l-1}\mathbf{Y}_{jl}^m$ are vector solutions of the Laplace equation. However, we are interested in those solutions which can be written in the form (82), i.e., which are obtained by acting with the operators $\mathbf{L}\ (=-i\mathbf{r}\times\nabla)$ and ∇ on the scalar solutions of the Laplace equation. Let us try to take the static limit in (81). For this we expand $\mathbf{A}_l^m$ and $\mathbf{B}_l^m$ in series in powers of k:

$$\begin{aligned}
&\mathbf{A}_l^m(\tau)=k^{-l-2}[\mathbf{A}_{1l}^m(\tau)+k^2\mathbf{A}_{2l}^m(\tau)]\\
&\mathbf{B}_l^m(\tau)=k^{l-1}[\mathbf{B}_{1l}^m(\tau)+k^2\mathbf{B}_{2l}^m(\tau)],\quad \tau=E,\ L,\\
&\mathbf{A}_l^m(M)=k^{-l-1}\mathbf{A}_{1l}^m(M),\quad \mathbf{B}_l^m(M)=k^l\mathbf{B}_{1l}^m(M).
\end{aligned}\tag{A5}$$

Here

$$\begin{aligned}
&\mathbf{A}_{1l}^m(E)=\frac{2\alpha_l}{\sqrt{l(l+1)}}\nabla\times(\mathbf{L}r^{-l-1}Y_l^m),\\
&\mathbf{A}_{2l}^m(E)=\frac{\alpha_l}{\sqrt{l(l+1)}}\frac{1}{2l-1}\nabla\times(\mathbf{L}r^{1-l}Y_l^m),\\
&\mathbf{B}_{1l}^m(E)=-\frac{i\beta_l}{\sqrt{l(l+1)}}\nabla\times(\mathbf{L}r^lY_l^m),\\
&\mathbf{B}_{2l}^m(E)=\frac{i\beta_l}{\sqrt{l(l+1)}}\frac{1}{2(2l+3)}\nabla\times(\mathbf{L}r^{l+2}Y_l^m),\\
&\mathbf{A}_{1l}^m(L)=2i\alpha_l\nabla r^{-l-1}Y_l^m,\quad \mathbf{A}_{2l}^m(L)=\frac{i\alpha_l}{2l-1}\nabla r^{1-l}Y_l^m,\\
&\mathbf{B}_{1l}^m(L)=\beta_l\nabla r^lY_l^m,\quad \mathbf{B}_{2l}^m(L)=-\frac{1}{2}\beta_l\frac{1}{2l+3}\nabla r^{l+2}Y_l^m,\\
&\mathbf{A}_{1l}^m(M)=\frac{2i\alpha_l}{\sqrt{l(l+1)}}\mathbf{L}r^{-l-1}Y_l^m,\\
&\mathbf{B}_{1l}^m(M)=\frac{\beta_l}{\sqrt{l(l+1)}}\mathbf{L}r^lY_l^m,\\
&\alpha_l=(-1)^{l+1}\sqrt{\pi}2^{l-1}/\Gamma\left(\frac{1}{2}-l\right),\\
&\beta_l=\sqrt{\pi}2^{-l-1}/\Gamma\left(l+\frac{3}{2}\right).
\end{aligned}\tag{A6}$$

The quantities $\mathbf{A}_{il}^m$ and $\mathbf{B}_{il}^m$ are independent of k. The terms for higher powers of k do not contribute in the long-wavelength limit and have therefore been omitted in the expansion (A5). The following expansion holds for the coefficients $a_l^m(\tau)$ entering into the definition of the VP [see (81)]:

$$\begin{aligned}
&a_l^m(\tau)=k^{l-1}[a_{1l}^m(\tau)+k^2a_{2l}^m(\tau)],\quad \tau=E,\ l,\\
&a_l^m(M)=k^la_{1l}^m(M),\quad a_{il}^m(\tau)=\int\mathbf{B}_{il}^m(\tau)^*\cdot\mathbf{j}dV.
\end{aligned}\tag{A7}$$

It follows from (A5) and (A7) that the contributions to the VP (81) from the electric and longitudinal multipoles taken separately diverge as k^{-2} for $k\to0$. Meanwhile, the expansion (A3), which is completely equivalent to (81), becomes (A4) in this limit. No singularities arise in taking this limit. This means that the singularities of the electric

and longitudinal multipoles in (81) cancel each other. This can also be verified in a different way, if we note that the singular term in (81) has the form

$$k^{-2}[a_{1l}^m(E)\mathbf{A}_{1l}^m(E)+a_{1l}^m(L)\mathbf{A}_{1l}^m(L)].$$

From the explicit form of a_{1l}^m and $\mathbf{A}_{1l}^m$ it follows that this expression is equal to zero. Taking this into account, we find the following expression for the static limit of (81):

$$\mathbf{A}=\frac{4\pi}{c}\sum\frac{1}{2l+1}\frac{1}{l(l+1)}\mathbf{C}_l^m(M)\cdot d_l^m(M)$$
$$+\frac{2\pi}{c}\sum\frac{1}{4l^2-1}C_l^m(E)\cdot d_l^m(L)$$
$$-\frac{2\pi}{c}\sum\frac{1}{(2l+1)(2l+3)}\mathbf{C}_l^m(L)\cdot d_l^m(E). \quad \text{(A8)}$$

Here

$$\mathbf{C}_l^m(M)=(\mathbf{r}\times\nabla)r^{-l-1}Y_l^m,\quad \mathbf{D}_l^m(M)=(\mathbf{r}\times\nabla)r^lY_l^m,$$

$$\mathbf{C}_l^m(E)=\left[\nabla-\frac{1}{l}\nabla\times(\mathbf{r}\times\nabla)\right]r^{1-l}Y_l^m,$$

$$\mathbf{D}_l^m(E)=\left[\nabla+\frac{1}{l+1}\nabla\times(\mathbf{r}\times\nabla)\right]r^{l+2}Y_l^m,$$

$$\mathbf{C}_l^m(L)=\nabla r^{-1-l}Y_l^m,\quad \mathbf{D}_l^m(L)=\nabla r^lY_l^m,$$

$$d_l^m(\tau)=\int\mathbf{D}_l^{m*}(\tau)\cdot\mathbf{j}dV. \quad \text{(A9)}$$

This is the required expression. The vector functions **C** and **D** involved in it satisfy the Laplace equation $\Delta C_l^m(\tau)=\Delta D_l^m(\tau)=0$. This is not obvious for $\mathbf{C}_l^m(E)$ and $\mathbf{D}_l^m(E)$. In fact, their component terms do not satisfy the Laplace equation; only linear combinations of them do. This, however, becomes obvious if we act on $\mathbf{C}_l^m(E)$ and $\mathbf{D}_l^m(E)$ with the operator Δ and use the identity

$$\Delta r^\alpha Y_l^m=(\alpha-l)(\alpha+l+1)r^{\alpha-2}Y_l^m,$$

in which we must take $\alpha=1-l$ for $\mathbf{C}_l^m(E)$ and $l+2$ for $\mathbf{D}_l^m(E)$. In addition, $\mathbf{C}_l^m(E)$ and $\mathbf{D}_l^m(E)$ satisfy the relations

$$\text{div}\,\mathbf{C}_l^m(E)=-2(2l-1)r^{-l-1}Y_l^m,$$

$$\text{div}\,\mathbf{D}_l^m(E)=2(2l+3)r^lY_l^m,$$

$$\text{curl}\,\mathbf{C}_l^m(E)=-\frac{2(2l-1)}{l}\mathbf{C}_l^m(M),$$

$$\text{curl}\,\mathbf{D}_l^m(E)=-\frac{2(2l+3)}{l+1}\mathbf{D}_l^m(M),$$

$$\text{curl}\,\mathbf{C}_l^m(M)=lC_l^m(L), \quad \text{(A10)}$$

$$\text{curl}\,\mathbf{D}_l^m(M)=-(l+1)D_l^m(L),$$

$$\text{div}\,\mathbf{C}_l^m(M)=\text{div}\,\mathbf{D}_l^m(M)=\text{div}\,\mathbf{C}_l^m(L)$$
$$=\text{div}\,\mathbf{D}_l^m(L)=\text{curl}\,\mathbf{C}_l^m(L)$$
$$=\text{curl}\,\mathbf{D}_l^m(L)=0.$$

Also, they are orthogonal on a sphere of arbitrary radius:

$$\int\mathbf{C}_l^m(\tau)\cdot\mathbf{C}_{l'}^{m'*}(\tau')d\Omega=\text{const}\cdot\delta_{ll'}\delta_{mm'}\delta_{\tau\tau'},$$

$$\int\mathbf{D}_l^m(\tau)\cdot\mathbf{D}_{l'}^{m'*}(\tau')d\Omega=\delta_{ll'}\delta_{mm'}\delta_{\tau\tau'}\cdot\text{const}.$$

If $\text{div}\,\mathbf{A}=0$, the second sum in (A8) vanishes, and the coefficient $d_l^m(E)$ simplifies:

$$d_l^m(E)=\frac{2(2l+3)}{l+1}\int r^lY_l^{m*}(\mathbf{rj})dV.$$

Let us now take the static limit in Eqs. (A1) and (A2):

$$r^{-l-2}\mathbf{Y}_{l,l+1}^m=\frac{1}{[(l+1)(2l+1)]^{1/2}}\mathbf{C}_l^m(L),$$

$$r^l\mathbf{Y}_{l+1,l}^m=\frac{1}{[(l+1)(2l+3)]^{1/2}}\mathbf{D}_{l+1}^m(L),$$

$$r^{-l}\mathbf{Y}_{l,l-1}^m=\frac{1}{2}\sqrt{\frac{l}{2l+1}}\mathbf{C}_l^m(E),$$

$$r^{l+1}\mathbf{Y}_{l,l+1}^m=-\frac{1}{2}\sqrt{\frac{l+1}{2l+1}}\mathbf{D}_l^m(E), \quad \text{(A11)}$$

$$r^{-l-1}\mathbf{Y}_{ll}^m=\frac{i}{\sqrt{l(l+1)}}\mathbf{C}_l^m(M),$$

$$r^l\mathbf{Y}_{ll}^m=\frac{i}{\sqrt{l(l+1)}}\mathbf{D}_l^m(M).$$

From this it follows that the expansions (A4) and (A8) coincide. However, the representation that we have found for $r^l\mathbf{Y}_{jl}^m$ and $r^{-l-1}\mathbf{Y}_{jl}^m$ in the form of differential operators (A11) is new. The $\mathbf{A}_l^m(\tau)$ satisfy the relations

$$\text{curl}\,\mathbf{A}_l^m(M)=ik\mathbf{A}_l^m(E),\quad \text{curl}\,\mathbf{A}_l^m(E)=-ik\mathbf{A}_l^m(M).$$

For $k\to0$ they become

$$\text{curl}\,\mathbf{A}_{1l}^m(M)=i\mathbf{A}_{1l}^m(E),$$

$$\text{curl}[\mathbf{A}_{1l}^m(E)+k^2\mathbf{A}_{2l}^m(E)]=-ik^2\mathbf{A}_{1l}^m(M). \quad \text{(A12)}$$

The first of Eqs. (A12) is satisfied automatically, owing to the definitions (A6). Collecting terms in the second equation with identical powers of k, we find

$$\text{curl}\,\mathbf{A}^m_{1l}(E)=0,\quad \text{curl}\,\mathbf{A}^m_{2l}(E)=-i\mathbf{A}^m_{1l}(M). \tag{A13}$$

The validity of these equations is easily verified independently by using the relations

$$\text{curl}(\mathbf{r}\times\nabla)r^\alpha Y^m_l = -(\alpha+1)\nabla r^\alpha Y^m_l+(\alpha-l)(\alpha+l+1)\mathbf{r}r^{\alpha-2}Y^m_l. \tag{A14}$$

Setting $\alpha=-l-1$, we obtain

$$\text{curl}(\mathbf{r}\times\nabla)r^{-l-1}Y^m_l=l\nabla r^{-l-1}Y^m_l. \tag{A15}$$

Since [see (A16)] $\mathbf{A}^m_{1l}(E)$ is proportional to the left-hand side of (A15), the first of Eqs. (A13) is satisfied. For $\alpha=1-l$, from (A14) we obtain

$$\text{curl}(\mathbf{r}\times\nabla)r^{1-l}Y^m_l=(l-2)\nabla r^{1-l}Y^m_l-2(2l-1)\mathbf{r}r^{-l-1}Y^m_l.$$

Acting on both sides of this equation with the curl operator, we verify that the second of Eqs. (A13) is valid. For $\alpha=l$ and $l+2$, from (A14) we obtain relations between the $\mathbf{B}^m_{il}$:

$$\text{curl}\,\mathbf{B}^m_{1l}(E)=0,\quad \text{curl}\,\mathbf{B}^m_{2l}(E)=-i\mathbf{B}^m_{1l}(M).$$

From (A15) it follows that the same vector function can be both a gradient and a curl. The analogous relation for positive powers of r is

$$\text{curl}(\mathbf{r}\times\nabla)r^lY^m_l=-(l+1)\nabla r^lY^m_l. \tag{A16}$$

Let us return to the original definitions (A1) and (A2). For $\tau=E$, L we expand both sides of these expressions in powers of k. Equating the coefficients of k^{-l-2} in (A1), we arrive at expressions already contained in (A9)–(A11). Equating the coefficients of k^{-l}, we have

$$\text{curl}(\mathbf{r}\times\nabla)r^{1-l}Y^m_l = l(2l-1)\sqrt{\frac{l+1}{2l+1}}r^{-l}\left(\mathbf{Y}^m_{l,l+1}-\sqrt{\frac{l+1}{l}}\frac{1}{l-1/2}\mathbf{Y}^m_{l,l-1}\right),$$

$$\nabla r^{1-l}Y^m_l = (2l-1)\sqrt{\frac{l+1}{2l+1}}r^{-l}\left(\mathbf{Y}^m_{l,l+1}+\sqrt{\frac{l}{l+1}}\frac{1}{l-1/2}\mathbf{Y}^m_{l,l-1}\right). \tag{A17}$$

We invert these expressions:

$$r^{-l}Y^m_{l,l-1}=\frac{1}{2}\sqrt{\frac{l}{2l+1}}\left[\nabla-\frac{1}{l}\text{curl}(\mathbf{r}\times\nabla)\right]r^{1-l}Y^m_l,$$

$$r^{-l}Y^m_{l,l+1}=\frac{1}{2l-1}\sqrt{\frac{l+1}{2l+1}}\left[\nabla+\frac{1}{l+1}\times\text{curl}(\mathbf{r}\nabla)\right]r^{1-l}Y^m_l. \tag{A18}$$

The first relation is a consequence of (A9) and (A11). Similarly, expanding (A2), we obtain

$$\text{curl}(\mathbf{r}\times\nabla)r^{l+2}Y^m_l = -(l+1)(2l+3)\sqrt{\frac{l}{2l+1}}r^{l+1}\left(\mathbf{Y}^m_{l,l-1}+\sqrt{\frac{l}{l+1}}\frac{1}{l+3/2}\mathbf{Y}^m_{l,l+1}\right),$$

$$\nabla r^{l+2}Y^m_l = (2l+3)\sqrt{\frac{l}{2l+1}}r^{l+1}\left[\mathbf{Y}^m_{l,l-1}-\sqrt{\frac{l+1}{l}}\frac{1}{l+3/2}\mathbf{Y}^m_{l,l+1}\right]. \tag{A19}$$

Or, inverting these,

$$r^{l+1}Y^m_{l,l+1}=-\frac{1}{2}\sqrt{\frac{l+1}{2l+1}}\left[\nabla+\frac{1}{l+1}\text{curl}(\mathbf{r}\times\nabla)\right]r^{l+2}Y^m_l,$$

$$r^{l+1}\mathbf{Y}^m_{l,l-1}=-\frac{1}{2l+3}\sqrt{\frac{l}{2l+1}}\left[\nabla-\frac{1}{l}\text{curl}(\mathbf{r}\nabla)\right]\times r^{l+2}Y^m_l. \tag{A20}$$

Again, the first of these expressions follows from (A9) and (A10). We multiply the first of Eqs. (A19) by the current density $\mathbf{j}$ and integrate over the volume:

$$\int \text{curl}(\mathbf{r}\times\nabla)r^{l+2}Y^m_l\mathbf{j}dV = -(l+1)(2l+3)\sqrt{\frac{l}{2l+1}}\int r^{l+1}\left(\mathbf{Y}^m_{l,l-1}+\sqrt{\frac{l}{l+1}}\frac{1}{l+3/2}\mathbf{Y}^m_{l,l+1}\right)\mathbf{j}dV. \tag{A21}$$

The integral on the right-hand side coincides with the toroidal moment.[12] Therefore, Eq. (A21) gives a new representation for the toroidal moment. If $\text{div}\,\mathbf{j}=0$, the integral on the left-hand side of (A21) simplifies:

$$2(2l+3)\int r^lY^{m*}_l(\mathbf{rj})dV. \tag{A22}$$

Therefore, the toroidal moment naturally arises as the coefficient of k^{l+1} in the expansion of the electric form factor $a^m_l(E)$. Equations (A8) are useful for solving various magnetostatic and electrostatic problems. For example, the conditions, obtained in Sec. 3, that the magnetic field H and the vector potential $\mathbf{A}$ vanish outside a given region of space follow almost automatically from (A8). As a new illustration, we use (A8) to calculate the static vector potential of the toroidal solenoid $(\rho-d)^2+z^2=R^2$. Let us calculate the coefficients $d^m_l(\tau)$ entering into (A8). For $\tau=M$ we have

$$d^m_l(M)=\int(\mathbf{r}\times\nabla)r^lY^{m*}_l\mathbf{j}=-\int r^lY^{m*}_l(\mathbf{r}\,\text{curl}\,\mathbf{j})dV.$$

For the poloidal current (3), $\text{curl}\,\mathbf{j}$ has only a φ component. Therefore, $\mathbf{r}\,\text{curl}\,\mathbf{j}=0$ and $d^m_l(M)=0$. Furthermore, from the continuity equation ($\text{div}\,\mathbf{j}=0$) it follows that $d^m_l(L)=0$. For the same reason, in the integrand for

$d_l^m(E)$ the component of $\mathbf{D}_l^m(E)$ proportional to ∇ does not contribute. Finally, for the VP we obtain the expression

$$A=-\frac{2\pi}{c}\nabla\sum\frac{1}{2l+1}\frac{1}{2l+3}\frac{1}{l+1}\frac{1}{r^{l+1}}Y_l^m$$
$$\times\int\operatorname{curl}(\mathbf{r}\nabla)r^{l+2}Y_l^{m*}\mathbf{j}dV$$
$$=-\frac{4\pi}{c}\nabla\sum\frac{1}{2l+1}\frac{1}{l+1}\frac{1}{r^{l+1}}Y_l^m\int r^lY_l^{m*}(\mathbf{rj})dV. \tag{A23}$$

Using the explicit expression (3) for $\mathbf{j}$, we obtain

$$\mathbf{rj}=\frac{gc}{4\pi}\frac{\delta(\tilde{R}-R)}{d+R\cos\psi}d\sin\psi.$$

In (A23) only the terms with $m=0$ are nonzero:

$$\mathbf{A}=-\frac{1}{2}gdR\nabla\sum\frac{1}{l+1}\frac{1}{r^{l+1}}P_l(\cos\theta)$$
$$\times\int\rho^lP_l\left(\frac{R\sin\psi}{\rho}\right)\sin\psi\,d\psi,$$
$$\rho^2=d^2+R^2+2dR\cos\psi. \tag{A24}$$

Here P_l are the Legendre polynomials $[P_l(x)=(1/2^ll!)(d^l/dx^l)(x^2-1)^l]$. Only the terms with odd l are nonzero in (A24). Setting $l=2n+1$, we find

$$\mathbf{A}=-\frac{1}{2}gdR\nabla\sum\frac{1}{n+1}\frac{1}{r^{2n+2}}P_{2n+1}(\cos\theta)$$
$$\times\int\rho^{2n+1}P_{2n+1}\left(\frac{R\sin\psi}{\rho}\right)\sin\psi\,d\psi. \tag{A25}$$

For an infinitesimally thin solenoid ($R\ll d$) this expression simplifies:

$$\mathbf{A}=-\frac{1}{4}\pi gR^2\nabla\sum(-1)^n$$
$$\times\frac{(2n+1)!!}{2^n(n+1)!}\frac{d^{2n+1}}{r^{2n+2}}P_{2n+1}(\cos\theta). \tag{A26}$$

These expressions are valid outside the sphere of radius $d+R$. Inside the sphere of radius $d-R$ we have

$$\mathbf{A}=\frac{1}{2}gdR\nabla\sum\frac{1}{l}r^lP_l(\cos\theta)$$
$$\times\int\frac{1}{\rho^{l+1}}P_l\left(\frac{R\sin\psi}{\rho}\right)\sin\psi\,d\psi \tag{A27}$$

for a finite solenoid and

$$\mathbf{A}=-\frac{1}{2}\pi gR^2\nabla\sum(-1)^n$$
$$\times\frac{(2n-1)!!}{2^nn!}\frac{r^{2n+1}}{d^{2n+2}}P_{2n+1}(\cos\theta) \tag{A28}$$

for an infinite solenoid.

Let us make the physical meaning of the expansion of the VP (A8) more precise. For this we ask why we must impose the condition div $\mathbf{A}=0$ by hand. We note that the initial nonstatic VP (81) satisfies the Lorentz gauge condition div $\mathbf{A}+\dot{\Phi}/c=0$. Here

$$\Phi=2\pi^2ik\exp(-i\omega t)\sum q_l^mh_lY_l^m,$$

$$q_l^m=\int j_lY_l^{m*}\rho_0dV,\quad\rho=\rho_0\exp(-i\omega t).$$

The relation $q_l^m=(i/c)a_l^m(L)$ guarantees that the Lorentz gauge condition is satisfied automatically. Applying the div operator to (81), we obtain

$$\operatorname{div}\mathbf{A}=-\frac{1}{c}2\pi^2k^2\sum a_l^m(L)h_lY_l^m=-\frac{\dot{\Phi}}{c}.$$

It is easily checked that this expression for $k\to0$ tends to the finite quantity

$$\frac{1}{c}\pi^{5/2}\Sigma,\quad\Sigma\equiv\sum\left(-\frac{2}{r}\right)^{l+1}\frac{1}{\Gamma\left(\frac{1}{2}-l\right)}a_l^m(L)Y_l^m.$$

On the other hand, from the relation div $\mathbf{A}+\dot{\Phi}/c=0$ it would seem to follow that for $k\to0$, $\dot{\Phi}$ and, consequently, div $\mathbf{A}$ must vanish. To understand the reason for this contradiction, we write Φ as

$$\Phi=-2\pi^2\frac{k}{c}\exp(-i\omega t)\sum a_l^m(L)h_lY_l^m.$$

If $kR\ll1$ and $kr\ll1$ (R is the size of the region in which ρ, $\mathbf{j}\neq0$, and r is the distance from this region to the observation point), we can take the limit $k\to0$ under the summation sign. Then

$$\Phi=-\frac{i\pi^{5/2}}{kc}\exp(-i\omega t)\Sigma.$$

We have not yet specified the time interval under consideration, and therefore we have not replaced $\exp(-i\omega t)$ by unity. The physical potential is equal to the real part of this expression:

$$\Phi=-\frac{i\pi^{5/2}}{kc}\sin\omega t\Sigma.$$

Since we have kept the time dependence in Φ, it must also be kept in the VP. For this Eq. (A8) must be multiplied by $\cos\omega t$. For $\omega t\ll1$ for the VP we return to (A8), while Φ becomes $-\pi^{5/2}t\Sigma$. Therefore, if we do not impose the additional condition div $\mathbf{A}=0$, the vector potential corresponds to a scalar potential Φ growing linearly in time (for $\omega t\ll1$). The conjugate solution is obtained if only the imaginary parts are kept in Φ and A. Then

$$\Phi=-\frac{i\pi^{5/2}}{kc}\cos\omega t\Sigma,$$

and the VP is obtained by multiplying (A8) by $(-\sin\omega t)$.

To conclude: the expression describes [when the time factor $\exp(-i\omega t)$ is included and the gauge condition

div $\mathbf{A}=0$ is not used] a wider range of phenomena than pure magnetostatics, which is obtained for div $\mathbf{A}=0$.

[1)]It is interesting to understand what the elementary vector potentials become in the static limit ($k\to 0$). This is discussed in the Appendix.
[2)]Here Ψ_0 is the WF describing the scattering on the sphere with the boundary condition (130) and no TS inside the sphere.

[1]M. A. Miller, Izv. Vyssh. Uchebn. Zaved. Radiofiz. **19**, 991 (1986) [in Russian].
[2]D. R. Saledin, IEEE Trans. Magn. **Mag-20**, 381 (1984).
[3]G. N. Afanasiev, J. Phys. A **23**, 5755 (1990); J. Comput. Phys. **69**, 196 (1987).
[4]Status Report on Controlled Thermonuclear Fusion, IAEA, Vienna (1990).
[5]IEEE Trans. Plasma Sci. **17**, No. 3 (1989); IEEE Trans. Magn. **25**, No. 1 (1989); **27**, No. 1 (1991).
[6]G. N. Afanas'ev and V. M. Dubovik, in *Physics and Technology of Millimeter and Submillimeter Radio Waves* [in Russian] (1991), Part 1, p. 71.
[7]D. F. Bartlett and B. F. L. Ward, Phys. Rev. D **16**, 3453 (1977).
[8]M. Peshkin and A. Tonomura, *The Aharonov–Bohm Effect* (Springer-Verlag, Berlin, 1989).
[9]V. L. Lyuboshits and Ya. A. Smorodinskiĭ, Zh. Eksp. Teor. Fiz. **75**, 40 (1978) [Sov. Phys. JETP **48**, 19 (1978)].
[10]G. N. Afanasiev, Phys. Lett. **142A**, 222 (1989); G. N. Afanasiev and V. M. Shilov, J. Phys. A **22**, 5195 (1989); J. Phys. A **26**, 743 (1993).
[11]Ya. B. Zel'dovich, Zh. Eksp. Teor. Fiz. **33**, 1531 (1957) [Sov. Phys. JETP **6**, 1184 (1958)].
[12]V. M. Dubovik and V. V. Tugushev, Phys. Rep. **187**, 145 (1990).
[13]G. N. Afanasiev, V. M. Dubovik, and S. Misicu, Preprint E2-92-177, JINR, Dubna (1992) [to be published in J. Phys. A].
[14]V. L. Ginzburg and V. N. Tsytovich, Zh. Eksp. Teor. Fiz. **88**, 84 (1985) [Sov. Phys. JETP **61**, 48 (1985)].
[15]G. N. Afanasiev, Fiz. Elem. Chastits At. Yadra **21**, 172 (1990) [Sov. J. Part. Nucl. **21**, 74 (1990)].
[16]G. N. Afanasiev, Fiz. Elem. Chastits At. Yadra **23**, 1264 (1992) [Sov. J. Part. Nucl. **23**, 552 (1992)].
[17]G. N. Afanasiev, Preprint E2-91-544, JINR, Dubna (1991).
[18]V. M. Dubovik and A. A. Cheshkov, Fiz. Elem. Chastits At. Yadra **5**, 791 (1974) [Sov. J. Part. Nucl. **5**, 318 (1975)]; V. M. Dubovik and L. A. Tosunyan, Fiz. Elem. Chastits At. Yadra **14**, 1193 (1983) [Sov. J. Part. Nucl. **14**, 504 (1983)].
[19]Y. Aharonov and A. Casher, Phys. Rev. Lett. **53**, 319 (1984).
[20]G. N. Afanasiev, J. Phys. A **26**, 731 (1993).
[21]V. R. Petukhov, Preprint 105-91, ITEP, Moscow (1991) [in Russian].
[22]V. R. Petukhov, Preprint 106-91, ITEP, Moscow (1991) [in Russian].
[23]G. N. Afanasiev, J. Phys. A **23**, 5185 (1990).
[24]G. N. Afanasiev and V. M. Dubovik, J. Phys. A **25**, 4869 (1992).
[25]A. Cimino, G. I. Opat, A. C. Klein *et al.*, Phys. Rev. Lett. **63**, 380 (1989).
[26]E. E. Radescu, Phys. Rev. D **32**, 1266 (1985); I. Yu. Kobzarev and L. B. Okun', in *Problems in Theoretical Physics* (Nauka, Moscow, 1972), p. 219 [in Russian].
[27]V. M. Dubovik, S. S. Krotov, and V. V. Tugushev, Kristallografiya **32**, 540 (1987) [Sov. Phys. Crystallogr. **32**, 314 (1987)].
[28]R. C. Casella, Phys. Rev. Lett. **65**, 2217 (1990).
[29]J. D. Jackson, *Classical Electrodynamics* (Wiley, New York, 1975).
[30]B. Carrascal, G. A. Estevez, and V. Lorenzo, Am. J. Phys. **51**, 233 (1991).
[31]S. Olariu and I. I. Popescu, Rev. Mod. Phys. **52**, 339 (1985).
[32]V. M. Dubovik, L. A. Tosunyan, and V. V. Tugushev, Zh. Eksp. Teor. Fiz. **90**, 590 (1986) [Sov. Phys. JETP **63**, 344 (1986)].
[33]M. E. Rose, *Multipole Fields* (Wiley, New York, 1955) [Russian transl., IL, Moscow, 1957].
[34]A. I. Akhiezer and V. B. Berestetskii, *Quantum Electrodynamics* (Wiley, New York, 1965) [Russian original, Fizmatgiz, Moscow, 1959]; J. M. Blatt and V. F. Weisskopf, *Theoretical Nuclear Physics* (Wiley, New York, 1952) [Russian transl., IL, Moscow, 1954].
[35]W. F. Brown, in *Handbuch der Physik*, Vol. 17: Dielectrics, edited by S. Flügge (Springer, Berlin, 1956), p. 1; P. W. Forsbergh, *ibid.*, p. 264.
[36]J. A. Stratton, *Electromagnetic Theory* (McGraw-Hill, New York, 1941) [Russian transl., OGIZ, Moscow, 1948].
[37]O. D. Jefimenko, Am. J. Phys. **58**, 625 (1990).
[38]M. A. Martsenyuk and N. M. Martsenyuk, Pis'ma Zh. Eksp. Teor. Fiz. **53**, 229 (1991) [JETP Lett. **53**, 243 (1991)].
[39]N. A. Tolstoĭ and A. A. Spartakov, Pis'ma Zh. Eksp. Teor. Fiz. **52**, 796 (1990) [JETP Lett. **52**, 161 (1990)].
[40]D. F. Bartlett and G. Gengel, Phys. Rev. A **39**, 938 (1989).
[41]R. G. Barrera, G. A. Estevez, and J. Giraldo, Eur. J. Phys. **6**, 287 (1985).
[42]G. A. Ryazanov, *Electrical Modeling with Applications to Vortex Fields* [in Russian] (Nauka, Moscow, 1969).
[43]T. Takabajasi, Hadr. J. Suppl. **1**, 219 (1985).
[44]Y. Aharonov and D. Bohm, Phys. Rev. **115**, 485 (1959).
[45]M. Razavy, Phys. Rev. A **40**, 1 (1989).
[46]J. M. Levy-Leblond, Phys. Lett. **125A**, 441 (1987).
[47]S. K. Bose, Indian J. Phys. B **61**, 274 (1987).
[48]U. Percoco and V. M. Villalba, Phys. Lett. **140A**, 105 (1989).
[49]S. Olariu, Phys. Lett. **144A**, 287 (1990).
[50]A. W. Thomas, in *Advances in Nuclear Physics*, edited by J. W. Negele and E. Vogt (Plenum, New York, 1984), Vol. 13, p. 1; J. Vepstas and A. D. Jackson, Phys. Rep. **187**, 111 (1990).
[51]Y. Aharonov, C. K. Au, E. C. Lerner, and J. Q. Liang, Phys. Rev. D **29**, 2396 (1984); B. Nagel, Phys. Rev. D **32**, 3328 (1985); R. A. Brown, J. Phys. A **18**, 2497 (1985).
[52]T. T. Wu and C. N. Yang, Phys. Rev. D **12**, 3845 (1975).
[53]S. M. Roy and V. Singh, J. Phys. A **22**, L425 (1989).
[54]S. M. Roy and V. Singh, Nuovo Cimento A **79**, 391 (1984).
[55]Y. Aharonov, in *Proc. of the Intern. Symp. on the Foundations of Quantum Mechanics*, edited by S. Kamefuchi, Japan Physics Society, Tokyo (1984), p. 10; C. N. Yang, *ibid.*, p. 5.
[56]W. Pauli, Helv. Phys. Acta **12**, 147 (1939) [Russian transl., Nauka, Moscow, 1977].
[57]S. M. Roy, Phys. Rev. Lett. **44**, 111 (1980).
[58]M. Born and E. Wolf, *Principles of Optics*, 4th ed. (Pergamon Press, Oxford, 1970) [Russian transl., Nauka, Moscow, 1970].
[59]G. Matteucci, Am. J. Phys. **58**, 1143 (1990).
[60]M. V. Berry, Eur. J. Phys. **2**, 240 (1980).
[61]A. Tonomura, N. Osakabe, T. Matsuda *et al.*, Phys. Rev. A **34**, 815 (1986).
[62]J. Komrska, in *Advances in Electronics and Electron Physics* (Academic Press, New York, 1971), Vol. 30, p. 139.
[63]H. W. Fink, W. Stocker, and H. Schmid, Phys. Rev. Lett. **65**, 1204 (1990).
[64]M. A. Berger and G. B. Field, J. Fluid Mech. **147**, 133 (1984).
[65]M. K. Moffat, Nature **347**, 367 (1990).
[66]H. Pfistor and W. Gekelman, Am. J. Phys. **59**, 497 (1991).
[67]M. A. Berger, J. Phys. A **23**, 2787 (1990).
[68]A. O. Barut, M. Bozic, and Z. Maric, Ann. Phys. (N.Y.) **214**, 53 (1992).
[69]E. G. Flekkoy and J. M. Leinaas, Int. J. Mod. Phys. **6**, 5327 (1991).

Translated by Patricia A. Millard